La chute n'est pas un échec.
L'échec est de rester là où on est tombé.
Socrate

# IDENTIFICATION OF A MICRORNA CONTROLLING HEPATIC CELL DIFFERENTIATION

**Céline Demarez**

*June 2016*

Université Catholique de Louvain

de Duve Institute – Liver and Pancreas Development Unit

Thèse présentée en vue de l'obtention du grade de docteur en sciences biomédicales et pharmaceutiques

## JURY MEMBERS

### Supervisor

Prof. Frédéric Lemaigre

*Université Catholique de Louvain*

### President

Prof. Thomas Michiels

*Université Catholique de Louvain*

### UCL jury members

Prof. Guido Bommer

*Université Catholique de Louvain*

Prof. Frédéric Clotman

*Université Catholique de Louvain*

Prof. Isabelle Leclercq

*Université Catholique de Louvain*

### External jury members

Prof. Anne Dubart-Kuperschmitt

*INSERM - Université Paris-Sud*

Prof. Leo Van Grunsven

*Vrije Universiteit Brussel*

# REMERCIEMENTS

Dans un de mes films favoris, Forrest Gump a dit : «La vie, c'est comme une boite de chocolats : on ne sait jamais sur quoi on va tomber». Et bien, de mon point de vue, on peut en dire autant de la thèse! Durant ces quatre dernières années, certains chocolats m'ont laissé un goût amer, d'autres m'ont laissé sur ma faim, et d'autres encore m'ont découragée... Cependant, après ces quelques déceptions et moments de doute, il n'est très vite resté que les meilleurs chocolats dans la boite: ceux avec un goût de promesse et de réussite. Et plus important encore, de nombreuses personnes avec qui les partager! En effet, si cette thèse était avant tout un défi personnel que je m'étais lancé, elle n'en est pas moins devenue un moment de rencontres, de collaboration et d'amitié. Alors à vous tous qui avez partagé ces moments de peines, de doutes et de démotivations mais surtout de joies, de rires et de partage, je vous dis du fond du cœur : MERCI !

Mes premiers remerciements vont bien entendu à mon promoteur **Frédéric Lemaigre**. Frédéric, merci de m'avoir accueillie dans votre laboratoire et de m'avoir accordé votre confiance. Vous m'avez permis de m'épanouir scientifiquement en me confiant rapidement les rênes de mon projet, tout en m'apportant un soutien sans faille dans les moments plus difficiles. Il faut bien le dire, ce projet nous aura fait transpirer! J'ai beaucoup apprécié travailler avec vous, tant pour vos qualités scientifiques qu'humaines, votre disponibilité, vos histoires d'oiseaux en réunions ou les petites discussions à propos de tout et de rien que l'on pouvait avoir dans votre bureau. Votre bienveillance quasi paternelle restera longtemps gravée dans ma mémoire. Merci d'avoir fait de ce labo un endroit où l'on prend plaisir à évoluer chaque jour. Enfin, après m'avoir tant apporté, j'espère de mon côté vous avoir donné l'envie de mettre de la couleur dans vos présentations! Et pourquoi pas du rose?! Encore merci pour tout…

Je remercie également les membres de mon comité d'encadrement, les professeurs **Thomas Michiels**, **Guido Bommer**, **Frédéric Clotman** et **Isabelle Leclercq** pour m'avoir suiviz et guidée toutes ces années. J'ai une petite pensée particulière pour Thomas qui, après m'avoir acceptée dans son laboratoire pour mon master, a accepté de devenir le

président de mon jury de thèse et m'a toujours encouragée avec optimisme durant ces quatre années. Merci également aux professeurs **Anne Dubart-Kuperschmitt** et **Leo Van Grunsven** d'avoir accepté d'évaluer mon travail de doctorat et d'avoir animé de milles questions ma défense privée. Merci aussi au docteur **Christine Sempoux** pour notre belle et sympathique collaboration.

S'il est vrai que la thèse demande beaucoup de travail et d'investissement personnel, ma vie au labo aurait été bien différente sans la bonne ambiance régnant au sein de notre équipe! Merci à tous mes super collègues d'avoir rendu mon quotidien aussi joyeux! **Sabine**, merci pour ton aide quotidienne, pour toutes nos discussions (sérieuses ou pas!), merci de nous avoir organisé de si chouettes sorties de labo avec toujours autant d'entrain et surtout, merci de ton amitié. **Claude**, après un petit stage d'adaptation à ton humour et à tes chansons (après tout, rien n'est impossible, j'ai bien survécu à Jean-Bernard!), j'ai découvert un petit mec super sympa avec qui le courant est tout de suite bien passé. Je te remercie sincèrement d'avoir participé à l'ambiance du bureau et suis très contente d'avoir collaboré avec toi sur notre papier! Par contre… je te remercie un peu moins pour ton modèle mathématique ;-) J'espère que l'on continuera à se retrouver autour de quelques pas de danse! Merci également à **Patrick** pour ses conseils avisés en réunion, à **Pierre-Paul** et **Géraldine** pour m'avoir fait intégrer le club des cools, à **Adrien**, **Boris**, **Janne**, **Elsa**, **Vitaline**, **Freddy**, **Bianca**, **Thoueiba**, **Nora** et **Alexis** pour votre bonne humeur, et à **Mourad** et **Younes** sans qui le travail sur les souris n'aurait pas été possible. Enfin, un grand merci à nos collègues de chez **GEPI** avec qui nous partageons l'étage et à tous ceux que j'aurais oublié de citer.

La thèse, c'est fatigant! Alors quoi de mieux qu'une super bande de potes pour se changer les idées? **Thib et Sarah**, je ne compte plus nos années d'amitié… Merci pour tous ces moments de complicités que l'on partage depuis si longtemps, pour tous ces bons moments passés ensemble, pour nos milles et une soirées à la maison, nos fous-rires… **Alex**, officiellement mon compétiteur numéro un lors de nos soirées Mario Kart, je te remercie pour l'attention que tu sais me porter et pour ton amitié de longue date elle aussi. **Châu**, merci pour tes encouragements, tes bons petits plats et tes soirées

d'anniversaires tellement originales! **Julien**, merci pour ton aide, pour tous nos petits moments de délires et pour toutes nos soirées ciné, jeux de société, bbq et j'en passe. **Cécile**, ma coupine, ma Tic… Entre-nous, un seul regard a suffi et le groupe des papoteuses du couloir était né! Aujourd'hui tu le sais, tu es plus qu'une collègue, tu es une amie. Toujours là pour moi, tu m'as offert un soutien inconditionnel et tu as su partager mes peines et mes doutes. Merci pour nos discussions innombrables, nos commérages (innombrables eux aussi ^^), pour nos partages de «bons plans» pour les manips, ta bonne humeur communicative et pour m'avoir fait faire du sport comme jamais auparavant! Bref, merci pour tous ces moments qui ont fait que sans toi, ma thèse n'aurait pas été la même. Merci aussi à **Ben et Vivi**, **Jo et Olivia**, **Tit et Ju**, **Jen et Malou**, **Marie et Aurélie**. Les amis, vous êtes géniaux!

Un énorme merci à ma famille qui m'a toujours soutenue et encouragée pendant toutes ces années. **Laurent et Barbara**, **Papy et Mamy**, **Parrain et Katia**, **Claude**, merci de tout cœur de vous êtres toujours inquiétés pour moi et d'avoir suivi de loin l'avancement de mon projet.

Enfin, je remercie tendrement les personnes qui ont probablement vécu cette thèse aussi intensément que moi. **Maman**, même si tu n'as pas toujours très bien compris ce que je faisais, tu as toujours su trouver les mots justes dans les moments difficiles, que ça soit durant mes études ou pendant ma thèse. Je sais que tu as vécu cette thèse à travers moi, et aujourd'hui je suis très heureuse de te rendre si fière. Merci d'avoir toujours cru en moi. **Louks**, mon chéri, je ne te dirai jamais assez merci pour ton amour et ta patience. Tu es le mieux placé pour savoir que cela n'a pas toujours été facile. Pourtant, tu as toujours su tirer le meilleur de moi-même et rester positif quand je croyais tout perdu. Merci de m'avoir supportée, surtout en cette période de rédaction et de défense tellement stressante. Mais surtout, merci d'être toi. Ton optimiste et ta joie de vivre me tirent incontestablement vers le haut!

Merci à tous ! Je tourne une page et j'en ouvre une autre: vivement la suite!

## SUMMARY

Cell differentiation is tightly controlled by transcriptional regulatory networks. These networks consist in tissue-specific transcription factors which control expression of target genes that exert the cells' functions. In such networks, microRNAs (miRNA) modulate transcription factor levels and thereby participate in the control of cell differentiation.

In the present thesis, we first searched for miRNAs which, in developing liver, control differentiation of hepatic epithelial cells. More specifically, we looked for microRNAs that control hepatobiliary lineage segregation, namely the differentiation of liver progenitor cells into either hepatocytes or cholangiocytes. Using a combination of *in vitro* and *in vivo* approaches resorting to transgenic mice, we identified miR-337-3p as a novel regulator of lineage segregation in the developing liver. MiR-337-3p stimulates expression of cholangiocyte genes and represses hepatocyte genes. Beyond the stage of lineage segregation, miR-337-3p controls the transcriptional network dynamics of developing hepatocytes and cholangiocytes and its action requires Notch and TGF-β signaling. In addition, we developed a mathematical model and supplied experimental data showing that miR-337-3p might exert a biphasic control on HNF4α expression.

Since differentiation grade of tumor cells in cholangiocarcinoma is a prognosis factor, determining if miRNAs play a role in tumor differentiation is important to identify molecular markers of prognosis and potential therapeutic targets. To address this issue we verified, in the second part of the thesis, if the expression of miRNAs and molecular differentiation markers, including cholangiocyte-specific transcription factors and miRNAs, correlate with the tumor differentiation grade as defined by histopathological criteria. Our investigation of intrahepatic cholangiocarcinoma surprisingly revealed a lack of correlation between the expression of molecular differentiation markers and the histologically-defined differentiation grade. Therefore, our data point toward necessary caution when investigating the prognosis of intrahepatic cholangiocarcinoma on the basis of histological cell differentiation criteria.

In conclusion, we have identified a miRNA that controls normal hepatic cell differentiation, and found that expression of miRNAs in cholangiocarcinoma does not reflect the tumor's histological differentiation grade.

# ABBREVIATIONS

| | |
|---|---|
| **Afp** | α-fetoprotein |
| **Alb** | Albumin |
| **Alfp** | Albumin/α-fetoprotein |
| **BMP** | Bone Morphogenic Proteins |
| **C/EBP** | CCAAT/enhancer binding protein |
| **CA 19-9** | Carbohydrate antigen 19-9 |
| **CA-125** | Carcinoembryonic antigen 125 |
| **CCA** | Cholangiocarcinoma |
| **CFTR** | Cystic Fibrosis Transmembrane conductance Regulator |
| **CK** | Cytokeratin |
| **CT** | Computed tomography |
| **CYP7A** | Cholesterol 7-α hydroxylase |
| **dCCA** | Distal cholangiocarcinoma |
| **DLK** | Delta-like homologue |
| **DNMT** | DNA methyltransferase |
| **E-cad** | E-cadherin |
| **ECM** | Extracellular matrix |
| **ESC** | Embryonic stem cell |
| **FACS** | Fluorescence-activated cell sorting |
| **FGF** | Fibroblast Growth Factors |
| **Fox** | Forkhead box |
| **G6pc** | Glucose-6-phosphatase |
| **GFP** | Green fluorescent protein |
| **gp** | Glycoprotein |
| **Grhl** | Grainyhead-like |
| **GSEA** | Gene Set Enrichment Analysis |
| **HCC** | Hepatocellular carcinoma |
| **HDGF** | Hepatoma-Derived Growth Factor |
| **Hes** | Hairy and enhancer of split homolog |
| **HGF** | Hepatocyte Growth Factor |
| **Hhex** | Hematopoietically expressed homeobox |
| **HNF** | Hepatocyte Nuclear Factor |
| **iCCA** | Intrahepatic cholangiocarcinoma |
| **IFFL** | Incoherent feed-forward loop |

| | |
|---|---|
| **IGFBP** | Insulin-like growth factor binding protein |
| **iPSC** | Induced pluripotent stem cells |
| **Jag** | Jagged |
| **LETF** | Liver-enriched transcription factors |
| **MACS** | Magnetic cell sorting |
| **miRNA** | microRNA |
| **MRI** | Magnetic resonance imaging |
| **Muc** | Mucin |
| **NF1A** | Nuclear factor 1-A |
| **OC** | Onecut |
| **OPN** | Osteopontin |
| **OSM** | Oncostatin M |
| **pCCA** | Perihilar cholangiocarcinoma |
| **PDS** | Primitive ductal structures |
| **PEPCK** | Phosphoenol pyruvate carboxykinase |
| **PFK2** | 6-phosphofructo-2-kinase |
| **PPAR** | Peroxisome Proliferator Activated receptors |
| **Prox** | Prospero homeobox protein |
| **PSC** | Primary sclerosing cholangitis |
| **RBPJκ** | Recombination signal binding protein for immunoglobulin kappa J |
| **SOX** | SRY-related HMG box transcription factor |
| **SRY** | Sex-determining region of the Y chromosome |
| **STAT** | Signal Transducer and Activator of Transcription |
| **Tat** | Tyrosine aminotransferase |
| **Tbx** | T-box transcription factor |
| **TEAD** | TEA domain |
| **TGF** | Transforming Growth Factor |
| **TNM** | Tumor Node Metastasis |
| **Ttr** | Transthyretin |
| **TβRII** | TGFβ receptor type II |
| **WT** | Wild-type |
| **Yap** | Yes-associated protein |

# TABLE OF CONTENT


**I. INTRODUCTION 19**

**1. LIVER ARCHITECTURE AND FUNCTIONS 19**

**2. EMBRYONIC DEVELOPMENT OF THE LIVER 20**

2.1. ONSET OF THE LIVER DEVELOPMENT 21

2.2. HEPATOBILIARY SEGREGATION 23

*2.2.1. Timing of hepatobiliary segregation 24*

*2.2.2. Transcriptional control of lineage segregation 24*

*2.2.3. Signaling pathways controlling lineage segregation 27*

2.3. HEPATOCYTE DEVELOPMENT 30

*2.3.1. Hepatocyte maturation and morphogenesis 31*

*2.3.3. Signaling pathways controlling hepatocyte maturation 36*

2.4. INTRAHEPATIC BILIARY TRACT DEVELOPMENT 37

*2.4.1. Morphogenesis of the intrahepatic biliary tree 37*

*2.4.2. Transcriptional control of bile duct development 39*

*2.4.3. Signaling pathways controlling bile duct morphogenesis 41*

**3. MICRORNAS AND LIVER DEVELOPMENT 44**

3.1. MICRORNAS AND GENE REGULATORY NETWORKS 45

3.2. GLOBAL IMPACT OF MICRORNAS ON LIVER FUNCTION 47

3.3. ROLE OF SPECIFIC MICRORNAS IN EMBRYONIC LIVER DEVELOPMENT 48

**4. CELL DIFFERENTIATION IN INTRAHEPATIC CHOLANGIOCARCINOMA 51**

4.1. GENERAL INFORMATION 52

*4.1.1. Epidemiology and etiology of iCCA 52*

*4.1.2. Pathophysiology of iCCA 52*

4.2. DIAGNOSIS AND MANAGEMENT OF INTRAHEPATIC CHOLANGIOCARCINOMA 53

4.3. PROGNOSIS OF INTRAHEPATIC CHOLANGIOCARCINOMA 54

*4.3.1. Classification and prognosis 54*

*4.3.2. Hepatic differentiation markers and prognosis 56*

*4.3.3. MicroRNAs and prognosis 58*

**II. AIMS OF THE THESIS 59**

**III. RESULTS 61**

**1. MIR-337-3P BALANCES HEPATOBILIARY GENE EXPRESSION IN DEVELOPING LIVER AND CONTROLS THE DYNAMICS OF HEPATOCYTE DIFFERENTIATION 61**

**2. EXPRESSION OF MOLECULAR DIFFERENTIATION MARKERS DOES NOT CORRELATE WITH HISTOLOGICAL DIFFERENTIATION GRADE IN INTRAHEPATIC CHOLANGIOCARCINOMA 103**

**IV. GENERAL DISCUSSION AND PERSPECTIVES 125**

**1. INVESTIGATING MIR-337-3P FUNCTIONS DURING LIVER EMBRYOGENESIS 125**

1.1. WHAT ARE THE MIR-337-3P TARGETS? 125

1.2. MECHANISM OF ACTION OF MIR-337-3P 127

**2. MICRORNAS, FINE TUNERS OF DEVELOPMENTAL PROCESSES 130**

**3. *IN VITRO* GENERATION OF HEPATIC CELLS 131**

**4. CHOLANGIOCYTE DIFFERENTIATION MARKERS, MICRORNAS AND ICCAS 133**

**5. GENERAL CONCLUSION AND PERSPECTIVES 135**

**V. ANNEXES 137**

**1. PROLIFERATION-INDEPENDENT INITIATION OF BILIARY CYSTS IN POLYCYSTIC LIVER DISEASES 137**

**VI. REFERENCES 153**

# I. INTRODUCTION

## 1. LIVER ARCHITECTURE AND FUNCTIONS

With a mass that accounts for 2% to 5% of the body weight, the liver is the largest gland of the body. This vital organ exhibits both endocrine and exocrine functions. Endocrine functions include the secretion of several hormones such as Insulin-like growth factors, Angiotensinogen or Thrombopoietin in the bloodstream, while the major exocrine function consists in bile secretion into the biliary tract down to the small intestine. The liver also secretes a broad range of plasma proteins including Albumin and Apolipoproteins and plays critical functions in the regulation of physiological processes such as lipid and carbohydrate metabolism, drug detoxification, hemostasis and urea metabolism (Si-Tayeb et al., 2010).

Histologically, the adult liver is mainly composed of hepatocytes which represent 80% of the liver parenchyma and carry out most of the liver functions. The remaining 20% of cells is composed of cholangiocytes/biliary cells, endothelial cells, Kupffer cells (macrophages), hepatic stellate cells and pit cells (natural killers cells) (Blouin et al., 1977).

The liver landscape is organised in functional and structural units called lobules (Figure 1). Each lobule is hexagonally shaped and consists of hepatocytes cords lined by sinusoidal capillaries radiating toward a central vein. Hepatocytes are separated from the endothelial cells by the space of Disse, which houses the stellate cells. Hepatic lobule corners are characterized by the presence of a portal triad, consisting of a branch of the portal vein, one or two bile ducts and a branch of the hepatic artery. The hepatic artery supplies the liver with oxygenated blood while the portal vein carries nutrient-rich blood drained from the digestive tract. Blood flows through the sinusoids and irrigates liver lobules before being collected by the central vein, which eventually reaches the systemic circulation.

Hepatocytes are polarized epithelial cells. The basolateral pole of hepatocytes face fenestrated sinusoidal endothelial cells, thereby facilitating endocrine secretion and capturing nutrients from the bloodstream, while the apical pole produces and secretes the bile into bile canaliculi delineated by tight junctions between adjacent hepatocytes. Bile flows from the canaliculi to the bile duct within the portal triad and is further collected by extrahepatic ducts before being stored in the gallbladder. Since the blood flows from portal triads toward central vein, bile and blood streams are anti-parallel in the liver (Figure 1).

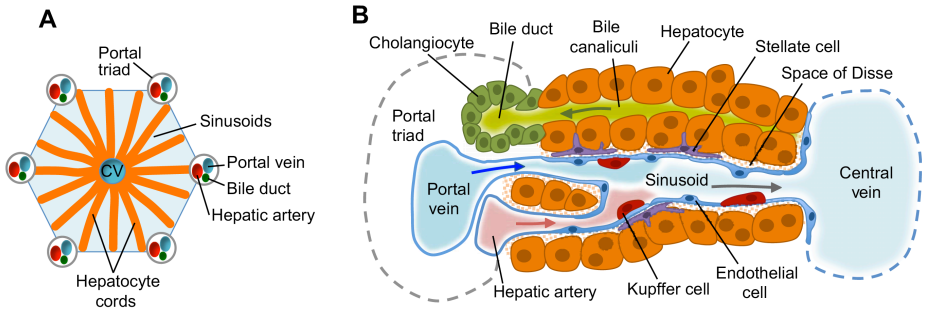



**Figure 1. Liver architecture and cell types** (from Gordillo et al., 2015). Schematic representation of the hepatic lobule **(A)** and the organisation of cells and bile/blood flows within the lobule **(B)**.

## 2. EMBRYONIC DEVELOPMENT OF THE LIVER

Liver organogenesis starts at embryonic day (E) 8.0 in the mouse and proceeds until the perinatal period. Hepatocytes and cholangiocytes, which are the two main epithelial cell types of the organ, derive from a common embryonic precursor cell called hepatoblast, while non-parenchymal cells have a mesodermal origin (Zhao and Duncan, 2005). Hepatoblasts are bipotent progenitors arising from the endoderm. They differentiate either to immature hepatocytes or cholangiocytes, and the latter cell types eventually mature into fully functional hepatic cells. These developmental steps will be described in the following chapter.

## 2.1. Onset of the liver development

The liver originates from the endoderm, one of the three germ layers generated at the time of gastrulation. During the foregut closure, hepatic progenitors located in three distinct domains of the endoderm converge to generate a single prehepatic domain in close proximity to the septum transversum and the cardiac mesoderm (Tremblay and Zaret, 2005; Zaret and Grompe, 2008) (Figure 2).

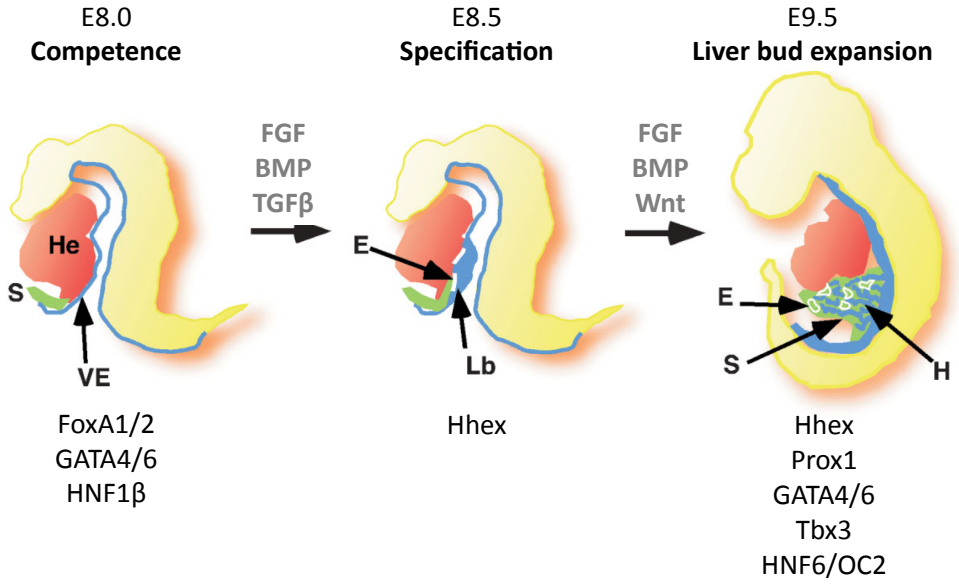



**Figure 2. Early steps of liver development in the mouse embryo** (adapted from Zhao and Duncan, 2005). Illustration of the initial steps of liver development with key transcription factors and extracellular signaling pathways involved at specific stages. He: heart, S: septum transversum, VE: ventral endoderm, E: endothelial cells, Lb: liver bud, H: hepatoblasts.

Around E8.0, cells of the prehepatic domain are primed to respond to liver-inducing signals and are then called "competent" (Figure 2). The acquisition of competence is driven by the "pioneer" transcription factors Forkhead box (Fox) A and GATA4, which bind to liver-specific genes and allow their transcription by decompacting their chromatin, thereby providing access to additional transcription factors (Bossard and Zaret, 1998; Cirillo et al., 2002; Gualdi et al., 1996; Lee et al., 2005). Hepatocyte Nuclear Factor (HNF) 1β is also required for ventral endoderm competence where it stimulates FoxA1 and

FoxA2 expression in the pre-hepatic domain. Mice lacking HNF1β fail to express liver-specific genes (Lokmane et al., 2008).

Hepatic specification occurs shortly after the acquisition of competence and provides the first molecular evidence of liver development. Thanks to their close proximity, the competent cells of the endoderm respond to extracellular signals such as Bone Morphogenic Proteins (BMP) and Fibroblast Growth Factors (FGF) arising from the septum transversum and the cardiac mesoderm (Figure 2). FGF and BMP induce expression of the early hepatic fate markers Albumin (Alb), Transthyretin (Ttr), α-fetoprotein (Afp) and HNF4α (Calmont et al., 2006; Miller et al., 2000; Rossi et al., 2001). Moreover, FGF, BMP and Transforming Growth Factor (TGF) β are required for proper antero-posterior patterning of the endoderm, and determine the position of hepatic precursors in the vicinity of pancreatic precursors (Loh et al., 2014; Serls et al., 2005; Wandzioch and Zaret, 2009). In addition, Wnt signaling must be repressed in the anterior endoderm to allow liver development (McLin et al., 2007).

Once specified, hepatic precursor cells are called hepatoblasts and line the liver diverticulum, an evagination of the endoderm. They progressively become columnar and undergo a transition to pseudostratified epithelium driven by the Hematopoietically expressed homeobox factor (Hhex) (Bort et al., 2006). Hepatoblasts then start to proliferate, thereby thickening the epithelium and inducing the formation of a liver bud surrounded by a basement membrane. Shortly after, hepatoblasts migrate through the membrane and invade the septum transversum (Figure 3). These developmental steps are under tight control of a transcription factor network that includes Hhex (Denson et al., 2000; Keng et al., 2000; Martinez Barbera et al., 2000), GATA4/6 (Watt et al., 2007; Zhao et al., 2005), Prospero homeobox protein (Prox) 1 (Seth et al., 2014; Sosa-Pineda et al., 2000), T-box transcription factor (Tbx) 3 (Ludtke et al., 2009), HNF6 and Onecut (OC) 2 (Margagliotti et al., 2007)(Figure 2). The transcription factor CCAAT/enhancer binding protein (C/EBP) α is required for liver outgrowth in zebrafish (Yuan et al., 2015), but its role in mouse liver outgrowth requires further investigations (Westmacott et al., 2006).

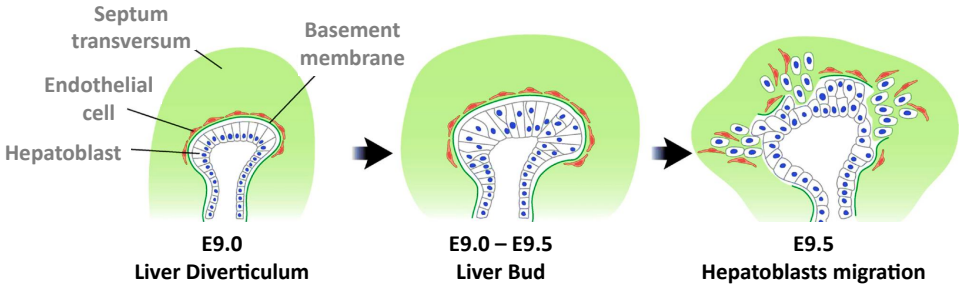



**Figure 3. Liver budding out of the endoderm** (adapted from Lemaigre et al., 2009). Schematic representation of the morphological changes underwent by the hepatoblasts during liver budding and septum transversum invasion.

After invading the septum transversum, hepatoblasts continue to proliferate in order to expand the liver mass. Several growth factors secreted by the septum transversum or by hepatoblasts themselves are involved in this process. These include Hepatocyte Growth Factor (HGF) (Monga et al., 2002; Schmidt et al., 1995), TGFβ1, -2 and -3(Weinstein et al., 2001), BMP4(Rossi et al., 2001; Yanai et al., 2008), FGF8 and -10 (Berg et al., 2007; Jung et al., 1999), Wnt (Tan et al., 2008), Hepatoma-Derived Growth Factor (HDGF) (Enomoto et al., 2002) and retinoic acid (Wang et al., 2006). Moreover, liver outgrowth is also controlled by soluble signals provided by the surrounding endothelial cells. Indeed, mice lacking endothelial cells exhibit complete arrest of hepatoblasts migration from the liver bud, while Wnt9a secretion from the sinusoidal wall is essential for hepatoblasts proliferation in chick embryo (Matsumoto et al., 2008; Matsumoto et al., 2001).

## 2.2. Hepatobiliary segregation

As mentioned previously, hepatoblasts are bipotent progenitors that can differentiate either to the hepatocyte or to the cholangiocyte lineage. Despite intense investigations, the concept of lineage commitment remains difficult to describe in clear molecular terms. Indeed, since it is a continuous process, the timing of molecular events driving lineage commitment cannot be determined accurately. Furthermore, hepatobiliary segregation is

governed by a sophisticated network of transcription factors and extracellular signals that is currently only partially understood. These two aspects are discussed further below.

### *2.2.1.* TIMING OF HEPATOBILIARY SEGREGATION

Between E9.5 and E12.5, hepatoblasts already express markers such as Alb, Ttr, HNF4α and Afp, which are characteristic of hepatocyte functions, thereby blurring the molecular limit between hepatoblasts and hepatocytes. However, there is evidence suggesting that hepatocyte differentiation has already begun in E12.0 livers. Indeed, electron micrographs identified a subpopulation of hepatoblasts presenting with abundant rough endoplasmic reticulum and lipid vesicles (Lemaigre, 2009). Beyond E12.0, hepatocyte-specific functions are gradually acquired and hepatocytes organise as cords. Regarding cholangiocyte development, the onset of biliary commitment is currently associated with the detection of SRY-related HMG box transcription factor (SOX) 9 in the liver parenchyma. Rare SOX9-expressing cells are detected around E11.5, and since SOX9 is the most specific and earliest marker of cholangiocytes in developing liver, E11.5 is considered as the starting point of biliary differentiation (Antoniou et al., 2009).

### *2.2.2.* TRANSCRIPTIONAL CONTROL OF LINEAGE SEGREGATION

Several transcription factors are involved in lineage cell commitment (Figure 4).

**HNF6 and OC2.** The transcription factor HNF6 (also known as OC1) plays a crucial role in cell fate decision of various precursor cells such as pancreatic or neural cells, as well as in hepatoblasts. HNF6 is expressed in hepatoblasts, hepatocytes and cholangiocytes, and can be considered as a key element in the differentiation network. Indeed, in the absence of HNF6 periportal hepatoblasts give rise to cyst-like structures presenting with a hybrid hepatobiliary phenotype, meaning that they express both hepatoblast/hepatocyte and cholangiocyte markers (Clotman et al., 2002). In the absence of its paralog OC2, which is partially redundant to HNF6, a similar but milder phenotype is observed (Clotman et al., 2005). However, in knockout mice for both HNF6 and OC2, the phenotype is dramatically

increased since hybrid cells are not only observed in the vicinity of the portal vein but throughout the liver parenchyma (Clotman et al., 2005).

**Hhex.** Livers depleted in the transcription factor Hhex also display hybrid cells positive for both hepatocyte and biliary features, and are associated with a decrease of HNF6 expression (Hunter et al., 2007).

**C/EBPα, Tbx3 and Prox1.** C/EBPα is expressed in hepatoblasts and hepatocytes and must be repressed in developing cholangiocytes in order to allow biliary differentiation (Shiojiri et al., 2004). However, appropriate levels of C/EBPα are required since its liver-specific inactivation again leads to hybrid cells development in the liver parenchyma (Yamasaki et al., 2006). Interestingly, in this case, the observed phenotype is associated with overexpression of HNF6, which is in accordance with the fact that C/EBPα can directly bind to the HNF6 promoter and inhibit its transcription (Rastegar et al., 2000). Moreover, in Tbx3-deficient mice, C/EBPα expression is repressed while HNF6 expression increases, resulting in enhanced biliary commitment (Ludtke et al., 2009). Similarly, in Prox1-deleted livers, biliary differentiation is promoted at the expense of hepatocyte differentiation as shown by the increase in SOX9-positive cells and the lower abundance of HNF4α-positive cells in the liver parenchyma (Seth et al., 2014). In addition, the loss of Tbx3 affects Prox1 expression while Tbx3 expression is maintained in Prox1 knockout livers and thus suggests that Tbx3 is upstream of Prox1 (Ludtke et al., 2009; Seth et al., 2014). Altogether, these data suggest that Hhex, C/EBPα, Tbx3 and Prox1 form a network that tightly regulates HNF6 expression in order to allow proper hepatobiliary segregation.

**SOX4 and SOX9.** As SOX9, SOX4 is expressed in biliary cells since the onset of biliary development (E12.5). In normal condition, SOX9 is specific to developing biliary cells, but SOX4 is also expressed in the portal mesenchyme and in rare parenchymal cells during liver development (Poncy et al., 2015). SOX4 and SOX9 both control cholangiocyte differentiation. Indeed, following liver-specific deletion of SOX4 or SOX9, cholangiocyte precursors at the time of lineage segregation express low levels of biliary markers, and show persistent expression of HNF4α. This phenotype is exacerbated after combined

deletion of SOX4 and SOX9. This suggests that SOX4 and SOX9 cooperatively regulate biliary commitment (Antoniou et al., 2009; Poncy et al., 2015). Since SOX9 expression is decreased inHNF6 knockout livers, HNF6 is thought to be upstream of SOX9 (Antoniou et al., 2009). Beyond the stage of lineage segregation, maturation of ducts is delayed or inhibited (see below).

**FoxM1B, Sall4 and C/EBPβ.** Finally, a few others transcription factors have been identified as regulators of the cell fate decision step. FoxM1B is critical for hepatoblasts differentiation toward biliary cells (Krupczak-Hollis et al., 2004), while *in vitro* overexpression of Sall4 in purified hepatoblasts enhances the expression of cholangiocyte markers and inhibits the expression of hepatocyte markers (Oikawa et al., 2009). Finally, while C/EBPα has been shown to promote hepatocyte differentiation, C/EBPβ exhibits the opposite effect by inducing biliary differentiation in hepatoblasts generated from human embryonic stem cells (hESCs) (Takayama et al., 2014).

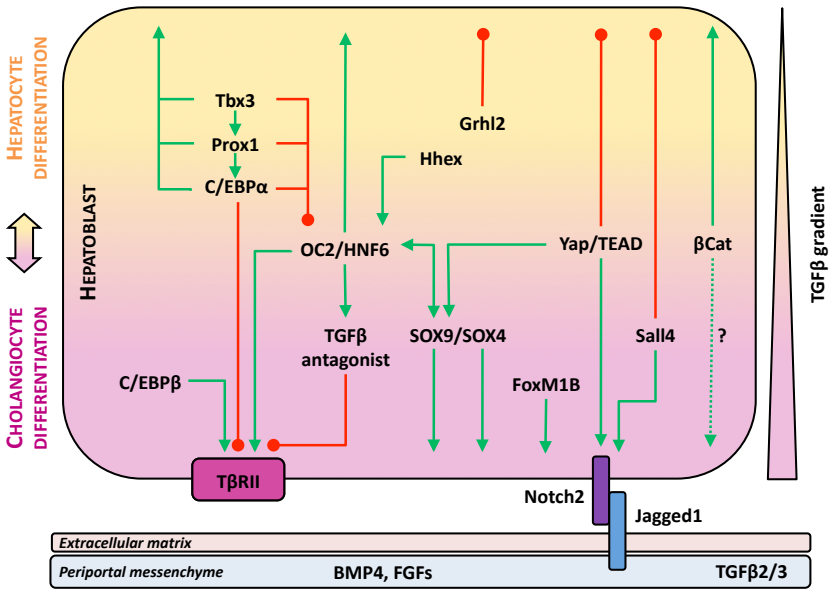



**Figure 4. Schematic overview of the major regulators of lineage cell commitment.** Transcription factors and extracellular cues participating in the hepatobiliary segregation network are illustrated. *Green arrows*, stimulation; *red dots*, repression.

### *2.2.3.* SIGNALING PATHWAYS CONTROLLING LINEAGE SEGREGATION

**TGFβ.** Several signaling pathways have been described as important contributors to hepatobiliary segregation (Figure 4). Among them, the TGFβ signaling pathway is a strong activator of biliary fate commitment. Indeed, the biliary program is initiated in E12.5 liver explants or hESCs-derived hepatoblasts upon treatment with TGFβ/Activin (Clotman et al., 2005; Takayama et al., 2014). Inversely, injecting pregnant mice with anti-TGFβ neutralizing antibodies prevents biliary differentiation in the foetal livers (Clotman et al., 2005). The TGFβ ligands TGFβ2 and TGFβ3 are abundantly expressed by the periportal mesenchyme, namely in cells adjacent to hepatoblasts that differentiate to cholangiocytes (Antoniou et al., 2009). TGFβ signaling occurs as a gradient extending from the portal vein to the liver parenchyma. Experiments using mice harbouring a TGFβ-responsive green fluorescent protein (GFP) reporter showed high signaling activity near the portal vein, where hepatoblasts commit to cholangiocytes, and progressively decreasing TGFβ activity progressing into the parenchyma, where hepatoblasts differentiate to hepatocytes (Clotman et al., 2005). The dynamics of TGFβ signaling implies accurate regulation of the pathway to prevent wrong cell fate commitment. Indeed, the severe biliary phenotype observed in HNF6 and HNF6/OC2 knockout mice results from an excess of TGFβ signaling in the liver parenchyma: in the absence of Onecut factors, high TGFβ signaling extends further in the parenchyma and superimposes a biliary differentiation program on developing hepatocytes, thereby generating hybrid hepatobiliary cells (Clotman et al., 2005). This indicates that HNF6 and OC2 are required to determine the slope of the TGFβ gradient, most likely by stimulating the expression of the TGFβ receptor type II (TβRII) as well as α2-macroglobulin and follistatin, two Activin/TGFβ repressors (Clotman et al., 2005; Plumb-Rudewiez et al., 2004). Finally, it has recently been shown that the transcription factors C/EBPα and C/EBPβ are fine-tuners of TGFβ signaling. Their opposite effect on hepatoblasts differentiation (see above) can be explained by their regulation of TβRII expression: C/EBPα and C/EBPβ bind to the same sites of the TβRII promoter, but they respectively repress or activate its transcription (Takayama et al., 2014).

**Notch.** Mutations in the human Notch ligand Jagged1 (Jag1) or in the Notch2 receptor genes cause Alagille syndrome, which is characterized by bile duct paucity and cholestasis (Li et al., 1997; McDaniell et al., 2006; Oda et al., 1997). Consequently, involvement of Notch signaling in biliary development has been widely studied. Notch signaling requires cell-to-cell contact. Since cholangiocytes develop around the portal vein, Notch ligand-expressing cells are assumed to be located in adjacent cells. Indeed, Jag1 is expressed in the portal endothelium and the portal mesenchyme and later in bile ducts, while Notch1 and Notch2 are expressed in hepatoblasts (Kodama et al., 2004; Tanimizu and Miyajima, 2004; Zong et al., 2009). *In vitro* gain- and loss-of-function experiments on purified hepatoblasts demonstrated that Notch activation favours biliary fate at the expense of hepatocyte differentiation (Tanimizu and Miyajima, 2004). This was further validated *in vivo*. Early deletion of RBPJκ, a key transcriptional effector of Notch signaling, leads to a strong reduction in the number of biliary cells and eventually to their complete loss in the liver parenchyma (Zong et al., 2009). Moreover, deletion of mesenchymal Jag1 strongly reduces the number of SOX9-positive cells in the liver parenchyma (Hofmann et al., 2010). Along the same lines, loss of Jag1 or Notch2 in zebrafish larvae is associated with a disruption of biliary development and hybrid cells exhibiting both biliary and hepatocyte features are detected in the liver. Similar results were obtained when growing the larvae in the presence of a Notch inhibitor (Lorent et al., 2010; Lorent et al., 2004). Conversely, mice overexpressing Notch intracellular domain (NICD) show increased cholangiocyte differentiation, even ectopically in the liver parenchyma (Jeliazkova et al., 2013; Tchorz et al., 2009; Zong et al., 2009). Further, enhanced biliary commitment observed in Sall4 overexpressing hepatoblasts is associated with Notch1/2 and Jag1 upregulation, thereby suggesting that Sall4 acts via Notch signaling (Oikawa et al., 2009). Together, these data highlight the role of the Notch pathway in the regulation of embryonic biliary fate (Figure 4).

**Wnt.** Wnt signaling has also been investigated and its involvement in hepatobiliary segregation is still highly controversial. Wnt signaling was long considered as a stimulator of biliary differentiation: inactivation of Wnt signaling by ablation of β-catenin (βcat), its

downstream effector, strongly reduces biliary commitment, whereas stabilisation of the pathway leads to the opposite effect and represses hepatocyte differentiation (Decaens et al., 2008; Tan et al., 2008). Nevertheless, our lab has recently reinvestigated the phenotype of βcat deleted-livers and only partly confirmed the previous data: mutant mice showed hepatocyte differentiation defect but cholangiocyte differentiation was not impaired, suggesting that Wnt/βcat is required for hepatocyte commitment but is dispensable for biliary fate commitment (Cordi et al., 2016). Wnt ligands activating the canonical pathway that repress hepatocyte development remain unknown. However, the non-canonical Wnt5a induces a calmodulin-dependent pathway that blocks biliary fate and duct morphogenesis (Kiyohashi et al., 2013). Therefore, Wnt signaling needs to be considered keeping in mind that the signaling pathway downstream of the receptor will determine the exact function of the ligand.

**Hippo.** The Hippo/Yap pathway also influences liver cell fate. The Hippo pathway consists in cascades of protein kinases leading to the phosphorylation, cytoplasmic sequestration and degradation of Yes-associated protein (Yap). Inactivation of the Hippo pathway conversely results in Yap translocation to the nucleus where it exerts transcriptional activity by interacting with TEA domain (TEAD) transcription factor. Cholangiocytes express high levels of nuclear Yap while Yap is mainly detected in the cytoplasm of hepatocytes (Yimlamai et al., 2014). Moreover, liver-specific inactivation of Yap reduces the number of biliary cells (Zhang et al., 2010), while Yap overexpression stimulates acquisition of biliary features such as SOX9 expression and stimulates the cholangiocyte-inducing pathways TGFβ and Notch (Yimlamai et al., 2014). Since combined deletion of RBPJκ and Yap constitutive overexpression partially rescue the phenotype, Yap is likely to be upstream of Notch (Yimlamai et al., 2014). Taken together, these results underline the participation of Yap in biliary fate stimulation (Figure 4).

**FGF, BMP and extracellular matrix components.** Finally, other signaling pathways such as FGF, BMP and extracellular matrix (ECM) components have a role in liver cells differentiation (Figure 4). In chick embryos, some FGF receptors are specifically expressed in biliary cells. Moreover, chick liver explants cultured in presence of FGF upregulate

biliary markers, thereby suggesting that FGF promotes cholangiocyte differentiation. Finally, FGF synergizes with BMP4 and ECM components such as type IV collagen and laminin during biliary commitment (Yanai et al., 2008).

Interestingly, committed hepatocytes and cholangiocytes maintain some plasticity during fetal life and after birth. Indeed, cholangiocytes initially line up around the branches of the portal vein and only part of the initial cholangiocytes contributes to duct formation, while the others revert to a hepatocyte phenotype and differentiate as periportal hepatocytes (Carpentier et al., 2011). The mechanisms driving this cell fate reallocation are unknown. In addition, overexpression of Notch in mature hepatocytes is sufficient to reprogram cells toward cholangiocytes (Jeliazkova et al., 2013; Tchorz et al., 2009; Zong et al., 2009). Furthermore, constitutive Yap activation in hepatocytes silences the hepatocytic phenotype and induces gradual acquisition of biliary features, probably by acting on Notch signaling (Yimlamai et al., 2014). Regarding biliary cells, *in vitro* experiments on purified cholangiocytes demonstrated that cell plasticity is, at least in part, controlled by Grainyhead-like (Grhl) 2. Indeed, in neonatal cholangiocytes cultured in a medium that stimulates hepatocyte differentiation low Grhl2 expression maintains the cells in a state that permits transdifferentiation to hepatocytes. In contrast, high Grhl2 level in adult cholangiocytes prevents lineage reconversion upon hepatocytic stimulation (Tanimizu et al., 2013).

Taken together, these results point out the crucial need of tight regulation of each component of the cell fate-determining network. Indeed, misexpression of a single element can critically affect the hepatobiliary balance and consequently induce abnormal cell fate allocation.

## 2.3. Hepatocyte development

Once committed to the cholangiocyte or hepatocyte lineage, hepatic cells undergo a maturation process that consists in the progressive acquisition of lineage-specific gene expression profiles, morphological features and the full range of physiological functions.

Such maturation occurs throughout embryonic development and is continued during the neonatal period (Jochheim et al., 2003; Petkov et al., 2004). Hepatocyte and cholangiocyte maturation will be described below and in chapter 2.4 respectively.

### *2.3.1.* HEPATOCYTE MATURATION AND MORPHOGENESIS

Hepatoblasts that differentiate toward the hepatocyte lineage gradually organise as cord-like structures in the liver parenchyma. Hepatocyte polarization is a crucial step in this process since each pole of the cell is in contact with a different environment and deals with different functions. Hepatocyte cords consist of a single cell layer. Therefore, hepatocytes have two opposing basal surfaces that are separated from the fenestrated sinusoidal cells and blood by the space of Disse (Figure 5). Moreover, hepatocytes form a branching network of bile canaliculi that drain the secreted bile to the bile ducts. This network is formed by small apical domains at the lateral membrane of two adjacent hepatocytes and is unique to the liver (Figure 5) (Treyer and Musch, 2013; Tsukita et al., 2001). Acquisition and maintenance of hepatic polarity are strictly controlled by Par1b, which induces asymmetric inheritance of the plasma membrane domains through regulation of the mitotic spindle orientation (Slim et al., 2013). Moreover, tight junctions maintain hepatic polarity by creating a strong blood-bile barrier (Figure 5).

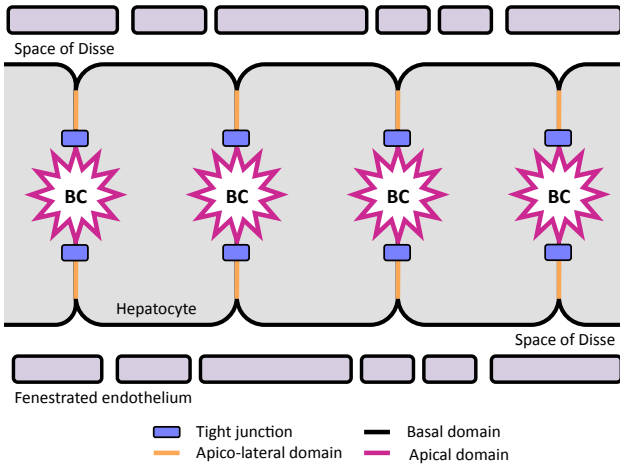



**Figure 5. Hepatocyte polarisation and cord-like organisation**. Hepatocytes are separated from blood by their two basal poles while bile canaliculi are formed by the apical pole of two adjacent cells. Tight junctions maintain cell integrity. *BC*, Bile canaliculi.

Although all hepatocytes appear similar when visualised by microscopy, their maturation status differs according to their location within the hepatic lobule. Indeed, hepatocytes located close to the central vein express different gene sets and exert different metabolic functions than periportal ones. This phenomenon is called liver zonation and takes place during the perinatal period (Gebhardt et al., 2007; Torre et al., 2011). The porto-central gradient in gene expression generates compartments that allow the liver to perform inverse metabolic functions such as gluconeogenesis and glycolysis within the same organ. As a consequence, each hepatocyte performs metabolic functions depending on its location along the periportal to pericentral axis (Torre et al., 2011). Liver zonation is regulated by a gradient of Wnt/β-catenin signaling that inversely controls the perivenous and periportal genetic programs (Torre et al., 2011).

### 2.3.2. TRANSCRIPTIONAL CONTROL OF HEPATOCYTE MATURATION

Hepatocyte-specific genes driving hepatocyte maturation in the embryo are tightly regulated by a complex and dynamic network of transcription factors referred to as liver-enriched transcription factors (LETFs). LETFs comprise 12 main members that are first expressed at low levels in hepatoblasts and that progressively raise when the latter differentiate to hepatocytes. Moreover, LETFs form a highly interconnected circuitry ruled by autoregulatory and cross-regulatory loops (Kyrmizi et al., 2006; Odom et al., 2006; Odom et al., 2004). Analysis of temporal and spatial expression patterns of LETFs during liver embryogenesis reveals a gradual increase in the number of interactions and in the complexity of these regulatory loops that leads to the stabilisation of the LETFs network (Kyrmizi et al., 2006). Within this network, a "core" of 6 transcription factors (HNF4α, HNF1α, HNF1β, HNF6, FoxA2 and Liver receptor homolog [LRH] 1) which occupy each other's regulatory regions and that of peripheral LETFs has been identified by Kyrmizi and coworkers (Kyrmizi et al., 2006) (Figure 6A).

Interestingly, these core factors synergistically and interdependently cooperate with coactivators in order to control the expression of common target genes (Beaudry et al., 2006). For example, HNF6 is involved in two cases of "synergistic interdependence". First,

HNF6 and HNF4α both require each other and need the recruitment of the coactivator PGC1α to stimulate the expression of the glucose-6-phosphatase (G6pc) gene, which catalyses the final step of gluconeogenesis. Second, a similar phenomenon occurs between HNF6 and C/EBPα, which synergise to recruit the CREB binding protein (CBP) coactivator, thereby regulating gluconeogenesis by stimulating FoxA2 expression (Yoshida et al., 2006). Finally, it has recently been demonstrated that Hippo signaling allows HNF4α and FoxA2 enhancer switching during liver development, thereby enabling them to fulfil distinct roles in a differentiation-dependent manner. Indeed, Yap and TEAD2 enhance the expression of embryonic genes by binding to regulatory regions co-occupied by HNF4α and FoxA2 (Alder et al., 2014). Importantly, threshold levels must be reached for synergistic interdependence to occur. Altogether, these processes enable stage-specific activation of hepatocyte-specific genes (Figure 6B).

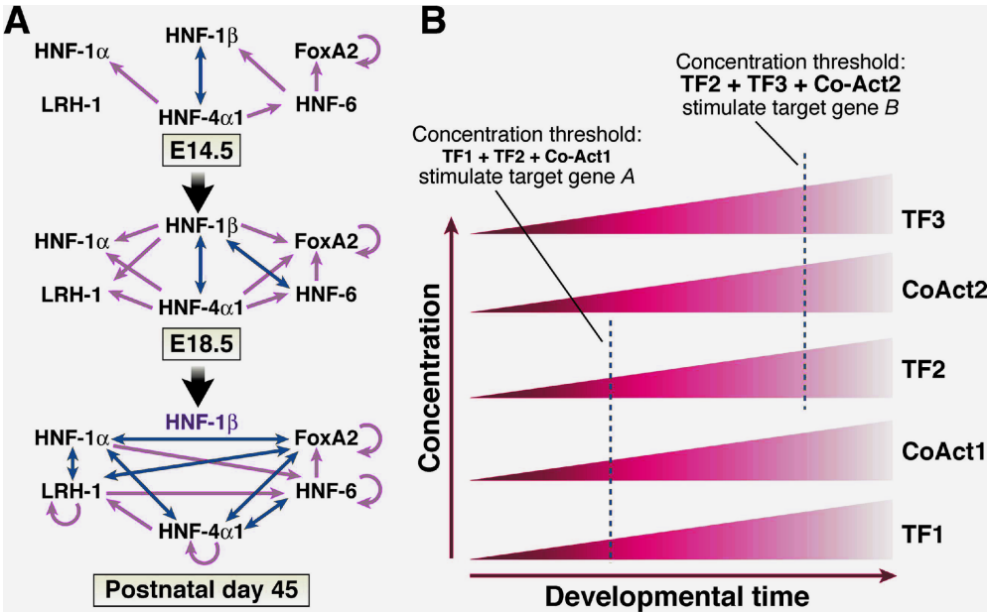



**Figure 6. Dynamic organisation of the liver-enriched transcription factors (LETFs) network controlling hepatocyte maturation** (adapted from Lemaigre et al., 2009). **(A)** Increased number of interactions among core LETFs during embryogenesis and in the adult. *Purple arrows*, unidirectional regulations; *blue double arrows*, reciprocal interactions. (B) Model of time-specific gene activation during liver development. The concentration of 3 transcription factors (TF) and 2 coactivators

(CoAct) increases throughout development. Stimulation of hepatocyte-specific genes A and B at specific time points occurs when the threshold concentration is reached.

The role of core LETFs in the establishment and maintenance of hepatocyte functions has been proven *in vitro* and in *vivo* by several studies using knockout mice:

**HNF4α.** HNF4α is crucial for acquisition and stabilisation of the core LETFs network during embryogenesis since its removal decreases the expression of all the other LETFs (DeLaForest et al., 2011; Kyrmizi et al., 2006). The function of HNF4α has been studied by inactivating its gene at several stages of development. Inactivation of HNF4α at the earliest stage of liver development is associated with early repression of hepatocyte genes: hepatocyte metabolic proteins, serum markers and apolipoptroteins are strongly downregulated (Li et al., 2000). Deletion of HNF4α in E15.5 hepatocytes results in impaired glycogen storage and decreased levels of genes involved in gluconeogenesis such as G6pc (Parviz et al., 2003). In addition, when deleted postnatally, the lack of HNF4α leads to abnormal lipids accumulation, reduced cholesterol levels and increased plasmatic concentration of bile acids (Hayhurst et al., 2001). HNF4α is also required for conferring epithelial character and polarity to hepatocytes. Indeed, in the absence of HNF4α, hepatocytes are small, rounded and fail to organise as cords, in part because they lack numerous genes involved in cell junction assembly and cell adhesion (Battle et al., 2006; Parviz et al., 2003). Finally, HNF4α suppresses expression of pericentral proteins in periportal hepatocytes and is therefore implicated in the establishment of the porto-central zonation (Stanulovic et al., 2007). Together, these data indicate that HNF4α is critical for hepatocyte maturation, function and morphogenesis.

**HNF1α and HNF1β.** HNF1α and HNF1β are the two members of the HNF1 family. Although they share identical DNA binding domains, they have distinct transcriptional activities (Schrem et al., 2002). While HNF1β-null embryos die at E7.5, HNF1α-null mice are viable and their livers develop normally, suggesting that HNF1α is not essential for liver development (Coffinier et al., 1999; Pontoglio et al., 1996). However, its absence is associated with partial reduction of Alb and α1-antitrypsin as well as a complete loss of the phenylalanine hydroxylase, an enzyme involved in the catabolism of amino acids

(Pontoglio et al., 1996). Survival of Hnf1α-null embryos likely reflects functional redundancy between HNF1α and HNF1β during hepatogenesis. Besides its role during hepatic specification, HNF1β is also implicated in the regulation of hepatocyte maturation. Indeed, HNF1β-depleted livers have defective fatty acids oxidation, hypercholesterolemia and perturbed bile acids sensing (Coffinier et al., 2002).

**HNF6.** In addition to its participation in hepatobiliary segregation, HNF6 regulates hepatocyte maturation. *In vitro* studies demonstrated that HNF6 stimulates G6pc expression (as mentioned above), partially mediates the effect of growth hormones and inhibits the glucocorticoid-induced enzymes 6-phosphofructo-2-kinase (PFK2) and phosphoenolpyruvate carboxykinase (PEPCK), two key enzymes of glucose metabolism (Beaudry et al., 2006; Lahuna et al., 2000; Pierreux et al., 1999). Moreover, *in vivo* studies on mice with bile duct ligation demonstrated that HNF6 regulates genes essential for bile acid synthesis and cholesterol catabolism, notably by directly inducing the expression of the cholesterol 7-α hydroxylase (CYP7A1), a rate-limiting enzyme involved in the conversion of cholesterol to bile acids (Wang et al., 2004).

**FoxA2.** Patients suffering from cholestatic syndromes, which are characterized by abnormal bile accumulation, present with a dramatic decrease in FoxA2 gene expression. In mice, deletion of FoxA2 in hepatocytes provides similar phenotype, which is mainly due to a drastic diminution of bile acid transporters and bile acid modifying enzymes (Bochkis et al., 2008). Moreover, FoxA2 deficient livers reveal that it controls gluconeogenesis during fasting by promoting the expression of PEPCK and insulin-like growth factor binding protein (IGFBP) 1 (Zhang et al., 2005).

**LRH1.** LRH1 belongs to the nuclear hormone receptor family. It is considered as an orphan nuclear receptor with an unknown regulatory hormone. However, recent evidences suggest that it could binds to phosphatidylinositols (Sablin et al., 2015). LRH1 controls bile acid metabolism by regulating CYP7A1. Moreover, mice with partially deleted LRH1 livers display hypercholesterolemia (Pare et al., 2004).

**C/EBPα and C/EBPβ.** Members of the C/EBP family do not belong to the core LETFs but deserve to be mentioned since they are important metabolic regulators (Lekstrom-Himes and Xanthopoulos, 1998). On one hand, C/EBPα knockout mice die soon after birth because of hypoglycaemia and dramatically low glycogen stores. This is notably due to the lack of stimulation of glycogen synthase, PEPCK and G6pc. Moreover, hepatocytes fail to accumulate lipids in these mice (Wang et al., 1995). On the other hand, a subset of C/EBPβ knockout mice also die shortly after birth and present with low levels of PEPCK, suggesting the involvement of C/EBPβ in gluconeogenic pathways (Croniger et al., 1997). Therefore, in spite of their opposite effect on lineage commitment during hepatobiliary segregation, C/EBPα and C/EBPβ share similar functions during hepatocyte maturation as being potent regulators of glucose and glycogen metabolism, as well as lipid homeostasis.

All the transcription factors described above are members of the LETFs network and are modulators of prenatal hepatocyte development. In adult hepatocytes, this complex network expands and integrates numerous additional transcription factors such as the Peroxisome Proliferator Activated receptors (PPARs) or the Sterol Regulatory Element-Binding Protein 1 (SREBP1), which control a wide set of metabolic functions. These additional transcription factors are often sensitive to hormonal, metabolic and xenobiotic signals (Locker, 2011).

### 2.3.3. SIGNALING PATHWAYS CONTROLLING HEPATOCYTE MATURATION

Several signaling pathways have been found to promote hepatocyte maturation. Hematopoiesis takes place in the liver during the embryogenesis, and hepatocytes are in close contact with hematopoietic cells in the developing liver. Hematopoietic cells secrete Oncostatin M (OSM), an Interleukin-6 family protein that signals through the glycoprotein (gp) 130 receptor, which is expressed at the hepatocyte membrane (Kamiya et al., 1999; Kinoshita et al., 1999). Upon OSM binding, gp130 induces a signaling cascade mediated by Signal Transducer and Activator of Transcription (STAT) 3 and thereby induces morphological changes as well as expression of hepatocyte metabolic genes such as the G6pc (Ito et al., 2000; Suzuki, 2003). However, other cytokines are expected to have

similar roles, since OSM receptor null-mice do not display hepatocyte defects (Tanaka et al., 2003). In addition, HGF and Wnt9a ligands, which are both expressed by the sinusoidal cells, regulate hepatocyte cord formation and stimulate glycogen accumulation (Matsumoto et al., 2008; Suzuki et al., 2006).

## 2.4. Intrahepatic biliary tract development

Hepatoblasts committed to cholangiocyte lineage undergo a progressive maturation process governed by morphological and differentiational cues that generate fully functional bile ducts draining and modifying the bile released at the apical surface of hepatocytes. Bile secretion is essential for fat emulsification and is transported through a network of intrahepatic ducts into the extrahepatic tract, the latter consisting of hepatic and cystic ducts, the gallbladder and the common bile duct. Despite their similar functionalities, extrahepatic and intrahepatic ducts do not share a common embryonic origin: intrahepatic cholangiocytes arise from hepatoblasts, while extrahepatic cholangiocytes develop from pancreatobiliary precursors located in portion of the endoderm that is posterior to the prehepatic endoderm (Si-Tayeb et al., 2010). In this section we will focus on intrahepatic duct maturation.

### 2.4.1. Morphogenesis of the intrahepatic biliary tree

Intrahepatic bile ducts development starts around E11.5 with the appearance of SOX9 positive cells in the vicinity of the portal vein (Antoniou et al., 2009). Progressively, an increasing number of hepatoblasts differentiate to SOX9-positive cholangiocytes and form a near continuous monolayered ring called "ductal plate" that surrounds the portal vein (Figure 7A). From that stage onward, the ductal plate undergoes sequential morphological changes leading to mature bile ducts at birth. Around E15.5, bilayered structures defining a lumen are detected at focal points of the ductal plate. These structures are called "primitive ductal structures (PDS)" and mark the onset of tubulogenesis, which is characterized by a transient asymmetry. Indeed, cells on the portal side of the PDS express typical biliary markers such as SOX9, Cytokeratin (CK) 19, Osteopontin (OPN) and high

levels of E-cadherin (E-cad), and repress HNF4α expression. On the contrary, cells on the parenchymal side are SOX9-negative and express HNF4α as well as low levels of E-cad (Figure 7B). This asymmetry is transient since hepatoblasts on the parenchymal side undergo a radial and progressive differentiation to biliary cells (Antoniou et al., 2009) (Figure 7C). In parallel to tubulogenesis, the periportal mesenchyme and the ECM progressively surround the forming bile ducts. In mice, ductal plate cells not involved in bile duct formation reorient their fate and give rise to periportal hepatocytes or adult liver progenitor cells (Carpentier et al., 2011). Finally, biliary tubulogenesis progresses according to a hilum-to-periphery axis in the liver lobes. As a consequence, during embryonic development mature ducts exhibiting radial symmetry are first seen near the hilum, while asymmetrical ductal structures are still detectable at the periphery. In adults, the ducts display a mature morphology throughout the lobes (Raynaud et al., 2011; Van Eyken et al., 1988).

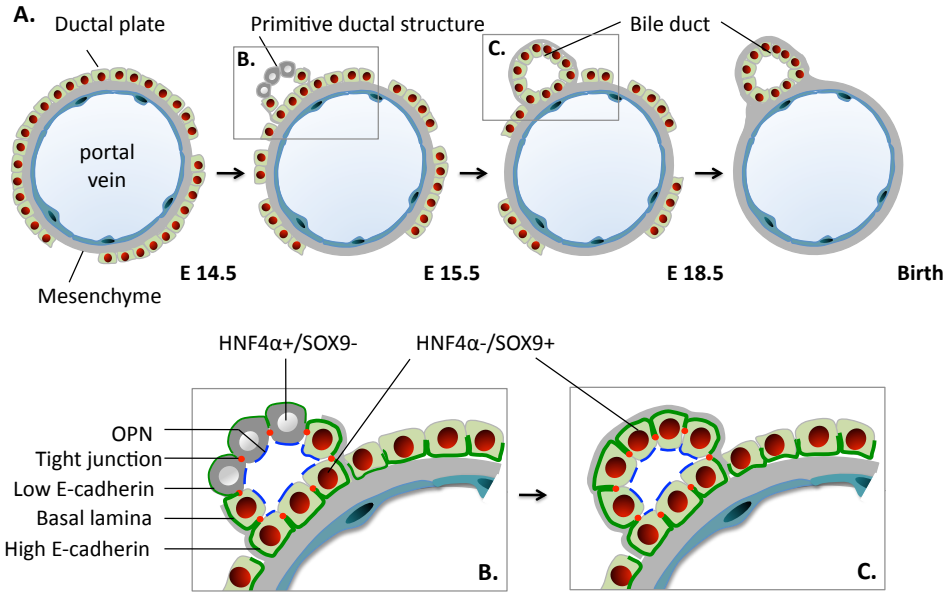



**Figure 7. Schematic representation of intrahepatic bile ducts morphogenesis** (adapted from Lemaigre et al., 2010). **(A)** Representation of the chronological events driving ducts tubulogenesis. **(B and C)** Magnification of boxed biliary structures.Genes expression at E15.5 (asymetrical structure) and E18.5 (symmetrical structure) are represented.

Concomitantly to bile duct formation, biliary cells gradually acquire cell polarity. Mature biliary cells exhibit an apico-basal polarity defined by an apical surface lining the lumen and a basal surface in close contact with the ECM. Polarisation of ductal cells starts early since OPN expression is already detected at the apical pole of all E15.5 PDS cells, including the HNF4α-positive cells (Antoniou et al., 2009) (Figure 7B).

Recently, Takashima and his team brought new insights into biliary morphogenesis (Takashima et al., 2015). Combining biliary labelling with *in silico* image analysis, they generated a three-dimensional (3D) spatiotemporal reconstruction of bile duct morphogenesis, and further refined the description of the tubulogenic process previously derived from 2D liver sections analysis. Indeed, their model proposes that bile duct maturation is fragmented and occurs from an increasing number of duct segments along the portal vein, which progressively connect to each other and to larger ducts, thereby generating the biliary tree. After birth, the number of duct segments and branches decreases, while the diameter of the remaining structures enlarges (Figure 8).

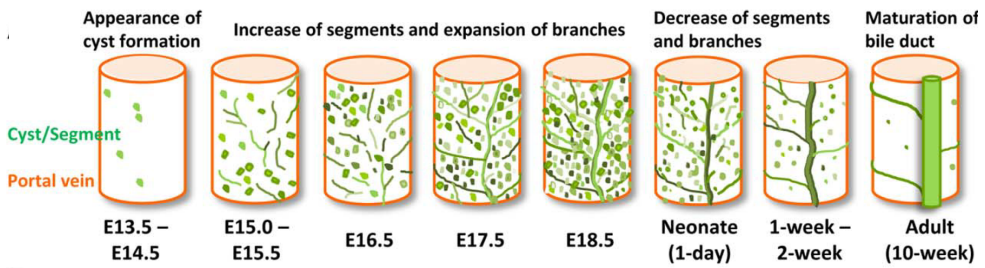



**Figure 8. Proposed mechanism for bile duct maturation** (from Takashima et al., 2015). Model of tubulogenesis in which bile duct maturation occurs by interconnection of small duct segments. Numerous duct segments as well as segment interconnections continuously increase until birth before involuting. The remaining ducts then enlarge.

### 2.4.2. TRANSCRIPTIONAL CONTROL OF BILE DUCT DEVELOPMENT

**SOX4 and SOX9.** Studies of livers depleted in SOX4 and/or SOX9 revealed that these two factors exert a pleiotropic regulation of bile duct maturation. First, SOX4 and SOX9 control the timing of bile duct morphogenesis since single deletion of SOX9 or SOX4 is characterised by the prolonged presence of asymmetrical PDS (Antoniou et al., 2009;

Poncy et al., 2015). Importantly, combined inactivation of SOX4 and SOX9 impairs intrahepatic duct formation, leading to cholestasis and portal fibrosis (Poncy et al., 2015). Second, SOX4 and SOX9 are required to establish apico-basal polarity. Indeed, SOX9-deleted livers transiently delay the appearance of apical markers such as OPN, while SOX4-deleted livers have prolonged absence of polarity markers and irregular cobblestone-like shaped biliary cells. Again, polarity defects is exacerbated in double-SOX-deleted livers since cell morphology is strongly perturbed and apical polarity markers are no longer detected (Poncy et al., 2015). Finally, SOX4 and SOX9 control signaling pathways involved in biliary development (see below in chapter *2.4.3*). Taken together, these data demonstrate that SOX9 and SOX4 cooperatively control cholangiocyte morphogenesis.

**HNF6 and HNF1β.** As described previously, HNF6 and HNF1β are members of the core LETFs and are thus expressed in developing hepatocytes. However, HNF6 and HNF1β were also among the first factors identified as regulators of bile ducts morphogenesis, cells in which they are expressed at higher levels than in hepatocytes. The absence of either factor results in very similar phenotypes characterized by ductal plate persistence and cyst-like biliary structures of variable size. Such cyst-like structures never incorporate into periportal mesenchyme and eventually collapse, therefore resulting in bile duct paucity at birth (Clotman et al., 2002; Coffinier et al., 2002). Accordingly, patients with heterozygous mutations in HNF1β display bile duct paucity (Roelandt et al., 2012). Finally, HNF6-depleted livers are associated with a transient lack of HNF1β and *in vitro* experiments demonstrated that HNF6 binds the HNF1β promoter and stimulates its expression (Clotman et al., 2002). Therefore, HNF6 and HNF1β are associated in a transcriptional cascade, explaining why similar morphological defects are seen in HNF6- or HNF1β-deleted livers.

**C/EBPα, Prox1 and Hhex**. C/EBPα knockout mice exhibit pseudoglandular structures that overexpress HNF6 and HNF1β in their liver parenchyma (Yamasaki et al., 2006). Similarly, hyperplastic bile ducts develop prematurely and ectopic bile ducts form in the parenchyma of Prox1-deleted mice. Again, the phenotype is associated with increased levels of HNF6 and HNF1β (Seth et al., 2014). On the other hand, livers specifically deleted

in Hhex also present with cyst-like structures which are, this time, associated with reduced levels of HNF6 and HNF1β (Hunter et al., 2007). Taken together, these results indicate that C/EBPα, Prox1 and Hhex regulate biliary tubulogenesis. In addition, as for hepatobiliary segregation, these data also suggest that HNF6 must be tightly controlled in order to allow proper tubulogenesis, since either an upregulation or a downregulation of the gene is associated with impaired biliary morphogenesis.

Collectively, these data identified a number of transcription factors involved in a transcriptional network regulating intrahepatic bile duct morphogenesis. However, since these factors also play a role during hepatobiliary segregation, it cannot be concluded if their effects on tubulogenesis are direct or result from an earlier defect at the time of cell fate commitment.

#### 2.4.3. SIGNALING PATHWAYS CONTROLLING BILE DUCT MORPHOGENESIS

Several studies addressed the question of extracellular cues regulating bile duct tubulogenesis. Interestingly, signaling pathways that regulate commitment to the cholangiocyte lineage also participate in bile duct morphogenesis.

**TGFβ.** At the onset of biliary commitment, TGFβ signals through its receptor TβRII. TβRII is initially expressed in all ductal plate cells. However, when PDS form, TβRII is no longer detected in biliary cells on the portal side while its expression persists in hepatoblasts of the parenchymal side. In mature ducts, all cholangiocytes are negative for TβRII (Antoniou et al., 2009). This process is most likely controlled by a negative feedback loop in which TGFβ represses its own receptor in cells that have differentiated to cholangiocytes. Indeed, upon TGFβ stimulation, cultured hepatoblasts commit to biliary cells but also repress TβRII expression (Antoniou et al., 2009). Based on these data, a model has been proposed in which TGFβ sequentially induces differentiation of cells on the portal side and then on the parenchymal side of the PDS before repressing its own receptor (Raynaud et al., 2011). Interestingly, delayed PDS maturation observed in livers deleted for SOX4, SOX9 or both SOX factors is associated with abnormal persistence of

TβRII on the portal side. Therefore, SOX factors modulate TGFβ signaling at the onset of PDS maturation (Poncy et al., 2015).

**Notch.** Several loss- and gain-of-function experiments described the role of Notch during cholangiocyte maturation. Liver-specific inactivation of Notch signaling during late stages of biliary development affects tubulogenesis without influencing biliary differentiation. Indeed, mice harbouring Notch2 (Geisler et al., 2008), RBPJκ (Jeliazkova et al., 2013; Zong et al., 2009)or combined Notch2/Jag1 (Lozier et al., 2008) deletion have normal ductal plate formation but suffer from bile duct paucity. Conversely, mice that overexpress Notch exhibit excessive number of bile ducts as well as ectopic tubulogenesis in the liver parenchyma (Jeliazkova et al., 2013; Tchorz et al., 2009; Zong et al., 2009). Interestingly, mice with conditional deletion of Jag1 in portal mesenchyme display bile duct paucity, while conditional deletion of Jag1 in portal endothelium has no impact on tubulogenesis (Hofmann et al., 2010). Therefore, these data reveal that the portal vein mesenchyme is a critical source of Jag1 which is required for proper bile duct morphogenesis.

Despite intense investigation, how Notch signaling promotes biliary development is not well understood yet. Jag1 and Hairy and enhancer of split homolog (Hes) 1, a transcription factor and direct target of Notch signaling, are initially expressed in ductal plate cells and in cells of the portal layer of PDS, and subsequently in cells of the parenchymal layer of PDS, thereby suggesting that Notch signaling is sequentially and radially activated in developing bile ducts (Antoniou et al., 2009; Zong et al., 2009). Thus, Notch could act via Hes1 induction. However, conflicting results about Hes1 were obtained. Indeed, Hes1-null mice do not form bile ducts (Kodama et al., 2004) while livers with specific Hes1 inactivation are devoid of biliary phenotype (Jeliazkova et al., 2013). Therefore, the role of Hes1 in biliary development requires more investigation. SOX9 could mediate Notch effects. Indeed, SOX9 has been identified as a Notch target gene and Notch inactivation is associated with downregulation of SOX9 (Hofmann et al., 2010; Zong et al., 2009). Inversely, the absence of SOX9 and/or SOX4 is associated with abnormally low levels of Hes1 in late-developing cholangiocytes (Poncy et al., 2015).

Finally, combined deletion of HNF6 and RBPJκ during late gestation impairs biliary development and is associated with almost complete loss of SOX9 and HNF1β expression, while single HNF6 or RBPJκ deletion only marginally affects biliary morphogenesis (Vanderpool et al., 2012). Consequently, these results suggest that Notch signaling and HNF6 cooperate by regulating SOX9 and HNF1β.

**Wnt.** Despite its controversial role during hepatic cell commitment, Wnt signaling has been shown to regulate biliary development. *In vivo* analysis with mutant mouse models showed that inactivation of Wnt signaling by ablation of βcat leads to bile ducts paucity (Tan et al., 2008). Inversely, stabilization of β-catenin promotes development of duct-like structures and bile duct hyperplasia (Cordi et al., 2016; Decaens et al., 2008), thereby suggesting that accurate regulation of β-catenin is necessary for proper bile duct development. Moreover, the Wnt non-canonical pathway was shown to inhibit bile duct formation. Indeed, formation of PDS is enhanced in mice harbouring Wnt5a ablation, while *in vitro* addition of Wnt5a inhibits duct-like structures normally formed by hepatoblasts cultured in 3D gels (Kiyohashi et al., 2013).

**Hippo.** Since Yap is upstream of the Notch pathway (see chapter *2.2.4*), it is not surprising that the Hippo pathway is involved in bile duct maturation. Indeed, bile ducts fail to develop in livers with specific deletion of Yap (Zhang et al., 2010), whereas Yap overexpression results in biliary hyperplasia (Yimlamai et al., 2014) and excessive number of tubular structures surrounded by stroma throughout the lobules (Zhang et al., 2010). These results are further supported by the fact that overexpression of a TEAD2-dominant negative mutant reduces Yap-induced biliary hyperplasia (Liu-Chittenden et al., 2012). Interestingly, while TEAD/Yap induces SOX9 expression (see chapter *2.2.3*), SOX4 in turn stimulates TEAD2. Indeed, TEAD2 is low in SOX4 and combined SOX4 and SOX9 knockout mice but not in SOX9 single knockout (Poncy et al., 2015).

**ECM components.** The basal pole of bile ducts is in close contact with the ECM, which is mainly composed of laminin. Among them, laminin α1, which signals through its β1 integrin receptor, is produced by fibroblasts located in the portal mesenchyme and is

essential to establish cholangiocyte apico-basal polarity. Indeed, hepatoblasts grown in 3D gel cultures develop apico-basal polarity and form cysts with a central lumen only in the presence of laminin α1 (Tanimizu et al., 2007). However, laminin α1 is dispensable for cyst maintenance and its function is progressively replaced by the laminin α5, which is expressed by cholangiocytes and also signals through β1 integrin (Tanimizu et al., 2012). Similarly, *in vivo*, laminin α1 is detected around PDS and its expression progressively decreases through time, while laminin α5 is first expressed along the portal side of PDS and later surrounds mature bile ducts. Together, these results suggest that laminin α1 and α5 regulate the sequential events occurring during biliary development. Consistently, laminin α5 deficient livers have reduced number of forming bile ducts despite normal biliary commitment (Tanimizu et al., 2012). In conclusion, laminin α1 is required for apico-basal polarity establishment and PDS initiation, whereas laminin α5 is required for tubulogenesis. Finally, it is interesting to note that a lack of laminin α5, but not α1, is observed in single and double SOX4 and SOX9 knockout mice (Poncy et al., 2015).

## 3. MICRORNAS AND LIVER DEVELOPMENT

Transcription factors and extracellular cues driving liver embryonic development have been widely studied and described above. In addition, microRNAs (miRNAs), which are important regulators of gene expression, also take part in these developmental processes. MiRNAs are key posttranscriptional regulators of gene expression that count no less than 2000 members in the mouse (Griffiths-Jones et al., 2006). These ~20-24 nucleotide-long noncoding RNAs constitute about 1-2% of genes in mammals (Bartel, 2009). Moreover, 60% of protein-coding genes are computationally predicted as miRNA targets (Friedman et al., 2009). MiRNAs and their targets are highly conserved between species, which suggests important functions. Their mode of action and involvement during liver development will be depicted hereafter.

## 3.1. MicroRNAs and gene regulatory networks

MicroRNAs take part in the regulation of almost all biological processes in which they confer robustness, mostly by reinforcing transcriptional programs and attenuating aberrant transcripts (Ebert and Sharp, 2012). Notably, they participate in the regulation of gene regulatory networks.

Gene regulatory networks contain the same type of network motifs among different organisms, thereby suggesting that they constitute important regulatory mechanisms of gene expression (Martinez and Walhout, 2009; Tsang et al., 2007). Feedback and feed-forward loops are common regulatory motifs. Both loop types are subdivided into coherent and incoherent loops. In coherent loops, the parallel paths have the same activatory or inhibitory effect, while in incoherent loops the regulatory paths have opposite effect (Figure 9). Interestingly, miRNAs take part in such regulatory loops:

**Feedback loops.** MiRNAs are known to be involved in feedback loops with transcription factors. Negative coherent feedback loops can lead to bi-stable expression of the miRNA and the transcription factor, and a transient signal can lock the loop into an irreversible state (Martinez and Walhout, 2009). This is the case of miR-223 and nuclear factor 1-A (NF1A) during granulocytic differentiation. NF1A suppresses expression of the primary miR-223 transcript in undifferentiated myeloid precursors. However, during granulocyte differentiation induced by retinoic acid, miR-223 accumulates and represses NF1A, thereby preventing a reversal to the precursor state (Fazi et al., 2005). Positive coherent feedback loops are motifs in which the expression of the miRNA and the transcription factor are amplified. Incoherent feedback loops, can result in oscillatory expression of both motif components. For example, miR-43 and LIN-26 function together in a loop in which LIN-26 stimulates miR-43, which in turn represses LIN-26 (Martinez et al., 2008). Such incoherent feedback loops are thought to fine-tune gene expression and eventually to maintain the steady-state of protein production (Tsang et al., 2007).

**Feed-forward loops.** In feed-forward loops a factor X regulates the expression of a target Z via a direct or indirect path, through a regulator Y (Figure 9). The c-Myc/E2F/miR-17-92 circuit is an example of coherent feed-forward motif. In this circuit, c-Myc activates both E2F and the miR-17-92 cluster, while E2F also stimulates the miRNA cluster. Particularly, this loop is embedded in a more complex circuit since the miR-17-92 cluster

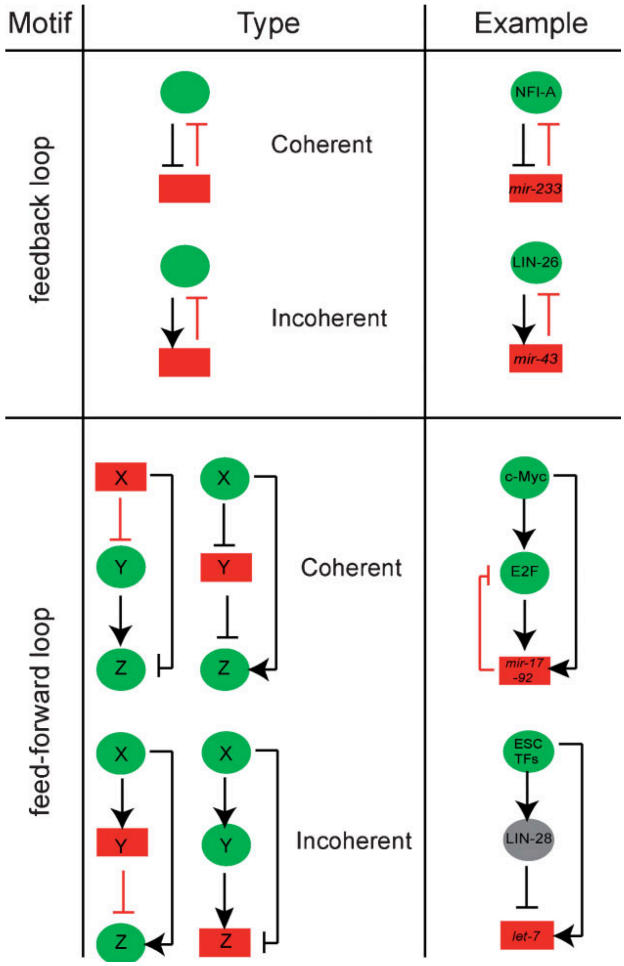



**Figure 9. Coherent and incoherent feedback and feed-forward loop motifs involving transcription factors and microRNAs** (from Martinez and Walhout, 2009). *Green circles*, transcription factors; *red rectangles*, miRNA; *gray circles*, other protein coding genes.

can repress E2F. Therefore, c-Myc induces E2F transcription but also limits its translation through the miRNA cluster, thereby providing a tight regulation of proliferative signals (Tsang et al., 2007). Such coherent feed-forward loops are often used in lineage commitment (Ebert and Sharp, 2012). Finally, incoherent feed-forward loop have been proposed to provide response acceleration upon signal detection (Tsang et al., 2007). For instance, Marson and colleagues have reported that the core embryonic stem cell (ESC) transcription factors, Oct4, Nanog, Sox2 and Tcf3, promote the transcription of let-7 and LIN-28 (Marson et al., 2008). Mature let-7 levels are low in ESC but abundant in differentiated cells. Upon signal detection, LIN-28 repression of let-7 is released and mature let-7 rapidly accumulates. Therefore, this circuit contributes to rapid cellular differentiation of ESCs. Interestingly, it has been proposed that extrinsic noise for a given gene could be reduced by such incoherent feed-forward loops (Ebert and Sharp, 2012). Extrinsic noise refers to variation arising from difference such as transcription factor concentration or cell-cycle stage.

## 3.2. Global impact of microRNAs on liver function

Constitutive loss of Dicer, the enzyme that generates mature miRNA, leads to embryonic lethality at E7.5 (Bernstein et al., 2003). Consequently, mice harbouring hepatocyte-specific inactivation of Dicer have been generated in order to investigate the overall role of miRNAs in the liver.

Adult Dicer knockout livers display impaired glucose and lipid metabolism characterized by steatosis and depletion of glycogen stores (Sekine et al., 2009a), as well as high rates of both proliferation and apoptosis (Hand et al., 2009b). Moreover, loss of Dicer progressively leads to liver damage and inflammation (Hand et al., 2009b), and to reactivation of fetal stage-specific genes such Afp (Sekine et al., 2009a). Finally, one third of the mice develop hepatic tumors after six month and the incidence increases with time (Sekine et al., 2009a). Interestingly, in accordance with the fact that miRNAs are fine-tuners of gene expression, liver zonation is impaired in Dicer-deficient livers. Indeed, the

porto-central gradient is perturbed and periportal genes are diffusely expressed throughout the lobules (Sekine et al., 2009b).

Together, these data suggest that miRNAs are required for normal liver function. However, the above experiments do not discriminate between phenotypic consequences of miRNA depletion or of loss of miRNA-independent Dicer functions. Moreover, there is evidence for Dicer-independent alternative miRNA biogenesis pathways, raising the possibility that single deletion of Dicer is not sufficient to drive complete ablation of mature miRNAs (Cheloufi et al., 2010; Chong et al., 2010; Cifuentes et al., 2010; Yang and Lai, 2011).

## 3.3. Role of specific microRNAs in embryonic liver development

In the above-described liver-specific Dicer knockouts, Dicer deletion only occurs postnatally, therefore preventing analysis of the role of microRNAs during liver embryogenesis. However, targeted approaches addressing the function of specific miRNAs during liver development have been set up. Several miRNAs involved in hepatic cell development have been identified; they are listed below and illustrated in Figure 10.

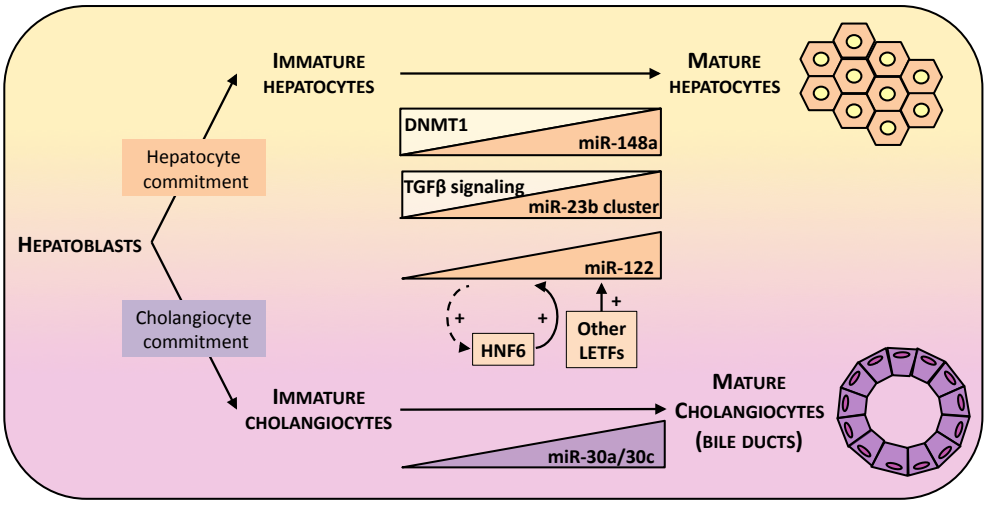



**Figure 10. MicroRNAs involved in hepatic cell development.** Schematic overview of microRNAs and their mode of action on cholangiocyte and hepatocyte development. MiR-148a, the miR-23b cluster

and miR-122 promote hepatocyte maturation while miR-30a and miR-30c promote bile ducts tubulogenesis. Triangles represent increasing or decreasing levels of expression. "+" represents stimulation.

**miR-122.** miR-122 is a liver-specific microRNA that accounts for 70% of the total liver miRNA population (Lagos-Quintana et al., 2002). It is expressed from E12.5 onward and increases until birth (Rogler et al., 2009). Moreover, *in situ* hybridizations showed that at E18.5, its expression is restricted to hepatocytes (Hand et al., 2009a). MiR-122 is controlled by HNF6, which directly binds to its promoter and stimulates its expression. Conversely, miR-122 also induces HNF6 expression via a mechanism that is still unknown, thereby revealing a positive feedback loop between HNF6 and miR-122 (Laudadio et al., 2012). Forced expression of miR-122 in transgenic mice promotes hepatocyte maturation in an HNF6-dependent fashion. Moreover, miR-122 overexpression also induces premature SOX9 expression in the parenchymal side of PDS and transient biliary hyperplasia independently of HNF6 (Laudadio et al., 2012). Interestingly, and accordingly to its role in hepatocyte maturation, several *in vitro* studies demonstrated that other LETFs than HNF6, namely HNF1α, HNF4α, FoxA2, C/EBPα, bind and stimulate the miR-122 promoter, thereby suggesting that miR-122 mediates at least some effects of the hepatocyte transcription network (Deng et al., 2014; Li et al., 2011; Xu et al., 2010). Finally, Tanimizu and his team recently demonstrated that Grhl2 restricts the hepatocytic differentiation potential of adult cholangiocytes by repressing miR-122 expression. Indeed, high Grhl2 levels in adult cholangiocytes prevent *in vitro*-programmed lineage conversion to hepatocytes by negatively regulating the promoter of miR-122 and thereby inhibiting hepatocyte differentiation (Tanimizu et al., 2014).

**miR-23b cluster.** The miR-23b cluster includes three miRNAs, namely miR-23b, miR-27b and miR24-1. At E17.5 its expression is restricted to hepatocytes and its level increases until birth (Rogler et al., 2009). *In vitro* experiments with cultured fetal hepatoblasts indicated that miR-23b cluster represses biliary-specific genes expression by inhibiting Smads, the mediators of the TGFβ signaling pathway. Indeed, in the absence of the miR-23b cluster, hepatocyte maturation proceeds but aberrant overexpression of biliary genes occurs. Conversely, repression of Smads by overexpression of the miR-23b

cluster blocks the formation of duct-like structures by hepatoblasts plated in 3D gels (Rogler et al., 2009). Since the miR-23b cluster influences TGFβ signaling, it is expected to participate in the establishment of the TGFβ gradient observed *in viv*o.

**miR-148a.** During *in vitro*-induced hepatocyte maturation, expression of DNA methyltransferase (DNMT) 1 rapidly decreases while DNMT3a and DNMT3b progressively increases, suggesting that DNMT1 repression is required for proper hepatocyte maturation (Gailhouste et al., 2013). Interestingly, miR-148a expression inversely correlates with DNMT1. Actually, it directly binds to DNMT1 mRNA and represses its expression. In addition, either DNMT1 inhibition or miR-148a overexpression promotes hepatocyte-specific genes expression (Gailhouste et al., 2013). Taken together, these experiments identified miR-148a as a stimulator of hepatocyte maturation.

**miR-30a and miR-30c.** Finally, miR-30a and miR-30c have been identified as regulators of tubulogenesis. In mouse liver, miR-30a and miR-30c are expressed from E12.5 onward. Interestingly, their levels increase until birth but progressively decrease postnatally, namely after completion of bile duct morphogenesis. Moreover, i*n situ* hybridization revealed that they are specifically expressed in biliary cells, and that this biliary expression pattern is conserved in human. That pattern is also conserved in zebrafish, in which miR-30a loss-of-functions experiment leads to impaired biliary morphogenesis characterized by fewer terminal ductules, thereby demonstrating the requirement of miR-30a in bile ducts morphogenesis (Hand et al., 2009a). However, the mode of action of miR-30a and miR-30c remains unclear, even though they were predicted by bioinformatic analyses to modulate the expression of Activin A, a ligand of the TGFβ signaling pathway (Hand et al., 2009a). In conclusion, miR-30a and miR-30c regulate late stages of zebrafish liver development by promoting bile duct morphogenesis; they could exert similar functions in mammalian liver.

## 4. CELL DIFFERENTIATION IN INTRAHEPATIC CHOLANGIOCARCINOMA

Defects in cell differentiation are a major characteristic of cancers. Indeed, tumor cells can re-express embryonic markers, while loss of cell differentiation is associated with poor survival in many cancers, including liver cancers.

Liver cancer is the sixth most frequent cancer and the third leading cause of cancer death worldwide (McGuire, 2016). Liver cancers most frequently arise from one of the two main epithelial cells of the organ, namely hepatocytes and cholangiocytes. Among them, hepatocellular carcinoma (HCC) is the most frequent. It derives from hepatocytes and accounts for about 75% of all liver cancers. Biliary tract tumors are called cholangiocarcinoma (CCA) and account for approximately 10%-20% of liver cancers. In addition, rare types of liver tumors include angiosarcoma and hemangiosarcoma, which originate from the endothelial cells, fibrosarcoma, which arises from mesenchymal cells, and hepatoblastoma, which usually develops in young children.

According to their anatomical location, CCA can be subdivided in three categories: the intrahepatic cholangiocarcinomas (iCCAs), which are located within the liver parenchyma, the perihilar cholangiocarcinomas (pCCAs), which are located outside of the liver but upstream of the cystic duct junction, and finally the distal cholangiocarcinomas (dCCAs), which are located downstream of the cystic duct (Razumilava and Gores, 2013) (Figure 11). The present introductory chapter will be devoted to iCCAs.

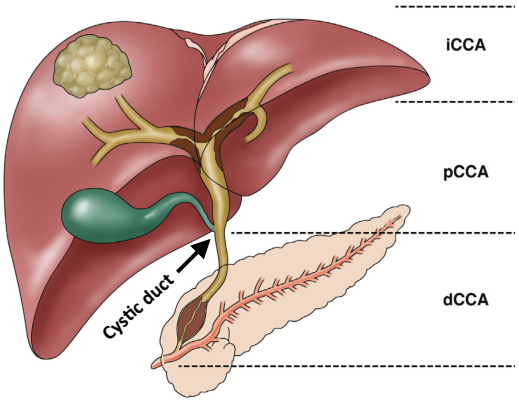



**Figure 11. Anatomical classification of cholangiocarcinomas (CCA)** (from Rivzi et al., 2013). CCAs are classified based on their anatomical location. *iCCA*, intrahepatic cholangiocarcinoma; *pCCA*, perihilar cholangiocarcinoma; *dCCA*, distal cholangiocarcinoma.

## 4.1. General information

### 4.1.1. EPIDEMIOLOGY AND ETIOLOGY OF ICCA

ICCA is the second most common primary liver tumor. It represents only 8% of cholangiocarcinoma cases but in contrast to pCCA and dCCA, which respectively represent 50% and 42% of total CCA cases, its incidence and mortality rates are sharply rising worldwide (Khan et al., 2012; Razumilava and Gores, 2014; Wadsworth et al., 2013). The peak incidence for iCCAs is between 55 and 75 years old (Haga and Patel, 2015), and the global incidence of iCCA varies widely among the different racial and ethnic groups. For instance, incidence can vary from 113 per 100.000 in Thailand to 0,1 per 100.000 in Australia, presumably because of genetic and risk factor diversity (Blechacz and Gores, 2008; Rizvi and Gores, 2013).

The etiology of iCCA remains obscure. However, a number of risk factors have been identified. These include chronic biliary tract inflammation, primary sclerosing cholangitis (PSC), liver cirrhosis, non-alcoholic steatosis, hepatitis B and C, hepatolithiasis and parasite infection such as *Opistorchis viverrini or Clonorchis sinensis* (Blechacz and Gores, 2008; Haga and Patel, 2015). Interestingly, some risk factors are strongly related to geographical location. For example, PSC is the most common predisposing condition for iCCA in Western countries, while iCCA is strongly associated with infection by O*pistorchis viverrini* in Asia (Rizvi and Gores, 2013).

### 4.1.2. PATHOPHYSIOLOGY OF ICCA

The current model of iCCA development proposes that chronic injury of the bile ducts induces cholangiocyte damage, reactive cholangiocytes proliferation, genetic mutations and epigenetic dysregulations, followed by neoplastic transformation (Fava and Lorenzini, 2012). However, emerging evidence suggests that iCCAs can also rise from other cell types than cholangiocytes. Indeed, it seems that iCCAs can derive from adult hepatic progenitor cells, from cells of the canal of Hering, or even from hepatocytes (Komuta et al., 2012; Komuta et al., 2008; Sempoux et al., 2011; Tanaka et al., 2004). Interestingly, two teams

demonstrated that in mice, conversion of hepatocytes into biliary cells was Notch-dependent and leads to iCCAs (Fan et al., 2012; Sekiya and Suzuki, 2012).

Several molecular alterations have been described in iCCA. These include activation and overexpression of growth-promoting factors, inactivation of tumor suppressors, overexpression of anti-apoptotic genes and of genes involved in angiogenesis and cell invasion (Blechacz and Gores, 2008; Braicu, 2009; Sirica et al., 2009).

## 4.2. Diagnosis and management of intrahepatic cholangiocarcinoma

In contrast to dCCA and pCCA, iCCA is clinically silent at early and mid-stages and is therefore often identified incidentally. Indeed, clinical manifestations of iCCA include non-specific symptoms such as abdominal pain, cachexia, fatigue and night sweats. ICCAs frequently present as intrahepatic mass lesions that can be visualised by medical imaging such as magnetic resonance imaging (MRI) or computed tomography (CT). Either MRI or CT are appropriate for evaluation of tumor size, presence of satellite lesions or status of vascular structures, and the results are normally used to plan further treatments. Interestingly, MRI can help to distinguish HCC from iCCA (Rizvi and Gores, 2013).

However, distinguishing iCCAs from hepatic tumors and distant adenocarcinoma can sometimes be challenging and diagnosis based only on clinical imaging may not be enough. Hence, molecular diagnosis using a broad range of serum and bile markers can be used in association with clinical imaging. Among the large variety of biomarkers, serum concentration of carbohydrate antigen 19-9 (CA 19-9) and carcinoembryonic antigen 125 (CA-125) is widely measured. However they are not specific to iCCA and elevated serum levels are found in other gastrointestinal or gynaecological malignancies, as well as in some non-tumor cholangiopathies (Haga and Patel, 2015). A potential solution could be to combine different biomarkers in order to improve sensitivity and specificity of the tests. Thus, there are currently no available biomarkers that can accurately diagnose iCCAs, and a definitive diagnosis therefore always requires analysis of a liver biopsy. For instance, liver biopsies are routinely stained for different cytokeratins in order to discriminate CCAs,

which express CK7 and CK19, from HCCs, which express CK8 and CK18 (Maeda et al., 1995; Moll et al., 1982).

Since an important difficulty when diagnosing iCCA is to distinguish iCCA from other liver pathologies or cancers, the use of miRNA signatures has been considered. For instance, distinct miRNA signatures have been shown to discriminate PSC from CCA (Bernuzzi et al., 2016), CCA from pancreatic adenocarcinoma (Collins et al., 2014) or HCC from iCCA (Karakatsanis et al., 2013). Moreover, some miRNA signatures were shown to be associated with iCCAs tumors when compared to normal liver tissue (Chen et al., 2009; Plieskatt et al., 2015). Depending on the assay, miRNAs were measured either from serum as biomarkers or directly from tissue after biopsy. Despite the fact that these results propose new paths for iCCA diagnosis, they are not yet used routinely since they need to be confirmed at larger scale and by other teams.

The treatment of choice for iCCA is surgical resection. However, tumors must meet different criteria with regard to size, vascularisation and location to be eligible for resection. About 60% of patients survive five years after resection. However, rates of recurrence are extremely high (60-65%). In some cases, liver transplantation can be considered but iCCA is again reported to recur in 70% of patients. Finally, in advanced-stage iCCAs not eligible for resection or transplantation, systemic chemotherapy is used (Guglielmi et al., 2009; Rizvi and Gores, 2013). In conclusion, iCCAs are tumors that are hard to identify and for which only few treatment options are available.

## 4.3. Prognosis of intrahepatic cholangiocarcinoma

#### 4.3.1. CLASSIFICATION AND PROGNOSIS

Classification of iCCAs is tricky because the field is in constant evolution. Indeed, new types or subtypes of iCCAs are constantly discovered and new proposed models emerge frequently. However, since prognosis and thus treatment options, is often associated to the different iCCAs categories, the importance of iCCAs classification should not be

underestimated. ICCAs can be classified according to three main categories that are described below.

***TNM staging.*** The Tumor Node Metastasis (TNM) staging is an international classification system that provides useful information about eligibility for tumor resection. As its name suggests, it is an anatomy-based system that records the primary and regional nodal extents of the tumor, as well as the absence or presence of metastasis. According to different criteria that are described in Table1, iCCAs are classified as stage I to stage IV tumors, stage IV being the worst case (Lazaridis and Gores, 2005).

| TNM classification of iCCAs | | | |
|---|---|---|---|
| **Stage** | **Tumor** | **Node** | **Metastasis** |
| **I** | T1 | N0 | M0 |
| **II** | T2 | N0 | M0 |
| **IIIA** | T3 | N0 | M0 |
| **IIIB** | T4 | N0 | M0 |
| **IIIC** | Any T | N1 | M0 |
| **IV** | Any T | Any N | M1 |

**Table 1. TNM classification of iCCAs** (fromLazaridis and Gores, 2005). T1, solitary tumor without vascular invasion; T2, solitary tumor with vascular invasion or multiple tumors, none >5 cm; T3, multiple tumors >5 cm or tumor involving a major branch of the portal or hepatic vein(s); T4, tumor with direct invasion of adjacent organs other than gallbladder or with perforation of visceral peritoneum; N0, no regional lymph node metastasis; N1, regional lymph node metastasis; M0, no distant metastasis; M1, distant metastasis.

**Morphological classification.** Macroscopically, iCCAs can be classified in four categories according to their growth patterns: mass-forming, periductal- or intraductal infiltrating and undefined subtypes (Razumilava and Gores, 2013). The mass-forming type corresponds to solid nodules demarcated from the adjacent liver parenchyma, the periductal infiltrating type shows infiltration along intrahepatic portal structures and the intraductal infiltrating type consists of tumors confined within large bile ducts (Sempoux et al., 2011). The mass-forming subtype is the most common and spreads via venous and

lymphatic vessels. Patients combining periductal-infiltrating tumors with mass-forming features have the worst prognosis. Conversely, patients presenting with superficial spreading, a rare type of iCCA that spreads along the biliary ducts but not in the liver parenchyma, have better outcomes.

Microscopically, iCCAs can be sorted as tubular or papillary adenocarcinomas, squamous or mucinous cell carcinomas, or lymphoepithelial-like type (Lazaridis and Gores, 2005; Nakanuma and Kakuda, 2015). However, iCCAs are usually tubular adenocarcinomas.According to their proportion of gland formation, they are categorizedas well, moderately or poorly differentiated. Well differentiated tumors have more than 95% of glandular tissue, moderately differentiated tumors exhibit between 50% and 95% of gland, while poorly differentiated tumors have less than 50% of glandular tissue. Importantly, the differentiation status inversely correlates with prognosis. Consequently, poorly differentiated tumors have the worst prognosis (Fan et al., 2011; Mazur et al., 2012; Uenishi et al., 2003)

**Immunohistological classification.** ICCAs can also be characterised by the presence of some histological markers. Among them, Mucin (Muc) 1 is the most used marker. Muc1 is a transmembrane protein that is normally expressed in developing cholangiocytes but not in adult ones. Numerous cases of iCCAS, predominantly of mass-forming type, re-express Muc1 and such Muc1-positives tumors are associated with poor prognosis. Along the same lines, Muc4 expression has also been reported as predicting poor outcomes (Braicu, 2009; Sirica et al., 2009). At last, it has recently been shown that stromal overexpression of EpCAM, a biomarker of cancer stem cells, is again correlated with poor prognosis (Sulpice et al., 2014).

#### 4.3.2. HEPATIC DIFFERENTIATION MARKERS AND PROGNOSIS

Interestingly, a number of cholangiocyte differentiation markers are expressed in iCCAs and have been investigated for their putative correlation with iCCA prognosis.

**OPN.** OPN overexpression is correlated with tumor aggressiveness and poor prognosis in several types of human cancers. Therefore, OPN expression was investigated in 73 surgically resected iCCAs. Among the tumors, only 32% were OPN-positive. Unexpectedly, overall survival was lower in patients with OPN-negative tumors. Moreover, the lack of OPN correlated with lymphatic permeation, perineural invasion and intrahepatic or lymph nodes metastasis. Therefore, in iCCAs, lack of OPN is correlated with poor prognosis (Terashi et al., 2004).

**SOX4.** Similarly to OPN, overexpression of SOX4 was described in several human malignancies but its prognostic value in iCCA was unclear. Therefore, SOX4 expression was studied in 58 iCCA samples. Slightly less than a third of the tumors overexpressed SOX4 and data demonstrated that SOX4 is an indicator of poor prognosis. Moreover, *in vitro* data revealed that SOX4 is an inhibitor of cellular migration and promotes epithelial-to-mesenchymal transition (EMT) (Wang et al., 2014).

**HNF1β**. Correlation of HNF1β with iCCAs prognosis was independently studied in two different tumors cohorts. The first study found high HNF1β expression in 67% of the iCCAs samples and low but detectable expression of HNF1β in the remaining tumors. However, while high HNF1β was associated to low serum Afp levels, no correlation was found with patient survival rates (Yu et al., 2015). Interestingly, in the second study, cytoplasmic and nuclear stainings of HNF1β were analysed separately. Intriguingly, 99% of the iCCAs showed cytoplasmic staining for HNF1β and 70% showed nuclear staining. However, again, no correlation was found with prognosis (Mazur et al., 2012).

**SOX9.** In the same study, Mazur and his team performed similar analyses with SOX9. Again, they found SOX9 cytoplasmic and nuclear staining in 80% and 90% of the tested iCCAs respectively. They concluded that lack of both nuclear and cytoplasmic SOX9 is correlated with high histological grade or high stage tumors, and that SOX9 expression is a prognostic factor for survival (Mazur et al., 2012). However, another study of a cohort of 43 iCCAs found the inverse correlation, namely that SOX9 overexpression in iCCAs is related to poorer outcomes (Matsushima et al., 2015).

Together, these results demonstrate that both lack of OPN and overexpression of SOX4 are related to poor cancer outcome, and suggest that SOX9 and HNF1β are not associated with iCCA prognosis.

#### 4.3.3. MICRORNAS AND PROGNOSIS

Several investigators characterized miRNA expression profiles in iCCA in order to identify profiles associated with prognosis. However, few correlations were found. First, when comparing miRNA expression between iCCAs and normal bile ducts, a 3-miRNA signature was recently identified for predicting survival of patients. The signature includes miR-675-5p, miR-652-3p and miR-338-3p (Zhang et al., 2015). Second, another team compared miRNA expression between iCCAs, normal bile ducts and normal liver tissue by laser capture microdissection on frozen tissues, and discovered two clusters of tumors with clearly distinguishable miRNA signatures. Interestingly, these two signatures were associated with high or low CA 19-9 serum levels, high CA19-9 levels being related to metastasis and high tumor grade (Chen et al., 2009). Finally, a transcriptomic profiling performed in well differentiated, moderately differentiated and papillary iCCAs allowed to identify miRNA signatures for each type of iCCA. This is of great interest, since the differentiation status of the tumor is known to inversely correlate with prognosis (Plieskatt et al., 2014). However, it is important to note that this study was performed exclusively in *Opistorchis viverrini*-infectedlivers. Therefore, these results might not be valid in ICCAs from other patients.

# II. AIMS OF THE THESIS

The host laboratory investigates how gene regulatory networks determine normal differentiation and morphogenesis of the liver, and how deregulation of such networks can initiate liver and pancreas tumorigenesis. In this context, the thesis aimed at identifying miRNAs that regulate cell differentiation in embryonic liver and in cholangiocarcinoma. The specific aims of the work were the following:

### AIM 1

Embryonic liver development is controlled by networks of transcription factors that stimulate the acquisition of hepatocyte and cholangiocyte features. MiRNAs take part in that process and participate in the control of cell differentiation. However, how and if miRNA exert a control on segregation of the hepatocyte and cholangiocyte lineages remained unknown. Therefore, the first aim of this thesis was to identify and characterise miRNAs involved in hepatobiliary segregation. This was performed by identifying microRNAs differentially expressed in developing hepatocytes and cholangiocytes, and by characterising the function of a selected miRNA through *in vitro* and *in vivo* gain- and loss-of-function experiments.

### AIM 2

In iCCA, the differentiation status of the tumors correlates with patient prognosis. However, only few molecular determinants of tumor differentiation and prognosis are available. Therefore, as an initial step in the characterisation of miRNA function in iCCA tumorigenesis, the second aim of this thesis was to investigate if the expression of miRNAs and molecular differentiation markers correlate with the tumor differentiation grade and thus with prognosis. This was performed by evaluating the expression of cholangiocyte-specific transcription factors and miRNAs in a set of 19 iCCAs with well-defined histological differentiation grade.

# III. RESULTS

## 1. MIR-337-3P BALANCES HEPATOBILIARY GENE EXPRESSION IN DEVELOPING LIVER AND CONTROLS THE DYNAMICS OF HEPATOCYTE DIFFERENTIATION

I performed the experiments of all figures except Fig. 3 b-e and Supplementary Fig. 4, which were performed by Claude Gérard. I contributed to study design, acquisition of data, analysis and interpretation of data and writing the manuscript.

**CONTEXT:** During liver embryogenesis, hepatoblasts differentiate either to hepatocyte precursors or to cholangiocyte precursor, which eventually mature into fully functional cells. These processes are under tight control of transcriptional networks and intercellular signaling pathways. Importantly, hepatobiliary segregation requires control mechanisms that set the right balance between hepatocyte and cholangiocyte gene expression, in order to avoid incomplete or inappropriate cell differentiation. Interestingly, miRNAs are known regulators of hepatic cell maturation. To date however, no miRNA has been identified as being involved in the segregation process. Therefore, in this first paper, we investigated the expression and the functions of such miRNAs, and identified miR-337-3p as a new regulator of hepatic cell differentiation.

# MiR-337-3P BALANCES HEPATOBILIARY GENE EXPRESSION IN DEVELOPING LIVER AND CONTROLS THE DYNAMICS OF HEPATOCYTE DIFFERENTIATION

Céline Demarez[1], Claude Gérard[1], Sabine Cordi[1], Alexis Poncy[1], Younes Achouri[1,2], Nicolas Dauguet[1], Frédéric P. Lemaigre[1*]

[1]Université catholique de Louvain, de Duve Institute, Avenue Hippocrate 75, Brussels, Belgium

[2]Université catholique de Louvain, Transgenic core facility, Avenue Hippocrate 55, Brussels, Belgium

* Correspondence and requests for materials should be addressed to FPL (email: frederic.lemaigre@uclouvain.be)

## ABSTRACT

Transcriptional networks regulated by intercellular signaling pathways control the differentiation of liver progenitor cells to hepatocytes and cholangiocyte. However, regulators that set the proper balance of hepatocyte and cholangiocyte gene expression during lineage segregation remain unknown. Here we identify miR-337-3p as a novel regulator of liver development. MiR-337-3p stimulates expression of cholangiocyte genes and represses hepatocyte genes in differentiating progenitor cells *in vitro* or in transgenic mouse livers. Beyond the stage of lineage segregation, miR-337-3p controls the transcriptional network dynamics of developing hepatocytes and cholangiocytes. Its action requires Notch and TGF-β signaling. Moreover, data are consistent with a mathematical model in which miR-337-3p exerts a biphasic control on HNF4a expression, a key component of the transcriptional network, via an incoherent feedforward loop. Together, our results highlight how network regulators exert a tight quantitative control during lineage segregation.

## INTRODUCTION

Hepatocytes and cholangiocytes are the main epithelial cells of the liver. Hepatocytes exert the major metabolic functions of the organ, and cholangiocytes line the biliary ducts and modulate the composition of bile. In developing liver, both cell types originate from bipotential precursors called hepatoblasts. Prior to segregation of the hepatocyte and cholangiocyte lineages, namely between embryonic day 9.5 (E9.5) and E12 in the mouse, hepatoblasts already express a number of hepatocyte-specific genes such as Albumin (Alb), Transthyretin (Ttr) and $\alpha$-foetoprotein (Afp). Around E12, *i.e.* at the time of hepatobiliary segregation, hepatocyte-specific gene expression rises in developing hepatocytes but becomes repressed in developing cholangiocytes. Concomitantly, biliary-specific genes are induced in cholangiocytes. Hepatocytes then progressively acquire the full set of hepatocyte functions and organize as cords that constitute the bulk of the liver parenchyma. Developing cholangiocytes form a single-layered sleeve of cells around the portal vein ("ductal plate"), and eventually give rise to the intrahepatic bile ducts (Lemaigre, 2009; Si-Tayeb et al., 2010; Zhao and Duncan, 2005).

A dynamic network of core liver-enriched transcription factors (LETFs) controls hepatocyte differentiation and maturation (Kyrmizi et al., 2006; Odom et al., 2006). LETFs are expressed at low levels in bipotential hepatoblasts. When the latter differentiate to hepatocytes, LETF expression persists and increases under control of intercellular signaling, thereby enabling stage-specific activation of hepatocyte genes (Alder et al., 2014; Beaudry et al., 2006; Kamiya et al., 1999). Among the core LETFs, Hnf4a is critical, since its inactivation at early stages of liver development is associated with impaired hepatocyte differentiation and disrupted liver morphogenesis (Parviz et al., 2003).

Notch and TGF-β signaling are among the main drivers of cholangiocyte differentiation from hepatoblasts (Clotman et al., 2005; Geisler et al., 2008; Hofmann et al., 2010; Lorent et al., 2004; Zong et al., 2009). Activation of these pathways is associated with induction of the biliary-specific SRY-related HMG box transcription factors 4 and 9 (Sox4 and Sox9), and with the set-up of a biliary transcriptional network in which

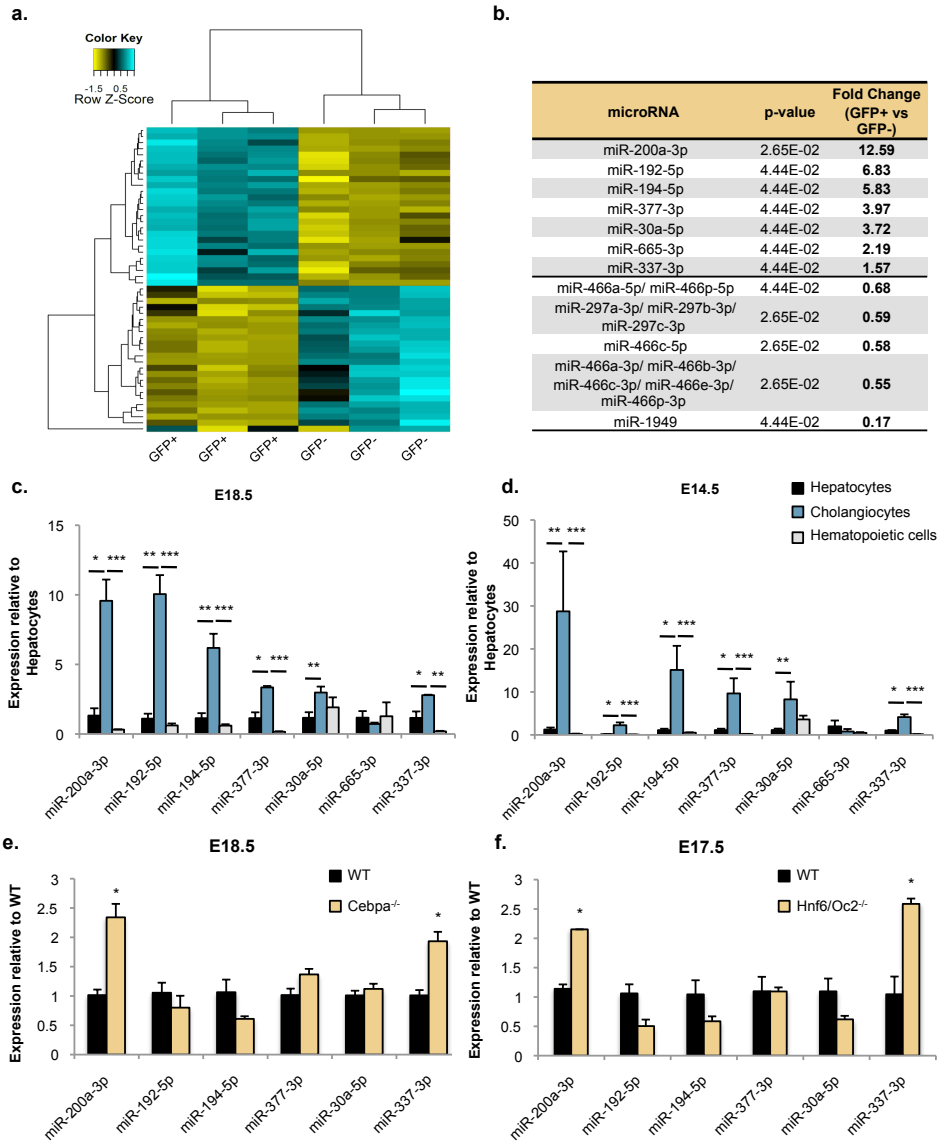
expression of the LETFs Hnf6, Hnf1b and Cebpb increases (Antoniou et al., 2009b; Clotman et al., 2002; Li et al., 2009; Poncy et al., 2015b; Takayama et al., 2014; Vanderpool et al., 2012). In contrast, hepatocyte functions and expression of the LETFs Hnf4a and Cebpa are repressed during cholangiocyte differentiation (Antoniou et al., 2009b; Ludtke et al., 2009; Shiojiri et al., 2004; Yamasaki et al., 2006).

These observations show that lineage segregation requires control mechanisms that set the right balance between hepatocyte and cholangiocyte gene expression, followed by accurate determination of the dynamics of transcription factor levels in the differentiating lineages. However, regulators that balance LETF expression in hepatoblasts differentiating to cholangiocytes and hepatocytes remain unknown. Here, we identify miR-337-3p as a novel regulator of liver development. Using experimental approaches combined with mathematical modelling, we show that miR-337-3p balances hepatobiliary gene expression in differentiating hepatoblasts, and further controls the dynamics of LETF expression in developing hepatocytes and cholangiocytes. Its role depends on Notch and TGF-β signaling, and it induces a incoherent feedforward loop that results in biphasic control on HNF4a, a master regulator of hepatocyte differentiation. Together, our results highlight how lineage segregation requires a tight quantitative control on gene expression.

## RESULTS

**MiR-337-3p is differentially expressed in developing hepatocytes and cholangiocytes and controls hepatobiliary gene expression.**

We reasoned that regulators which balance hepatocyte and cholangiocyte gene expression in embryonic livers should ideally be present in hepatoblasts and differentially expressed in developing cholangiocytes and hepatocytes. To identify such regulators, we focused on miRNAs and first compared the miRNome in differentiating cholangiocytes and hepatocytes. Sox9-GFP embryos express GFP specifically in cholangiocytes (Supplementary Fig. 1) and allow to separate GFP+ cholangiocytes from GFP- cells by fluorescence-activated cell sorting (FACS). To enrich the GFP- fraction in developing hepatocytes, hematopoietic cells were removed by magnetic cell sorting (MACS) using a cocktail of biotinylated antibodies directed against a panel of hematopoietic lineage antigens. We compared miRNA expression in the two cell populations at E18.5 by microarray analysis, and found 7 miRNAs upregulated in the cholangiocyte fraction (Fig. 1a-b). The miRNAs enriched in the hepatocyte fraction were not selected for further studies since miR-1949 and members of the miR-466/297 cluster are predicted to be misannotated microRNAs (Chiang et al., 2010). The cholangiocyte-enriched miRNAs, except for miR-665-3p, were all validated by qRT-PCR analysis of RNA from FACS-sorted cells at E18.5 and at the stage of lineage commitment, namely E14.5 (Fig. 1c-d). Moreover, among the six cholangiocyte-enriched miRNAs, only miR-200a-3p and miR-337-3p were upregulated in mouse models presenting with an excess of biliary differentiation, namely mice deficient in C/EBPa (Alfp-Cre;Cebpa$^{f/f}$) or doubly deficient in HNF6 and Onecut2 (Hnf6/Oc2$^{-/-}$) (Clotman et al., 2005) (Fig. 1e-f). This suggested that these two miRNAs might functionally be involved in controlling cholangiocyte *versus* hepatocyte development.




| microRNA | p-value | Fold Change (GFP+ vs GFP-) |
|---|---|---|
| miR-200a-3p | 2.65E-02 | **12.59** |
| miR-192-5p | 4.44E-02 | **6.83** |
| miR-194-5p | 4.44E-02 | **5.83** |
| miR-377-3p | 4.44E-02 | **3.97** |
| miR-30a-5p | 4.44E-02 | **3.72** |
| miR-665-3p | 4.44E-02 | **2.19** |
| miR-337-3p | 4.44E-02 | **1.57** |
| miR-466a-5p/ miR-466p-5p | 4.44E-02 | **0.68** |
| miR-297a-3p/ miR-297b-3p/ miR-297c-3p | 2.65E-02 | **0.59** |
| miR-466c-5p | 2.65E-02 | **0.58** |
| miR-466a-3p/ miR-466b-3p/ miR-466c-3p/ miR-466e-3p/ miR-466p-3p | 2.65E-02 | **0.55** |
| miR-1949 | 4.44E-02 | **0.17** |

**Figure 1. Identification of microRNAs differentially expressed in developing hepatocytes and cholangiocytes. (a)** Heatmap and unsupervised hierarchical clustering analysis of miRNA microarray data comparing developing hepatocytes (GFP-) and cholangiocytes (GFP+) at E18.5. The analysis was performed on all samples, and on the top 50 microRNAs with highest standard deviation. **(b)** List of miRNAs differentially expressed between developing hepatocytes and cholangiocytes (p-value <0.05). P-values are Benjamini-Hochberg adjusted. **(c-d)** Differential miRNA expression was validated by RT-qPCR at E18.5 and at the time of lineage segregation (E14.5). **(e-f)** Only miR-200a-3p and miR-337-3p were overexpressed in mouse models in which livers present with an excess of biliary differentiation. Data in (c-f) are mean ± SEM; *p<.05, **p<.01, ***p<.001; n≥3.

To confirm this hypothesis, we overexpressed miR-337-3p and miR-200a-3p by transfecting the corresponding miR-mimics in cultured immortalized hepatoblasts. We found that both miR-337-3p and miR-200a-3p repressed expression of hepatocyte markers, but only miR-337-3p was able to stimulate cholangiocyte gene expression (Fig. 2a-b). Considering these results, we selected miR-337-3p for further investigations.

**Notch and TGF-β-dependent control of hepatobiliary gene expression by miR-337-3p**

To determine the impact of miR-337-3p on hepatoblast differentiation, we analyzed the transcriptome of cultured hepatoblasts transfected with a miR-337-3p mimic or with a negative control. Microarray analysis identified 245 upregulated and 345 down-regulated genes (p-value <0.05; fold change <0.5 or >2). Gene Set Enrichment Analysis (GSEA) further revealed that miR-337-3p represses a large number of hepatocyte functions, such as detoxification, protein secretion, and metabolism of cholesterol, fatty acids, bile acids and carbohydrates (Table 1 and Supplementary Fig. 2). Moreover, miR-337-3p up-regulated a gene set related to Notch signaling, which is known to stimulate cholangiocyte differentiation while repressing hepatocyte gene expression (Geisler et al., 2008; Hofmann et al., 2010; Lorent et al., 2004; Tanimizu and Miyajima, 2004; Zong et al., 2009). Therefore, we next determined if the effect of miR-337-3p on hepatoblast differentiation depends on Notch signaling. Hepatoblasts were transfected with miR-337-3p mimic or control mimic in the presence or absence of the Notch pathway inhibitor N-[2S-(3,5-difluorophenyl)acetyl]-L-alanyl-2-phenyl-1,1-dimethylethyl-ester-glycine (DAPT) and gene expression was measured. MiR-337-3p stimulated expression of the Notch targets Hey1 and Hes1 (Fig. 2c). DAPT not only suppressed the miR-337-3p-mediated induction of Hes1 and Hey1, but it also inhibited the effects of this miRNA on hepatocyte and cholangiocyte gene expression (except for Sox4) (Fig. 2d).

Further, we found that miR-337-3p also stimulates TGF-β signaling, another biliary-promoting pathway. MiR-337-3p induced a TGF-β luciferase reporter construct and was unable to down-regulate hepatocyte markers when TGF-β signaling was blocked by SB431542, an inhibitor of the TGF-β receptor (Fig. 2e-f). Stimulation of the cholangiocyte

marker by miR-337-3p was only slightly affected by SB431542 (Fig. 2f). We concluded that Notch and TGF-β signaling are stimulated by miR-337-3p and that this stimulation is required, at least in part, for miR-337-3p-dependent control of hepatocyte and cholangiocyte gene expression.

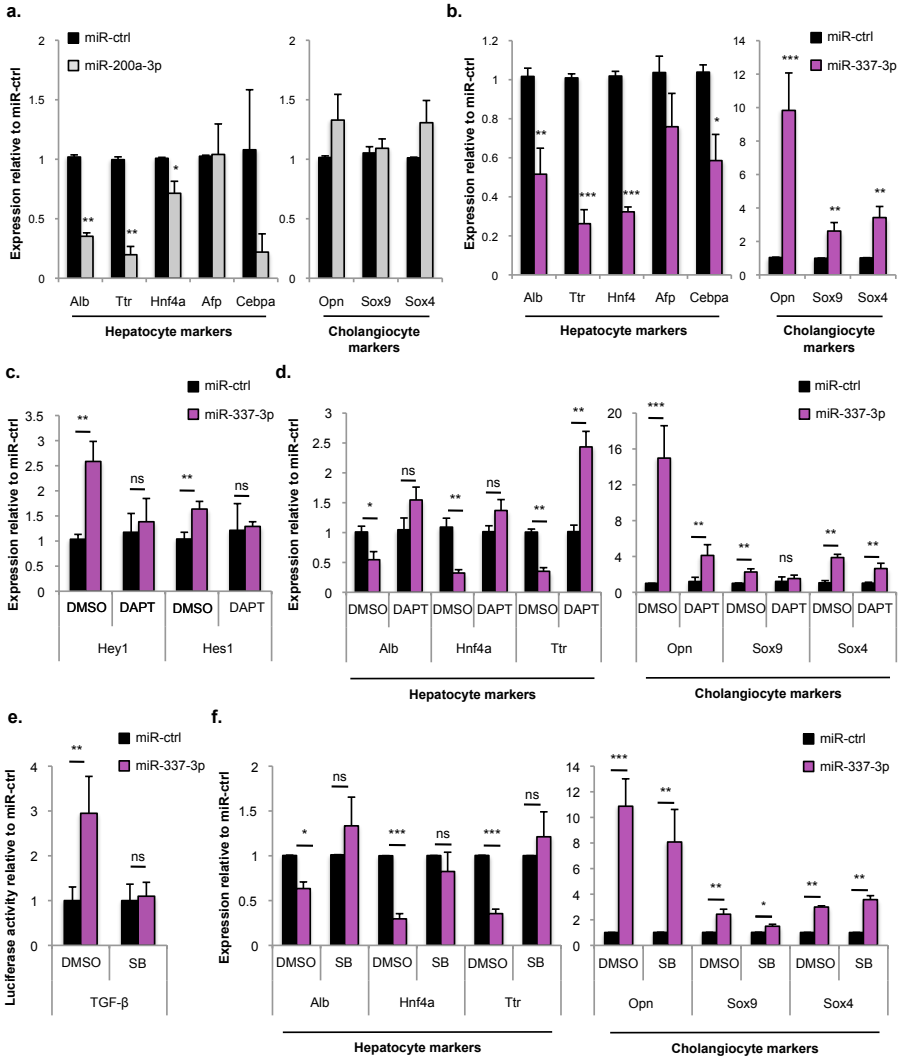



**Figure 2. Notch- and TGF-β-dependent control of hepatobiliary gene expression by miR-337-3p in cultured hepatoblasts. (a-b)** Cultured hepatoblasts were transfected with miR-200a-3p or miR-337-3p mimics. Both miRNAs repressed hepatocyte gene expression, but only miR-337-3p induced

cholangiocyte gene expression. **(c)** miR-337-3p mimic induces expression of Notch target genes Hey1 and Hes1, and DAPT (50 μM) inhibits the miR-337-3p-mediated induction of Hey1 and Hes1. (**d**) The effect of miR-337-3p effect is blocked by DAPT-mediated repression of Notch signaling. **(e)** miR-337-3p mimic induces a TGF-β reporter construct in the absence of the TGF-β inhibitor SB431542 (2 μM). (**f**) miR-337-3p did not repress hepatocyte markers or stimulate the biliary marker Sox9 in the presence of SB431542 (2 μM). Data are mean ± SEM; *p<.05, **p<.01, ***p<.001; n=3; ns, non-significant; miR-ctrl, miR-mimic negative control; SB, SB431542.

**Table1. List of hepatic pathways enriched by miR-337-3p.**

| Hepatocyte function | Gene set enriched | NES | p-val | FDR q-val |
|---|---|---|---|---|
| Lipid metabolism | Fatty acid metabolism | -2.35 | <0.001 | <0.001 |
| | Cholesterol homeostasis | -1.99 | <0.001 | <0.001 |
| | Adipogenesis | -1.93 | <0.001 | <0.001 |
| | Bile acid metabolism | -1.98 | <0.001 | <0.001 |
| Carbohydrate metabolism | Glycolysis | -1.50 | 0.002 | 0.029 |
| Detoxification and catabolism | Xenobiotic metabolism | -2.33 | 0.000 | 0.000 |
| | Reactive oxygen species pathway | -1.53 | 0.024 | 0.021 |
| Protein production and secretion | Protein secretion | -1.70 | 0.000 | 0.005 |
| | Coagulation | -1.49 | 0.006 | 0.028 |
| | Complement | -1.41 | 0.016 | 0.044 |
| Others | Oxidative phosphorylation | -1.84 | <0.001 | 0.001 |
| | MTORC1 signaling | -1.87 | <0.001 | 0.001 |
| | Heme metabolism | -1.47 | 0.006 | 0.027 |
| **Cholangiocyte function** | **Gene set enriched** | **NES** | **p-val** | **FDR q-val** |
| Signaling pathway | Notch signaling | 1.68 | 0.006 | 0.003 |

NES= normalized enrichment score

### MiR-337-3p regulates HNF4a via an incoherent feedforward loop

To further investigate the function of miR-337-3p, we also inhibited its expression in cultured hepatoblasts by transfecting antagomirs (Fig. 3a). The results showed that a subset of hepatocyte markers as well as the cholangiocyte marker Sox4 were downregulated. This further supported that miR-337-3p balances hepatobiliary gene expression, but surprisingly revealed that both antagomir-mediated inhibition and miR-mimic-dependent upregulation of miR-337-3p (Figs. 2b and 3a) induced a similar repression of Hnf4a, a master regulator of hepatocytefunctions (Parviz et al., 2003).

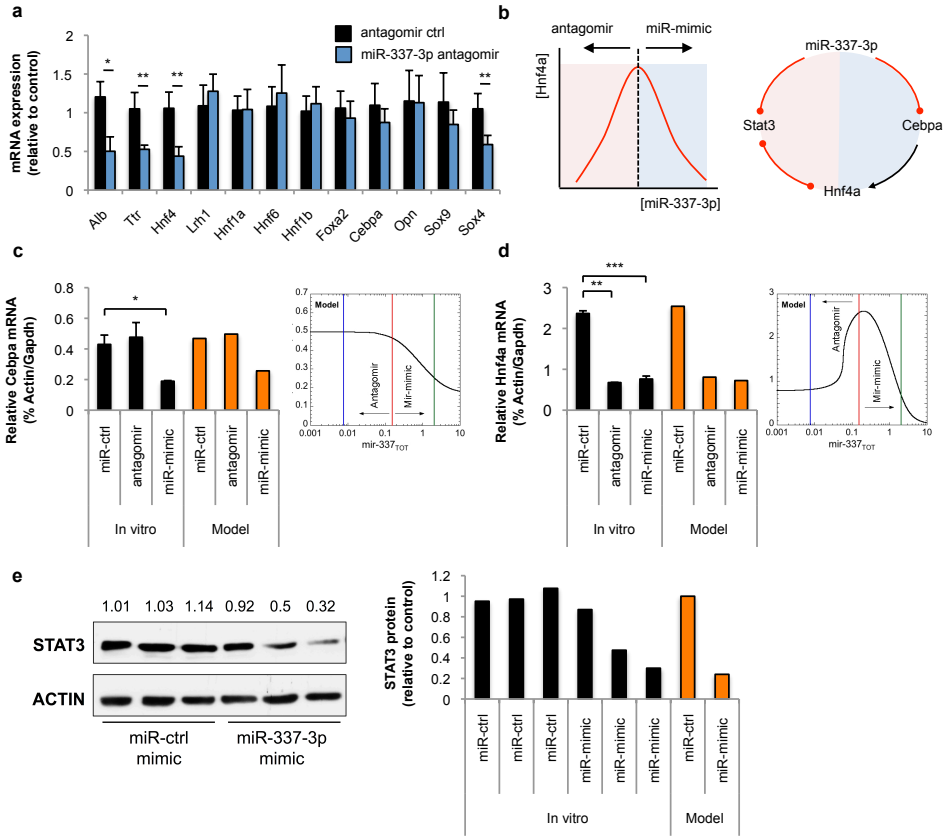



**Figure 3. MiR-337-3p regulates Hnf4a expression via an incoherent feedforward loop. (a)** Transfection of cultured hepatoblasts with a miR-337-3p antagomir did not affect cholangiocyte gene expression, except for Sox4, but repressed a subset of hepatocyte markers. **(b)** Model predictsjow Hnf4a might be biphasically regulated by an incoherent feedforward loop involving

Stat3 and Cebpa. **(c-e)** Expression of Cebpa mRNA (c), Hnf4a mRNA (d) and STAT3 protein (e) in cultured hepatoblasts transfected with miR-337-3p mimics or antagomirs was consistent with the output of a quantitative mathematical model predicting a biphasic expression of HNF4a in response to miR-337-3p acting via Cebpa/Hnf4a/Stat3. Vertical red, blue and green lines in c, d, e (right panels) correspond to the experimental control, antagomir or miR-mimic conditions. Data are mean ± SEM; *p<.05, **p<.01, ***p<.001; n=3. Parameter values and calibration of the mathematical model are described in Supplementary Information.

To resolve this apparent discrepancy we postulated that such control would be biphasic: a rise in miR-337-3p would first stimulate Hnf4a expression until it reaches a peak, and further increase of the miRNA would then lower Hnf4a levels. In other terms, cells expressing maximum Hnf4a levels would show reduction in HNF4a when miR-337-3p is either increased or repressed, as observed when treating hepatoblasts with miR-337-3p mimics or antagomirs. Biphasic control of Hnf4a by miR-337-3p would require a molecular network motif known as incoherent feedforward loop (IFFL) (Kim et al., 2008; Mangan and Alon, 2003). This IFFL would be defined by at least two opposing (stimulatory and inhibitory) pathways between miR-337-3p and Hnf4a (Kim et al., 2008; Mangan and Alon, 2003) (Fig. 3b). A literature search identified Cebpa as a candidate mediating the inhibitory pathway, and Stat3 as the mediator in the activation pathway (Hatziapostolou et al., 2011; Kyrmizi et al., 2006), with Stat3 and Cebpa being validated and predicted targets of miR-337-3p, respectively (Du et al., 2012; Dweep and Gretz, 2015).

To evaluate if miR-337-3p and Hnf4a can form a Cebpa- and Stat3-dependent IFFL, we first built a quantitative mathematical model that accounts for the dynamics of the loop. The model is based on a set of kinetic equations describing the time evolution of the expression levels of the network components (Table 2 and Supporting Information). It considers that miR-337-3p directly represses the translation of Stat3, as demonstrated by others (Du et al., 2012), and assumes that miR-337-3p represses the synthesis of Cebpa, which is consistent with our finding that Cebpa levels decrease in a dose-dependent manner upon transfection of miR-337-3p-mimic (Fig. 3c and Supplementary Fig. 3a). It also considers mutual inhibition between Stat3 and Hnf4a, as demonstrated by others (Hatziapostolou et al., 2011). For sake of simplicity, the model considers that miR-337-3p directly represses Cebpa. This assumption is theoretically acceptable since a direct

interaction between miR-337-3p and Cebpa is not a necessary condition to observe biphasic expression of Hnf4a in response to miR-337-3p (not shown).

The model predicts such biphasic response- (Fig. 3d), and reproduces the expression levels of Cebpa, Hnf4a and STAT3, measured in the control, miR-337-3p mimic and antagomir conditions (Fig. 3c-e and Supplementary Fig. 4). Dose-response curves are shown in Supplementary Fig. 3 and discussed in Supplementary Information. Taken together, the in vitro expression data supported by the mathematical model suggest that miR-337-3p, Stat3, Cebpa and Hnf4a constitute an IFFL. The biphasic response of Hnf4a as a function of miR-337-3p reveals that optimized expression levels of miR-337-3p in hepatoblasts ensures adequate expression of Hnf4a

**Table 2. Kinetic equations of the mathematical model**

| | |
|---|---|
| [1] | $\frac{dmSTAT3}{dt} = V_{SM1STAT3} + V_{SM2STAT3} \cdot \left( \frac{(K_{IHNF4})^n}{(K_{IHNF4})^n + HNF4a^n} \right) - k_1 \cdot miR337 \cdot mSTAT3 + k_2 \cdot mirmSTAT3 - k_{DMSTAT3} \cdot mSTAT3$ |
| [2] | $\frac{dSTAT3}{dt} = k_{SSTAT3} \cdot mSTAT3 - k_{DSTAT3} \cdot STAT3$ |
| [3] | $\frac{dmirmSTAT3}{dt} = k_1 \cdot miR337 \cdot mSTAT3 - k_2 \cdot mirmSTAT3 - k_{DMIR1} \cdot mirmSTAT3$ |
| [4] | $\frac{dmcEBPA}{dt} = V_{SM1CEBPA} + V_{SM2CEBPA} \cdot \left( \frac{cEBPA^n}{(K_{A2CEBPA})^n + cEBPA^n} \right) - k_3 \cdot mcEBPA \cdot miR337 + k_4 \cdot mirmcEBPA - k_{DMCEBPA} \cdot mcEBPA$ |
| [5] | $\frac{dcEBPA}{dt} = k_{SCEBPA} \cdot mcEBPA - k_{DCEBPA} \cdot cEBPA$ |
| [6] | $\frac{dmirmcEBPA}{dt} = k_3 \cdot mcEBPA \cdot miR337 - k_4 \cdot mirmcEBPA - k_{DMIR2} \cdot mirmcEBPA$ |
| [7] | $\frac{dmHNF4a}{dt} = V_{SM1HNF4A} + V_{SM2HNF4A} \cdot \left( \frac{(K_{ISTAT3})^n}{(K_{ISTAT3})^n + STAT3^n} \right) \cdot \left( \frac{cEBPA^n}{(K_{A1CEBPA})^n + cEBPA^n} \right) - k_{DMHNF4A} \cdot mHNF4a$ |
| [8] | $\frac{dHNF4a}{dt} = k_{SHNF4A} \cdot mHNF4a - k_{DHNF4A} \cdot HNF4a$ |

**MiR-337-3p represses hepatocyte-specific gene expression *in vivo***

To determine the function of miR-337-3p *in vivo*, we generated transgenic mice (hereafter called miR-337-3p Tg) that harbour the Alfp-Cre transgene and a Cre recombinase-dependent miR-337-3p overexpression construct (Fig. 4a). The temporal expression profile of miR-337-3p is illustrated in Supplementary Fig. 5. Alfp-Cre induces target gene recombination in early hepatoblasts (Kellendonk et al., 2000). MiR-337-3p expression was transiently increased in transgenic mice from E11.5 (1.3 fold) to E13.5 (1.9 fold) before returning to normal values (Fig. 4b). Interestingly, despite this modest and transient increase, hepatocyte differentiation markers were down-regulated (Fig. 4c and d). These markers include a large set of transcription factors, as well as functional markers. Together, these results confirm *in vivo* that miR-337-3p controls hepatocyte differentiation.

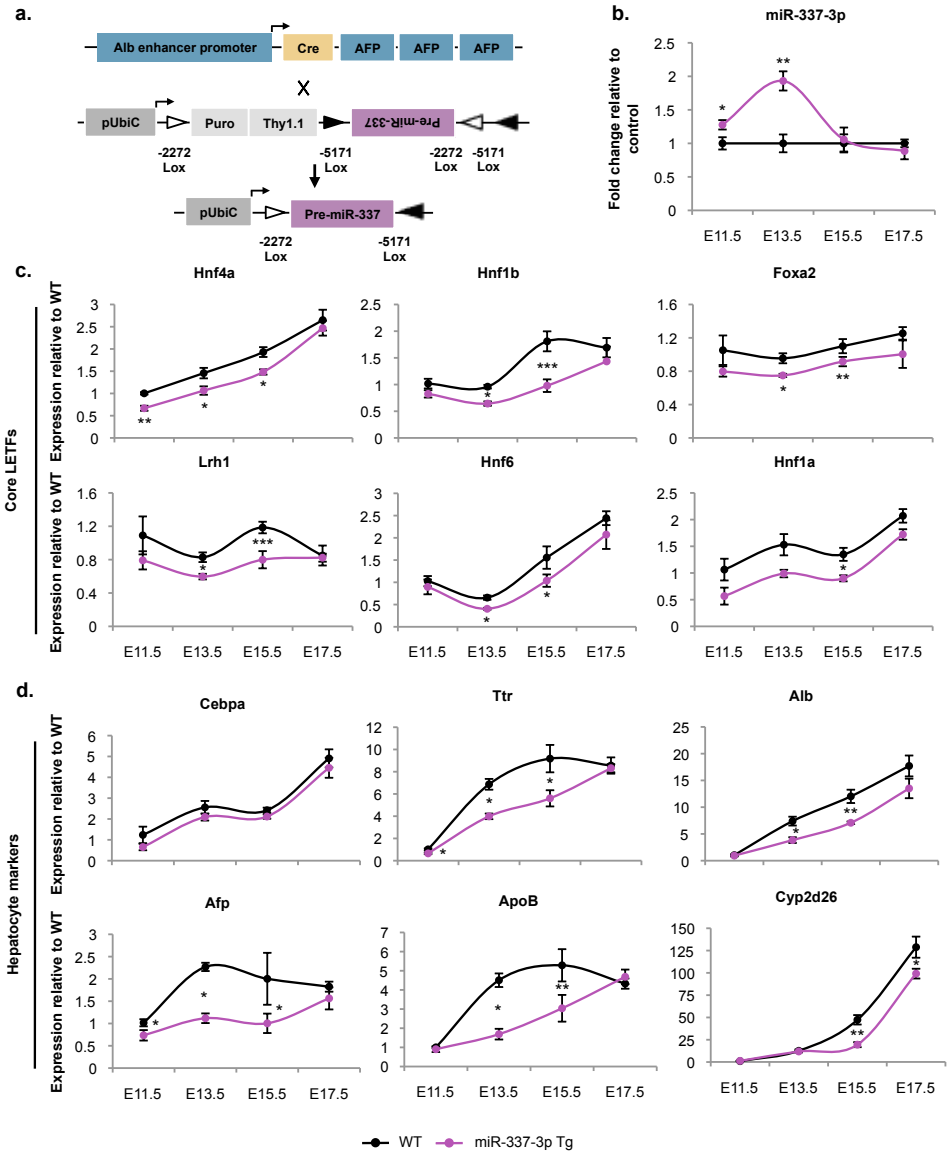
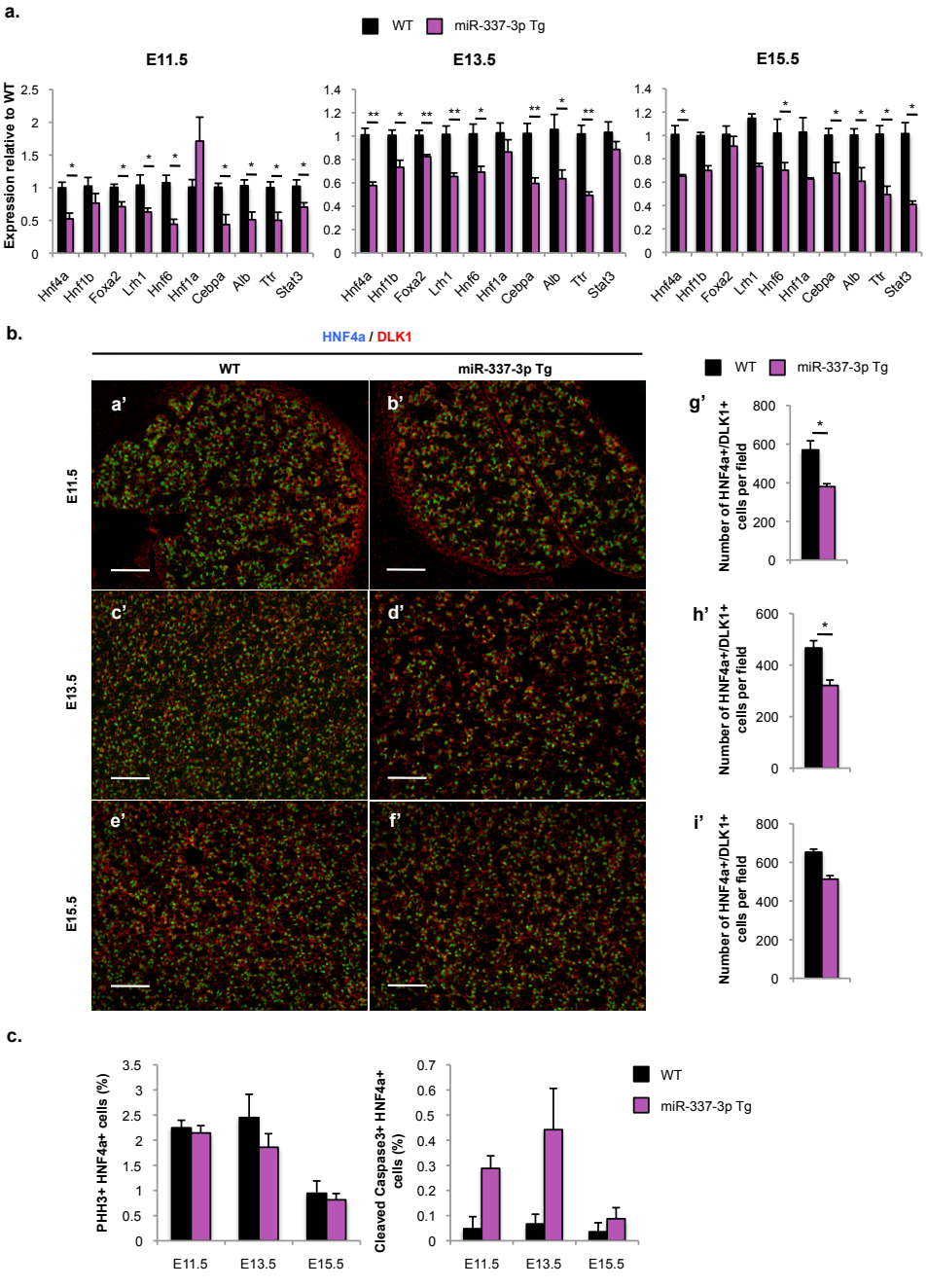



**Figure 4.** ***In vivo*** **miR-337-3p overexpression represses hepatocyte-specific gene expression. (a)** Constructions for generating miR-337-3p Tg mice. **(b)** Liver of miR-337-3p Tg mice transiently overexpress miR-337-3p from E11.5 to E13.5. **(c-d)** Overexpression of miR-337-3p represses expression of hepatocyte-specific genes during liver development. Data in (b-d) are mean ± SEM; *p<.05, **p<.01, ***p<.001; n≥4 for each time point.

Hepatoblasts specifically express Delta-like homologue 1 (DLK1) in their membrane (Tanimizu, 2003; Tanimizu et al., 2004) and gene expression analyses of MACS-purified DLK1+ hepatoblasts from WT and miR-337-3p Tg livers further strengthened previous results. Indeed, Fig. 5a shows that hepatocyte-specific gene expression was lower in hepatoblasts that overexpress miR-337-3p, indicating that the cells were less differentiated than their WT counterpart. Cebpa and Stat3 were also repressed, which is in line with the incoherent feedforward loop model described above. Our interpretation was further strengthened by immunofluorescence staining of liver sections. Livers from wild-type (WT) or miR-337-3p Tg embryos (E11.5 to E15.5) were co-stained for HNF4a and DLK1. Both WT and miR-337-3p Tg mice showed normal liver architecture, but miR-337-3p Tg livers had reduced numbers of HNF4a+/DLK1+ hepatoblasts (Fig. 5b). Proliferation (phosphohistone H3 staining) and apoptosis (cleaved caspase 3 staining) of these cells was not significantly affected (Fig. 5c). This suggested that miR-337-3p overexpression represses hepatoblast differentiation toward hepatocytes. Altogether, our results indicate that miR-337-3p represses hepatocyte gene expression at early stages of liver development.

**Figure 5. MiR-337-3p controls hepatocyte differentiation *in vivo*. (a)** DLK1+ hepatoblasts were purified and their differentiation status was assessed by RT-qPCR. Data show that hepatoblasts of miR-337-3p Tg mice are less differentiated than WT hepatoblasts. **(b)** Immunofluorescence analysis showed reduced number of hepatoblasts (HNF4a+/DLK1+) in miR-337-3p Tg livers at E11.5 and E13.5 **(c)** Proliferation and apoptosis in miR-337-3p livers were assessed by measuring the percentage of HNF4a+ hepatoblasts that stain positive for phosphohistone H3 (PPH3) and cleaved-caspase 3. Data are mean ± SEM; *p<.05, **p<.01; n=4 for each time point. Scale bars= 100 µm.


a.
WT
miR-337-3p Tg
E11.5
E13.5
E15.5
Expression relative to WT
Hnf4a
Hnf1b
Foxa2
Lrh1
Hnf6
Hnf1a
Cebpa
Alb
Ttr
Stat3
b.
HNF4a / DLK1
WT
miR-337-3p Tg
a'
b'
c'
d'
e'
f'
E11.5
E13.5
E15.5
g'
h'
i'
Number of HNF4a+/DLK1+ cells per field
c.
PHH3+ HNF4a+ cells (%)
Cleaved Caspase3+ HNF4a+ cells (%)

***In vivo* miR-337-3p controls ductal plate development**

When investigating biliary-specific gene expression in miR-337-3p Tg mice, we found significant upregulation of Sox4 at E13.5, but unchanged expression of Sox9 and Opn (Fig. 6a). However, immunostaining analysis revealed that the number of SOX9+ cells was slightly reduced, suggesting that the expression of SOX9 per cell is increased (Fig. 6b-d). Moreover, further immunostaining analysis of the ductal plate showed a strong reduction in the number of HNF1b+ and HNF6+ cells (data not shown). Importantly, this reduction only affects cells that constitute the monolayered part of the ductal plate and which are fated to differentiate to periportal hepatocytes (Antoniou et al., 2009b; Carpentier et al., 2011). Indeed, in miR-337-3p Tg mice, these cells express SOX9 but lack the expression of HNF1b and HNF6, while ductal plate cells that line developing ducts show normal SOX9, HNF1b and HNF6 expression (Fig 6b and c). Consistent with this, the number of developing ducts in miR-337-3p Tg livers was normal, as well as the number of cells lining the ducts (Fig. 6d). Therefore, we concluded that miR-337-3p promotes development of cholangiocytes fated to form bile ducts at the expense of cholangiocytes fated to become periportal hepatocytes.

Bile duct development normally starts with the formation of primitive ducts asymmetrically lined by cholangiocytes on the portal side and by hepatoblasts on the parenchymal side. These structures progressively mature to form ducts entirely and symmetrically lined by cholangiocytes (Antoniou et al., 2009b; Carpentier et al., 2011). We found no acceleration of bile duct maturation in miR-337-3p Tg livers. Indeed, the ratio of asymmetrical to symmetrical structures was identical in WT and miR-337-3p-overexpressing ducts (Fig. 6d). Also, the biliary marker CK19, which in our hands is only detected in WT cholangiocytes at E18.5, was not detected at an earlier stage in miR-337-3p Tg livers (Fig. 6e).

We concluded that overexpression of miR-337-3p increases development of cholangiocytes fated to become bile ducts without accelerating duct morphogenesis.

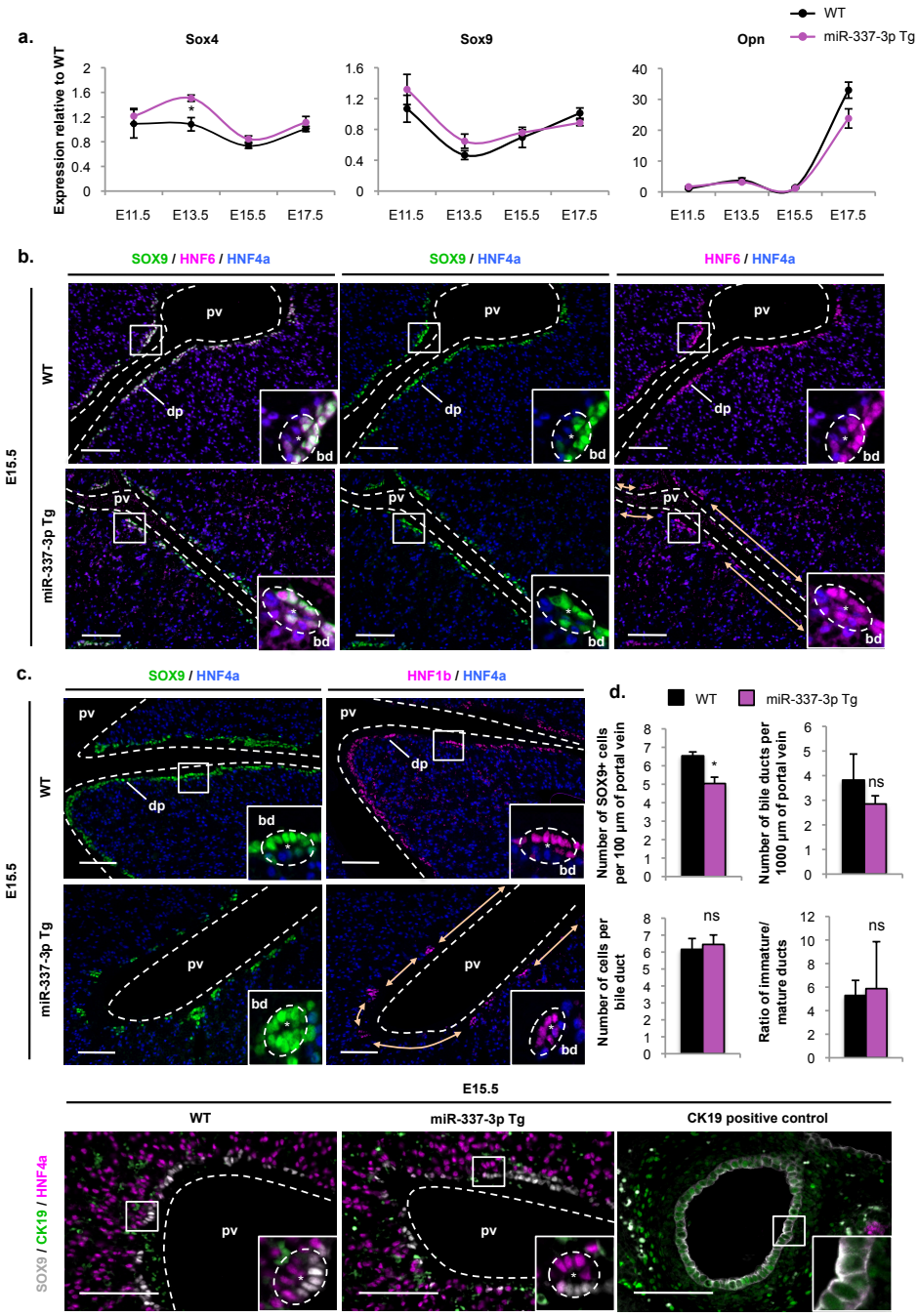



**Figure 6. MiR-337-3p promotes cholangiocyte development *in vivo*. (a)** Livers of miR-337-3p Tg mice overexpress the cholangiocyte marker Sox4 at E13.5 but not Sox9 and Opn. **(b-c)** E15.5 immunostainings show a reduction in the number of SOX9+ ductal plate cells, while ductal plate

cells not involved in bile duct formation do not express HNF1b and HNF6 in miR-337-3p livers. Arrows delineate the ductal plate areas lacking HNF1b and HNF6 staining. **(d)** Quantification of SOX9+ cells in E15.5 livers confirm the reduced amount of SOX9+ cells per portal vein distance in miR-337-3p Tg livers. The number of bile ducts and the number of cells per bile duct did not differ between WT and Tg livers. The ratio of immature to mature ducts is similar in WT and Tg mice, indicating that miR-337-3p does not accelerate bile duct maturation. **(e)** Lack of CK19 detection in WT and Tg cholangiocytes at E15.5 further supports normal maturation. Data in (a) and (d) are mean ± SEM; *p<.05; n≥4 for each time point. Scale bars= 100 μm; Dp= ductal plate, pv= portal vein, *Asterisk*= lumen of biliary structures.

## DISCUSSION

Hepatoblasts express a large set of hepatocyte functions, and it is commonly considered that intercellular signals such as Notch or TGF-β signaling redirect the fate of periportal hepatoblasts to the cholangiocyte lineage. The remaining hepatoblasts would then differentiate by default towards the hepatocyte lineage, with hepatocyte gene expression being further enhanced in response to extracellular signals such as Oncostatin M. Here we identified miR-337-3p as a novel regulator of liver development, which balances hepatobiliary gene expression (Fig. 7).

Known microRNAs function in maturing hepatocytes by stimulating hepatocyte functions (miR-148 or miR-122) or repressing cholangiocyte gene expression (miR-23b cluster)(Gailhouste et al., 2013; Laudadio et al., 2012; Rogler et al., 2009). MiR-30a-5p, which was identified in our microarray screen, is specifically expressed in developing cholangiocytes and regulates later stages of development by promoting bile duct morphogenesis (Hand et al., 2009). MiR-337-3pis initially found in hepatoblasts and then differentially expressed in both hepatocytes and cholangiocytes. It stimulates cholangiocyte genes while repressing hepatocyte functions, thereby balancing hepatobiliary gene expression.

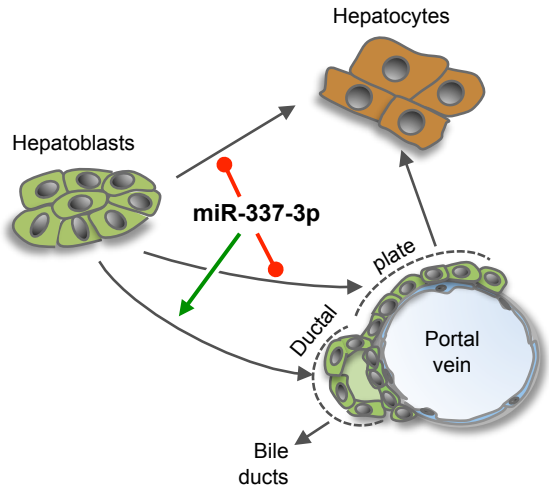



**Figure 7. Schematic representation of miR-337-3p function during liver development.** MiR-337-3p represses hepatocyte differentiation and stimulates cholangiocyte-specific gene expression. miR-337-3p also inhibits HNF1b and HNF6 expression in monolayered ductal plate cells that are normally fated to differentiate to periportal hepatocytes and promotes bile duct development.

MiR-337-3p represses a wide set of LETFs. The latter form a dynamic network characterized by an increasing number of autoregulatory and cross-regulatory loops that enhance the stability of the network (Kyrmizi et al., 2006; Lemaigre, 2009; Odom et al., 2006; Odom et al., 2004). Our experiments did not support that Hnf4a is directly targeted by miR-337-3p (Supplementary Fig. 6). Consistent with our mathematical model, we propose that miR-337-3p controls HNF4a expression via an incoherent feedforward loop acting via Cebpa and Stat3. Our finding implements in hepatic lineage segregation the notion that miRNA-dependent feedback and feedforward loops are recurrent network motifs in mammals (Tsang et al., 2007), (Alon, 2007). Such FFLs are common in hepatocyte transcriptional networks (Kyrmizi et al., 2006; Lemaigre, 2009; Martinez-Jimenez et al., 2010; Odom et al., 2006; Odom et al., 2004), but an incoherent feedforward loop has to our knowledge not yet been considered in embryonic liver. More importantly, this regulatory loop would underlie biphasic regulation of Hnf4a by miR-337-3p, characterized by the fact that gain- or loss-of-function of miR-337-3p can have similar repressive effects on HNF4a expression. If such biphasic response really takes place during liver development, this would underscore the fact that only small changes in miRNA concentration can be required to either stimulate or repress a gene network. The sensitivity of the hepatocyte network to small variations in gene regulators is further illustrated in our work by the repression of the LETF network and hepatocyte functions resulting from a limited increase in miR-337-3p in vivo.

Mir-337-3p stimulates cholangiocyte gene expression and we provide evidence that it stimulates Notch or TGF-β signaling, two pathways known to promote cholangiocyte differentiation. How miR-337-3p modulates these pathways remains to be determined. Since the effect of miR-337-3p is abrogated by γ-secretase and TGF-β receptor inhibitors (DAPT and SB431542), we expect that miR-337-3p directly targets these Notch and TGF-β mediators or upstream regulators thereof. In lines with this, we observed an overexpression of the TGF-β ligands TGFβ1 and TGFβ3 in cultured hepatoblasts transfected with the miR-337-3p mimic. Moreover, Notch2 and TGFβRI expression was

also increased in the presence of the miR-337-3p mimic, thereby suggesting that miR-337-3p acts upstream of Notch and TGFβ pathways

MiR-337-3p exerts differential functions within the ductal plate. Indeed, overexpression of miR-337-3p inhibited HNF1b and HNF6 expression in monolayered ductal plate cells, which are known to give rise to periportal hepatocytes (Antoniou et al., 2009b; Carpentier et al., 2011), but not in ductal plate cells fated to become bile ducts. How this cell-specific activity is exerted is not known yet, but it is consistent with a global hepatocyte-repressing and cholangiocyte-promoting function of miR-337-3p (Fig. 7). To our knowledge, it also represents the first regulatory event that distinguishes the monolayered ductal plate cells from the primitive ductal cells.

In conclusion, we have identified miR-337-3p as a novel regulator of hepatobiliary differentiation in developing liver. Our work is likely to impact on *in vitro* programming of cultured cells towards hepatocytes of cholangiocytes for cell therapy or pharmacological studies.

## METHODS

### Animals

AlfpCre (kindly provided by F. Tronche), Sox9-GFP and Hnf6/Oc2$^{-/-}$ mice have been described (Clotman et al., 2005; Gong et al., 2003; Kellendonk et al., 2000; Laudadio et al., 2012). MiR-337-3p Tg mice were generated by injection of fertilized oocytes with pLB2-FLIP-miR-337-3p construct. Experimental protocols were approved by the Animal Welfare Committee of the Université Catholique de Louvain.

### Plasmids

pLB2-FLIP-miR-337-3p was generated by inserting the genomic sequence coding for miR-337-3p plus 300 base pairs flanking each side into pLB2-FLIP (Stern et al., 2008). Primers used to amplify miR-337-3p coding sequences were 5'TCGATCGTTTAAACAGAGTAGGCCCAGGATCGAC3' and 5'TCGATCGCGGCCGCCATCCCTCTGCTCCCTCTC3'. psiCHECK-3'UTR-HNF4a was generated by cloning a PCR-generated fragment of the HNF4a 3'UTR region downstream of the Renilla luciferase in psiCHECK1 vector (Promega). Primers used were 5'TCGATCCTCGAGGTAATGGGGCCAGCTGATTA3' and 5'CGATCGAATTCGAGGACGTCTGCTTCTGACC3'.

### Cell Isolation

Pools of 20 livers at E18.5 and E14.5 Sox9-GFP livers were dissected, minced and cell-dissociated in DMEM-F12 (#31870-025, Gibco, Lifetechnologies) containing 1 mg/ml collagenase IV (#43E14253, Worthington), 1 mg/ml dispase (#17105-041, Gibco, Lifetechnologies) and 0.1 mg/ml of DNAse I (#11284932001, Roche) for 30 min at 37°C. Digestion was stopped by adding an equal volume of 10% FBS in phosphate buffered saline (PBS) and cells were resuspended in 40 µl of 2 mM EDTA, 0.5% bovine serum albumin (BSA) in PBS per $10^7$ cells and filtered on 40 µm cell strainer (#087711, Fisher Scientific). Hematopoietic cells were eliminated by MACS separation using the "Lineage

Cell depletion Kit" (#130090858, Miltenyi Biotech). Sox9-GFP+ cells and Sox9-GFP- cells were isolated by fluorescence-activated cell sorting. Total RNA was isolated as described below.

For isolation of Dlk1+ cells, individual livers were dissected and cell-dissociated in DMEM-F12/collagenase IV/dispase/DNaseI solution as described above. Cells were resuspended in 40 µl of 2 mM EDTA, 0.5% BSA in PBS (MACS buffer) per $10^7$ cells and incubated with 2 µl of biotinylated goat anti-Dlk1 antibody (#BAF-1144, R&D systems) for 15 min at 4°C. Cells were washed in 2 mM EDTA in PBS and resuspended in 80 µl of MACS buffer to which 20 µl of anti-biotin microbeads (#120-000-900, Miltenyi Biotech) were added per $10^7$ cells. After 15 min of incubation at 4°C, cells were washed and resuspended in 500 µl of MACS buffer. Dlk1+ cells were isolated using a MS column (#130-042-201, Miltenyi Biotech) according to the manufacturer's protocol.

**RNA extraction and analysis**

Total RNA was isolated from cultured cells or embryonic liver using Trizol (#1029602, Invitrogen, Life technologies). cDNA synthesis was performed with MMLV reverse transcriptase (#28025-13, Invitrogen, Life technologies) according to the manufacturer's protocol. Gene expression was quantified by RT-qPCR using Kapa SYBR Fast 2X Universal Master Mix (#KK4601, Sopachem). For measuring microRNA expression, specific stem-loop primers were used for reverse transcription, and RT-qPCR was performed using a specific forward primer and a common universal reverse primer. The primers are listed in Supplementary Table 4. mRNA and miRNA levels were normalized with *β-Actin* or *Gapdh* and *Rnu6* or *Rnu1a,* respectively. $2^{-\Delta\Delta Ct}$ method was used for gene quantification in all figures except for Fig. 3 and Supplementary Figs. 3 and 4 for which $2^{-\Delta Ct}$ method was used.

For miRNA microarray analysis, 200 ng of RNA were labelled and hybridized to miRCURY LNA array ($7^{th}$ Gen) by Exiqon S/A Profiling Services (Exiqon, Vedbaek, Denmark). Three biological samples, each representing a pool of 20 livers, of Sox9-GFP+ and Sox9-GFP- cells labelled with Hy3 were compared. miRNAs with Benjamini-Hochberg adjusted p-values< 0.05 were selected.

For mRNA microarray, total RNA was extracted from cultured hepatoblasts transfected with either miR-337-3p mimic or mimic negative control #1 (n=3). 100 ng of RNA was hybridized to GeneChip Mouse Gene 2.0 ST Array (#902462, Affymetrix) following the manufacturer's protocol. Data were analysed with the Affymetrix Transcriptome Analysis Console (TAC) Software. Gene Set Enrichment Analysis was performed as described (Subramanian et al., 2005). Enriched pathways were identified by comparing differentially expressed genes to the hallmark gene sets from the Molecular Signature Database (MSigDB) (Liberzon et al., 2015).

**Cell culture and transfection**

Mouse hepatoblast cell lines were obtained from E12.5 embryos as described (Strick-Marchand and Weiss, 2002), with the following modifications. Livers were dissected, minced and washed in cold PBS, and digested as described above. Cell pellets were resuspended in 3 ml culture medium and plated onto a 6-cm dish coated with rat-tail collagen I (#08-115, Millipore). Four hours later the plate was washed extensively with PBS and medium was replaced. Medium consisted of RPMI (#31870-025, Gibco, Life technologies) supplemented with 10 % FBS (#F6178, Sigma-Aldrich), 50 ng/mL EGF (#AF-100-15, Peprotech), ITS 1X (#41400-045, Gibco, Lifetechnologies) and 30 ng/mL IGF-II (#100-12, Peprotech). Cultures were passaged every 3-4 days for 2-3 weeks. Medium was then changed twice per week until colonies of self-immortalized cells began to develop, typically within 3-8 weeks. Individual colonies were manually removed and plated onto collagen-coated wells.

For transfection, cultured hepatoblasts were plated in 24-well plates (50000 cells/well) coated with collagen and transfected 1 day later using Lipofectamine 2000 Transfection Reagent (#11668019, ThermoFisher Scientific). MicroRNAs were overexpressed by transfecting 500 ng of miRIDIAN microRNA mmu-miR-337-3p mimic (#C-310545-09-0005, Dharmacon), or miRIDIAN microRNA mmu-miR-200a-3p mimic (#C-310500-05-0005, Dharmacon), or 500 ng of miRIDIAN microRNA Mimic Negative Control #1 (#CN-001000-01, Dharmacon). MicroRNA inhibition was performed by transfecting 500 ng of miRIDIAN

microRNA mmu-miR-337-3p hairpin Inhibitor (IH-HMR-XX-0005, Dharmacon) ormiRIDIAN microRNA Hairpin Inhibitor Negative Control #1 (#IN-001005-01, Dharmacon). In dose-response experiments, miR-mimic control was added to miR-337-3p-mimic to obtain a constant amount of 750 ng miR-mimic in all conditions.

For signaling inhibitor assays, transfected hepatoblasts were cultured in dimethylsulfoxide (vehicle control) or in 50 µM of N-[2S-(3,5-difluorophenyl)acetyl]-L-alanyl-2-phenyl-1,1-dimethylethyl-ester-glycine, DAPT (#D5942, Sigma Aldrich) or 2 µM SB431542 (#S4317, Sigma Aldrich). RNA was extracted 48 h after transfection.

**Luciferase reporter assays**

For TGF-β reporter assays, 500 ng of miRNA mimics were co-transfected in cultured hepatoblasts with 100 ng of pCAGA12x-Luc vector (Plumb-Rudewiez et al., 2004) and 10 ng of pRL-CMV (Promega) as internal control.

For measuring the response of HNF4a 3'UTR to miRNA in luciferase assays, 400 ng of miRNA mimics were co-transfected with 15 ng of psiCHECK-3'UTR-HNF4a and 100 ng of pGL3-CMV-Luc (Promega) as internal control. For both, luciferase activities were measured after 48 h with a TD-20/20 luminometer (Promega) using the Dual-Luciferase Reporter Assay System (#E1910, Promega) according to manufacturer's protocol. Luciferase activities were expressed as the ratio of reporter activity to internal control activity.

**Western blotting, immunostaining and quantification**

For detection of STAT3 by western blotting, cultured hepatoblasts were plated in 6-well plates coated with collagen and transfected the next day with 2.5 µg miRNA mimics for 48 hours. Cell lysis and western blotting were as described in (Arts et al., 2015).

Immunostainings were performed on sections of formalin-fixed and paraffin-embedded embryos. Tissues were sectioned at 7 µm, deparaffinized and micro-wave heated for 10 min in 10 mM sodium citrate pH 6.0 for antigen retrieval. Sections were permeabilized for

5 min in 0.3% Triton X-100 in PBS before blocking for 45 min in 0.3% milk, 10% bovine serum albumin, 0.3% Triton X-100 in PBS. Primary and secondary antibodies (listed in Supplementary Table 5) were diluted in blocking solution and incubated at 4°C overnight and room temperature for 1 h, respectively. Pictures were taken with an Axiovert 200 fluorescent microscope using AxioVision system.

Apoptosis and proliferation were assessed in miR-337-3p Tg livers by cleaved-caspase 3 and phospho-histone H3 immunostaining. For each developmental time point, pictures from 5 randomly chosen areas per section were taken per mouse ($n \geq 4$ for both wild-type and miR-337-3p Tg livers). Counting was performed with Adobe Photoshop CS5. The percentage of cleaved-caspase 3 and phospho-histone H3 positive hepatoblasts was calculated by dividing the number of hepatoblasts positive expressing cleaved caspase 3 or phospho-histone H3 by the total number of HNF4$\alpha$ positive hepatoblasts.

To quantify the impact of miR-337-3p on biliary development, SOX9/HNF4/b-CAT triple staining was performed on E13.5 and E15.5 livers. Three wild-type and three miR-337-3p Tg livers were analysed. Pictures form 8 areas were taken per section, 4 around the hilum and 4 in the periphery of the livers. Counting was performed with Adobe Photoshop CS5. For each picture, portal vein periphery was measured (µm) using the measurement tool of the AxionVision image capture system and the number of bile ducts and of SOX9+ cells was normalised per portal vein. For counting of symmetrical and asymmetrical biliary structures, bile ducts were considered asymmetrical if containing at least one HNF4a+ cell.

**Mathematical model**

The mathematical model of the incoherent feedforward loop (IFFL) between miR-337-3p and Hnf4a is based on a set of 8 kinetic equations representing the time evolution of the expression level of each network component (Fig. 3 and Table 2). All reaction steps in the model rest on mass-action kinetics. The variables of the model are defined in Table S1. The description of the parameters and the numerical values used in the simulations are in Tables S2 and S3. The mathematical model is defined by explicit dynamic variables such as free mRNAs of Stat3 (*mSTAT3*) in Eq. [1], of Cebpa (*mCEBPA*) in Eq. [4], and of Hnf4a

(*mHNF4a*) in Eq. [7]. Protein form for each component is considered: total *STAT3* protein in Eq. [2], *CEBPA*in Eq. [5], and *HNF4A* in Eq. [8]. Finally, we also consider the inactive complexes between miR-337-3p and each mRNA: *mirmSTAT3* in Eq. [3] and *mirmcEBPA* in Eq. [6]. The free form of miR-337-3p, *miR337*, is considered as an input parameter of the model. All simulations were performed using XPPAUTO (http://www.math.pitt.edu/~bard/xpp/xpp.html). Parameter values and calibration of the mathematical model are described in Supplementary Information.

**Statistical analysis**

Data are presented as means ± SEM. Significance was assessed by non-paired Mann-Whitney test, except for Fig.1 (c-d) and Fig. S3 which were assessed by Kruskal-Wallis test.

## ACKNOWLEDGEMENTS

The authors thank F. Tronche for providing Alfp-Cre mice, and the members of the laboratory for discussions. The work of FPL was supported by the Interuniversity Attraction Pole Programme (Belgian Science Policy, PVII-47), the D.G. Higher Education and Scientific Research of the French Community of Belgium (ARC 15/20-065), and the F.R.S.-FNRS (Belgium: Grants T.007214 and J.0058.15). CD and AP held a fellowship from Télévie.

## AUTHOR CONTRIBUTIONS

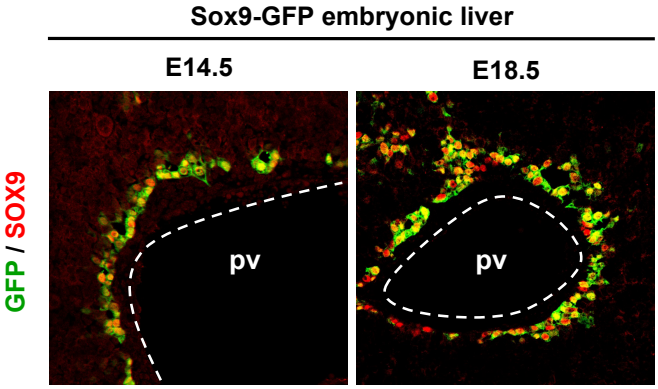
Performed the experiments: CD, CG, SC, YA, ND, IM. Conceived and designed experiments: CD, CG, AP, FL. Contributed material: BSP and IT. Wrote the paper: CD, CG, FL.

## COMPETING FINANCIAL INTERESTS

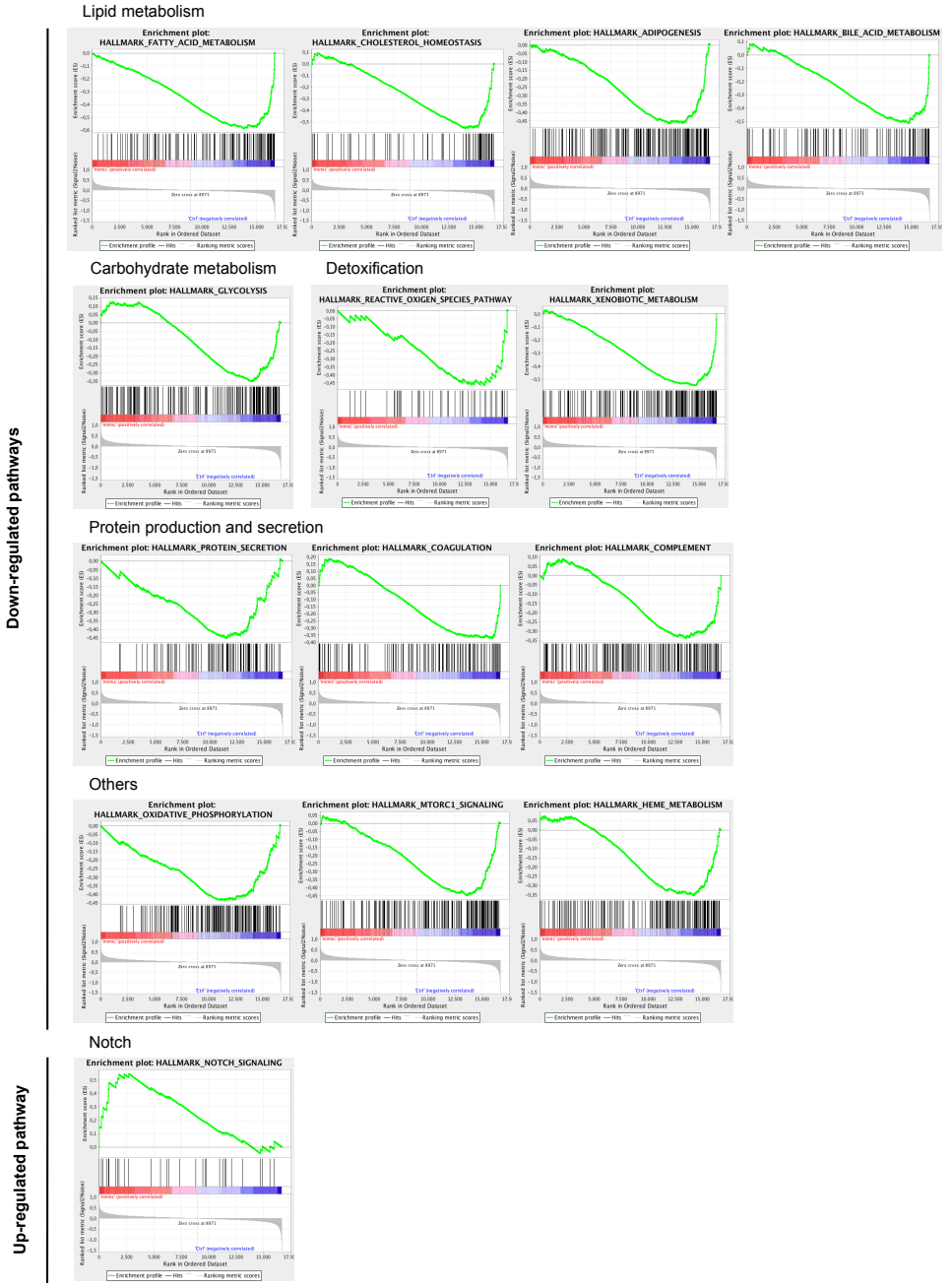
The authors declare no competing interest.

## SUPPORTING INFORMATION

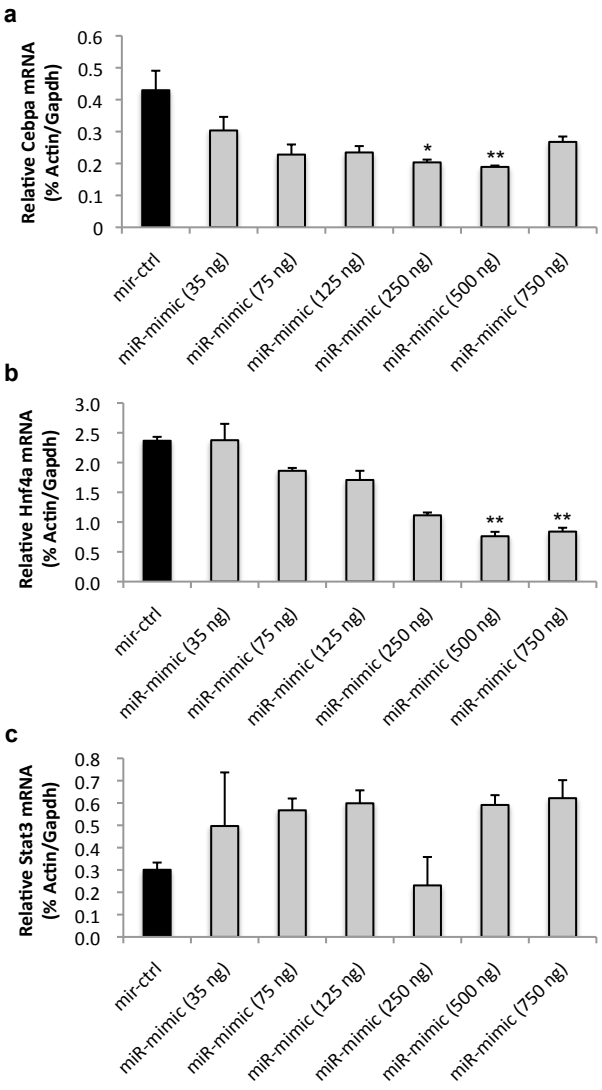
**Supplementary Figure 1. GFP expression is restricted to cholangiocytes in Sox9-GFP mice during development.** Immunostainings show that GFP expression co-localizes with the cholangiocyte marker SOX9 in liver from E14.5 and E18.5 Sox9-GFP embryos. pv = portal vein.



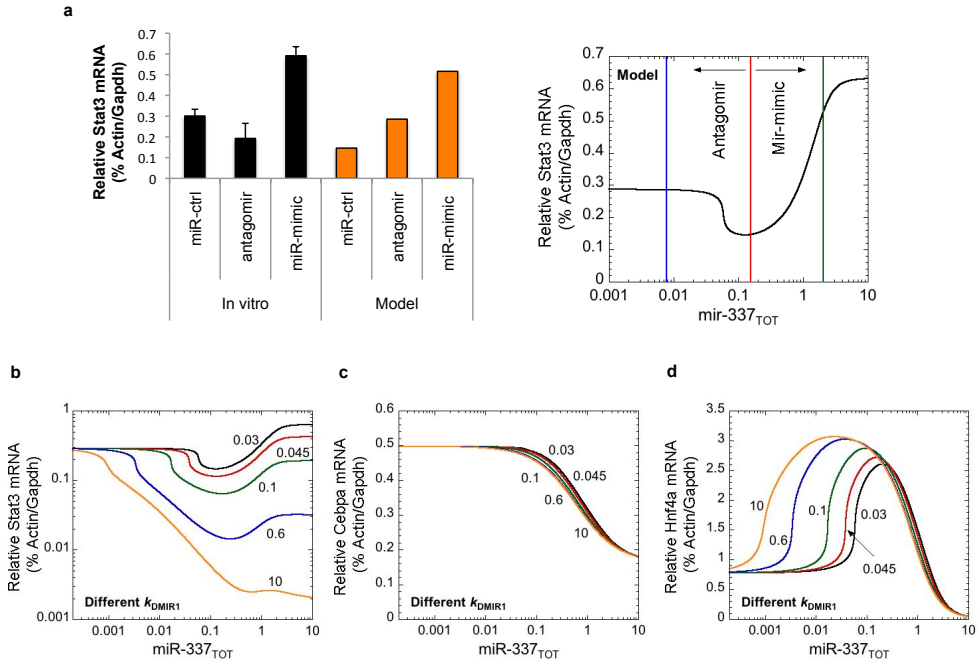
**Supplementary Figure 2. Gene Set Enrichment Analysis (GSEA) of cultured hepatoblasts transfected with miR-337-3p mimic.** GSEA reveals reduction of a broad range of hepatocyte metabolic functions and enrichment in genes involved in Notch signaling, a pathway stimulating cholangiocyte differentiation.



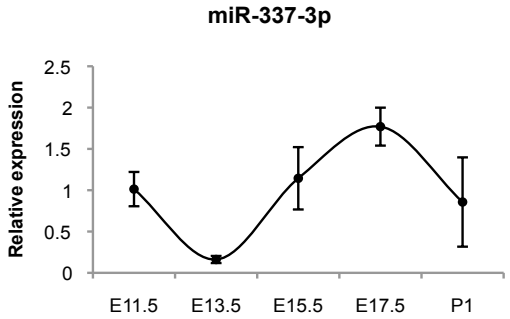
**Supplementary Figure 3. Dose-response of Cebpa, Hnf4a and Stat3 as a function of miR-337-3p.** Cultured hepatoblasts were transfected with increasing amounts of miR-337-3p mimic, as indicated, and Cebpa, Hnf4a and Stat3 mRNAs were measured by RT-qPCR.Data are mean ± SEM; *p<.05, **p<.01; n=3. Expression relative to the mean expression of Actin and Gapdh.



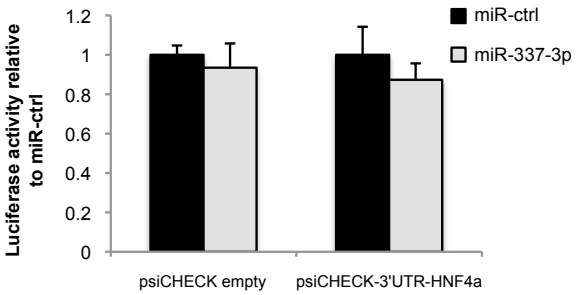
**Supplementary Figure 4. Effect of Stat3 expression profile on the biphasic dynamic levels of Hnf4a.**Expression of Stat3 mRNA (**a**) in cultured hepatoblasts transfected with miR-337-3p mimics or antagomirs was consistent with the output of a quantitative mathematical model predicting a biphasic expression of Hnf4a. Vertical red, blue and green lines in the right panel correspond to the control, antagomir or miR-mimic conditions. Predicted steady-state levels of Stat3 (**b**), Cebpa (**c**) and Hnf4a (**d**) mRNAs are shown for different degradation rates of the inactive complex between Stat3 mRNA and miR-337-3p, $k_{DMIR1}$. Data are mean ± SEM; *p<.05, **p<.01, ***p<.001; n=3. Expression relative to the mean expression of Actin and Gapdh. Parameter values used in the mathematical model are in Supporting Information.



**Supplementary Figure 5. Temporal expression of miR-337-3p.** MiR-337-3p expression during liver development. n≥4 for each time point




**Supplementary Figure 6. No evidence for direct targeting of Hnf4a gene by miR-337-3p.** Cultured hepatoblasts were co-transfected with the psiCHEK-3'UTR-HNF4a construct and with miR-337-3p mimic. MiR-337-3p did not affect luciferase activity controlled by an Hnf4a 3'UTR sequence predicted to bind miR-337-3p. Data are mean ± SEM; n=3.



**Detailed description and calibration of the mathematical model**

Each component of the IFFL in the model is calibrated with its corresponding expression levels in the different *in vitro* conditions (control, miR-337-3p antagomir and miR-mimic). The expression levels of the different mRNAs measured by RT-qPCR correspond to the total forms of each component. These levels are expressed relative to the percentage of Actin/Gapdh (expression is relative to the mean expression of Actin and Gapdh). In the mathematical model, these total forms can be calculated as follow:

$$miR337_{TOT} = miR337 + mirmSTAT3 + mirmcEBPA$$

$$mcEBPA_{TOT} = mcEBPA + mirmcEBPA$$

$$mSTAT3_{TOT} = mSTAT3 + mirmSTAT3$$

Thus, we calibrate the mathematical model by comparing the expression levels of the total forms of each component with their corresponding in vitro expression data. The steady-state expression level of each component is given by the balance between its rate of synthesis and its rate of degradation. Half-life of the mRNA and protein for each component is based on the literature (Supplementary Table 3). As previously observed experimentally [1], we also consider in the mathematical model that CEBPA can regulate its own synthesis (see Eq (4) in Table 2).

The existence of the IFFL between miR-337-3p and Hnf4a is a necessary but not sufficient condition to generate a biphasic behavior characterized by a maximum Hnf4a expression. In addition, we need to assume that the kinetics of association between miR-337-3p and Stat3 mRNA (activation pathway) is higher than the association kinetics between miR-337-3p and Cebpa messenger RNA (inhibition pathway). Such assumption ($k_1 > k_3$) ensures the presence of a maximum in the expression level of Hnf4a as a function of miR-337-3p. Indeed, at low levels of miR-337-3p, an increase in miR-337-3p preferentially promotes its binding to Stat3 messenger RNA, which favors the activation pathway and the rise in

Hnf4a; while at higher levels of miR-337-3p, Cebpa messenger RNA will also bind to miR-337-3p, eliciting the inhibition pathway and a decrease in Hnf4a.

Finally, *in vitro* data indicate that the expression of Stat3 mRNA increases in the presence of miR-337-3p-mimic,while its protein level decreases in the same condition (Fig. 3e and Supplementary Fig. 4a). To account for such counter-intuitive dynamical behavior, we assume that the complex consisting of mSTAT3 bound to miR-337-3p, mirmSTAT3, is not rapidly degraded (small $k_{DMIR1}$). Thus miR-337-3p is able to inhibit STAT3 protein synthesis by forming a stable complex with its mRNA but will not rapidly induce mRNA degradation. A small $k_{DMIR1}$ is crucial to observe a rise in Stat3 mRNA expression in vitro in the presence of miR-337-3p mimic, but is not needed to observe the biphasic expression behavior of Hnf4a as a function of miR-337-3p level, since increasing the degradation rate $k_{DMIR1}$ predicts that Stat3 mRNA will decrease as a function of miR-337-3p, while keeping a biphasic response of HNF4 (Supplementary Fig. 4b-d).

**Supplementary Table 1: Variables of the mathematical model**

| Equations | Symbol | Definition |
|---|---|---|
| 1 | *mSTAT3* | Free form of Stat3 messenger RNA |
| 2 | *STAT3* | Total form of the protein STAT3 |
| 3 | *mirmSTAT3* | Inactive complex between mSTAT3 and miR337-3p |
| 4 | *mcEBPA* | Free form of Cebpamessenger RNA |
| 5 | *cEBPA* | Transcription factor CEBPA |
| 6 | *mirmCEBPA* | Inactive complex between mCEBPA and miR337-3p |
| 7 | *mHNF4a* | Free form of HN4amessenger RNA |
| 8 | *HNF4a* | Transcription factor HNF4a |

**Supplementary Table 2: Parameters of the mathematical model**

| Symbol | Definition | Numerical value* |
|---|---|---|
| *miR337* | Free form of the microRNA miR-337-3p | 0.05: miR-ctrl<br>0.001: miR-antagomir<br>1.35: miR-mimic |
| $V_{SM1STAT3}$ | Basal transcription rate of Stat3 messenger RNA | 0.001 |
| $V_{SM2STAT3}$ | Transcription rate of Stat3 messenger RNA<br>repressed by HNF4a | 0.018 |
| $k_1$ | Bimolecular rate constant for binding of mSTAT3 to miR-337 | 12 |
| $k_2$ | Rate constant for dissociation of complex (mirmSTAT3) between mSTAT3 and miR-337-3p | 0.5 |
| $k_3$ | Bimolecular rate constant for binding of miR-337-3p to mcEBPA | 0.25 |
| $k_4$ | Rate constant for dissociation of complex (mirmcEBPA) between miR-337-3p and mcEBPA | 0.01 |
| $k_{DMSTAT3}$ | Rate constant for degradation of Stat3 messenger RNA | 0.054 |
| $k_{SSTAT3}$ | Rate constant for STAT3 translation | 88 |
| $k_{DSTAT3}$ | Rate constant for degradation of STAT3 protein | 0.031 |
| $k_{DMIR1}$ | Rate constant for degradation of mirmSTAT3 | 0.03 |
| $k_{DMIR2}$ | Rate constant for degradation of mirmcEBPA | 0.4 |
| $V_{SM1HNF4A}$ | Basal transcription rate of Hnf4a | 0.001 |
| $V_{SM2HNF4A}$ | Transcription rate of Hnf4a regulated by STAT3 and CEBPA | 0.3 |
| $k_{DMHNF4A}$ | Rate constant for degradation of Hnf4a messenger RNA | 0.067 |
| $k_{SHNF4A}$ | Rate constant for HNF4A translation | 206 |
| $k_{DHNF4A}$ | Rate constant for degradation of HNF4Aprotein | 0.074 |

| | | |
|---|---|---|
| $V_{SM1CEBPA}$ | Basal transcription rate of Cebpa | 0.065 |
| $V_{SM2CEBPA}$ | Transcription rate of Cebparegulated by itself | 0.015 |
| $k_{DMCEBPA}$ | Rate constant for degradation of Cebpamessenger RNA | 0.133 |
| $k_{SCEBPA}$ | Rate constant for CEBPA translation | 2000 |
| $k_{DCEBPA}$ | Rate constant for degradation of CEBPAprotein | 0.69 |
| $K_{IHNF4}$ | Constant for inhibition of STAT3 synthesis by HNF4A | 4400 |
| $K_{ISTAT3}$ | Constant for inhibition of Hnf4a transcription by STAT3 | 460 |
| $K_{A1CEBPA}$ | Constant for activation of Hnf4a transcription by CEBPA | 935 |
| $K_{A2CEBPA}$ | Constant for auto-activation of Cebpa transcription | 4975 |
| *n* | Coefficient of cooperativity mediated by the oligomerization of transcription factors (HNF4A, STAT3 or CEBPA) needed to promote the transcription of messenger RNA | 2 |

*The dynamic variables of the mathematical model are expressed relative to the percentage of the housekeeping genes, Actin and Gapdh, and are thus dimensionless. The time unit of the rate constants is in inverse hour ($h^{-1}$).

**Supplementary Table 3: Calibration of the mathematical model**

| | STAT3 | HNF4A | CEBPA |
|---|---|---|---|
| **Experimental mRNA half-life duration (h)** | 12.75 | 10.33 | 5.22 |
| **Experimental protein half-life duration (h)** | 22.12 | 9.4 | 1 |
| **Experimental Protein/mRNA ratio** | 1325 | 2800* | 2800* |
| **Free mRNA half-life duration in the model (h)** | 12.84 | 10.34 | 5.21 |
| **Protein half-life duration in the model (h)** | 22.36 | 9.37 | 1 |
| **Protein/mRNA ratio in the model** | 1327 | 2784 | 2794 |
| **References** | [2] | [3, 4] | [4, 5] |

*mean value of the protein/mRNA ratio measured in 5000 different genes [2].

**Supplementary Table 4: List of primer sequences used for RT-qPCR.**

| Gene | Primer sequence (5' ➔ 3') |
|---|---|
| β-Actin | Fw - TCCTGAGCGCAAGTACTCTGT<br>Rev - CTGATCCACATCTGCTGGAAG |
| Gapdh | Fw - GGTCCTCAGTGTAGCCCAAG<br>Rev - AATGTGTCCGTCGTGGATCT |
| Rnu6 | Fw - CTCGCTTCGGCAGCACA<br>Rev - AACGCTTCACGAATTTGCGT |
| Rnu1a | Fw - CCATGATCACGAAGGTGGTT<br>Rev - ATCCGGAGTGCAATGGATAA |
| Alb | Fw - GCTGAGACCTTCACCTTCCA<br>Rev - TCTTCAGTTGCTCCGCTGTA |
| Ttr | Fw - GGGCTCACCACAGATGAGAA<br>Rev - CAGAGTCGTTGGCTGTGAAA |
| Hnf4a | Fw - AGCTCGAGGCTCCGTAGTGTTT<br>Rev - GAAAATGTGCAGGTGTTGACCA |
| Afp | Fw - GGAGGCTATGCATCACCAGT<br>Rev - CATGGTCTGTAGGGCTTTGC |
| Cebpa | Fw - GCAGTGTGCACGTCTATGCT<br>Rev - AGCCCACTTCATTTCATTGG |
| Opn | Fw - TGAGATTGGCAGTGATTTGC<br>Rev - CTGCTTCTGAGATGGGTCAG |
| Sox9 | Fw - CAAGACTCTGGGCAAGCTCTG<br>Rev - TCCGCTTGTCCGTTCTTCAC |

| | |
|---|---|
| Sox4 | Fw - GAACGCCTTTATGGTGTGGT<br>Rev - GAACGGAATCTTGTCGCTGT |
| Hey1 | Fw - CATGAAGAGAGCTCACCCAGA<br>Rev - CGCCGAACTCAAGTTTCC |
| Hes1 | Fw - TGAAAACACTGATTTTGGATGC<br>Rev - GCTCGGGTCTGTGCTGAG |
| Hnf1b | Fw - GAAAGCAACGGGAGATCCTC<br>Rev - GACTGCCCAGGCCCCTGGTTCTGT |
| Foxa2 | Fw - CTCCGTGTCAGGAGCACAAG<br>Rev - GTGGCTGTGGTGATGTTGCT |
| Lrh1 | Fw - TGGTGGAAGGTGTCCAAGAG<br>Rev - GCAGCATCTCAATGAGGAGG |
| Hnf6 | Fw - TTCCAGCGCATGTCGGCGCTC<br>Rev - GGTACTAGTCCGTGGTTCTTC |
| Hnf1a | Fw - TATCAGCAGCCTCTCATGCC<br>Rev - TGAGGTGAAGACCTGCTTGG |
| ApoB | Fw - CTGGATTCGAGCACAGATGA<br>Rev - GCC-AGCAATCTGGAAGCTG |
| Cyp2d26 | Fw - TTCAAAAGCCTGGAAGCAGT<br>Rev - TCCACCAGAAGCAGGAAGAT |
| miR-200a-3p | Fw - ACACTCCAGCTGGGTAACACTGTCTGGTAA<br>Rev - CTCAACTGGTGTCGTGGAGTCGGCAATTCAGTTGAGACATCGTT |
| miR-192-5p | Fw - ACACTCCAGCTGGGCTGACCTATGAA<br>Rev - CTCAACTGGTGTCGTGGAGTCGGCAATTCAGTTGAGGGCTGTCAATT |

| | |
|---|---|
| miR-194-5p | Fw - ACACTCCAGCTGGGTGTAACAGCAACTCCA<br>Rev - CTCAACTGGTGTCGTGGAGTCGGCAATTCAGTTGAGTCCACATG |
| miR-377-3p | Fw - ACACTCCAGCTGGGATCACACAAAGGCAAC<br>Rev - CTCAACTGGTGTCGTGGAGTCGGCAATTCAGTTGAGACAAAAGT |
| miR-30a-5p | Fw - ACACTCCAGCTGGGTGTAAACATCCTCGAC<br>Rev - CTCAACTGGTGTCGTGGAGTCGGCAATTCAGTTGAGCTTCCAGT |
| miR-665-3p | Fw - ACACTCCAGCTGGGACCAGGAGGCTGAGG<br>Rev - CTCAACTGGTGTCGTGGAGTCGGCAATTCAGTTGAGAGGACCT |
| miR-337-3p | Fw - ACACTCCAGCTGGGTTCAGCTCCTATATGAT<br>Rev - CTCAACTGGTGTCGTGGAGTCGGCAATTCAGTTGAGAAAGGCATCA |

**Supplementary Table 5: List of primary and secondary antibodies used for immunostaining experiments.**

| Primary antibody | Species | Dilution | Source | Reference |
|---|---|---|---|---|
| HNF4a | Mouse IgG2 | 1/350 | R&D Systems | PP-H1415-00 |
| SOX9 | Rabbit | 1/500 | Chemicon | AB5535 |
| HNF6 | Guinea Pig | 1/10000 | Described in [6] | / |
| HNF1b | Rabbit | 1/200 | Santa Cruz | SC-22840 |
| DLK1 | Rabbit | 1/200 | Abcam | ab21682 |
| Cleaved Caspase 3 | Rabbit | 1/200 | Cell Signaling | 9661 |
| Phospho Histone H3 | Rabbit | 1/100 | Cell Signaling | 9701 |
| CK19 | Rat | 1/50 | Developmental Studies Hybridoma Bank | TROMA III |
| GFP | Goat | 1/250 | Abcam | Ab6673 |

| Secondary antibody | Species | Dilution | Source | Reference |
|---|---|---|---|---|
| Alexa Fluor 488 anti-rabbit | Donkey | 1/1000 | Invitrogen | A-21206 |
| Alexa Fluor 647 anti-mouse IGg2 | Goat | 1/1000 | Invitrogen | A-21235 |
| Alexa Fluor 594 anti-rat | Donkey | 1/1000 | Invitrogen | A-21209 |
| Alexa Fluor 594 anti-rabbit | Donkey | 1/1000 | Invitrogen | A-21207 |
| Alexa Fluor 594 anti-guinea pig | Goat | 1/1000 | Invitrogen | A-11076 |
| Alexa Fluor 594 anti-goat | Donkey | 1/1000 | Invitrogen | A-11058 |

## Supplementary references


1. Christy RJ, Kaestner KH, Geiman DE, Lane MD. CCAAT/enhancer binding protein gene promoter: binding of nuclear factors during differentiation of 3T3-L1 preadipocytes. Proceedings of the National Academy of Sciences of the United States of America 88, 2593-2597 (1991).

2. Schwanhausser B, et al. Global quantification of mammalian gene expression control. Nature 473, 337-342 (2011).

3. Hong YH, Varanasi US, Yang W, Leff T. AMP-activated protein kinase regulates HNF4alpha transcriptional activity by inhibiting dimer formation and decreasing protein stability. The Journal of biological chemistry 278, 27495-27501 (2003).

4. Sharova LV, Sharov AA, Nedorezov T, Piao Y, Shaik N, Ko MS. Database for mRNA half-life of 19 977 genes obtained by DNA microarray analysis of pluripotent and differentiating mouse embryonic stem cells. DNA research : an international journal for rapid publication of reports on genes and genomes 16, 45-58 (2009).

5. Shim M, Smart RC. Lithium stabilizes the CCAAT/enhancer-binding protein alpha (C/EBPalpha) through a glycogen synthase kinase 3 (GSK3)-independent pathway involving direct inhibition of proteasomal activity. The Journal of biological chemistry 278, 19674-19681 (2003).

## 2. EXPRESSION OF MOLECULAR DIFFERENTIATION MARKERS DOES NOT CORRELATE WITH HISTOLOGICAL DIFFERENTIATION GRADE IN INTRAHEPATIC CHOLANGIOCARCINOMA

I performed the experiments of all figures. I contributed to study design, acquisition of data, analysis and interpretation of data and writing the manuscript.

**CONTEXT:** The main goal of the thesis was to investigate the role of miRNAs during hepatic cell differentiation. In that context, we studied their role in iCCAs, which are characterized by cell differentiation abnormalities. In iCCA, the prognostic worsens when tumors are poorly differentiated. However, we found that regardless of the histological status, the expression of cholangiocyte differentiation markers does not correlate with prognosis. Therefore, in this second paper, we searched for a correlation between these differentiation markers (including miRNAs) and the histological grade of the tumors, in order to improve the prognosis value of differentiation criteria.

# EXPRESSION OF MOLECULAR DIFFERENTIATION MARKERS DOES NOT CORRELATE WITH HISTOLOGICAL DIFFERENTIATION GRADE IN INTRAHEPATIC CHOLANGIOCARCINOMA

Céline Demarez[1], Catherine Hubert[2], Christine Sempoux[3], Frédéric P. Lemaigre[1,*]

[1]de Duve Institute, Université catholique de Louvain, Avenue Hippocrate 75, B-1200 Brussels, Belgium

[2]Division of Hepato-Biliary and Pancreatic Surgery, Department of Abdominal Surgery and Transplantation, Cliniques universitaires Saint-Luc

[3]Service de Pathologie Clinique, Centre Hospitalier Universitaire Vaudois, CH-1011 Lausanne, Switzerland

*Corresponding author: Avenue Hippocrate 75/B1-7503, B-1200 Brussels, Belgium. Tel: +32 2 764 7583; Fax: +32 2764 7507; frederic.lemaigre@uclouvain.be

## ABSTRACT

The differentiation status of tumor cells, defined by histomorphological criteria, is a prognostic factor for survival of patients affected with intrahepatic cholangiocarcinoma (ICC). To strengthen the value of morphological differentiation criteria, we wished to correlate histopathological differentiation grade with expression of molecular biliary differentiation markers and of microRNAs previously shown to be dysregulated in ICC. We analysed a series of tumors that were histologically classified as well, moderately or poorly differentiated, and investigated the expression of cytokeratin 7, 19 and 903 (*CK7*, *CK19, CK903*), SRY-related HMG box transcription factors 4 and 9 (*SOX4, SOX9*), osteopontin (*OPN*), Hepatocyte Nuclear Factor-1 beta (*HNF1β*), Yes-associated protein (*YAP*), Epithelial cell adhesion molecule (*EPCAM*), Mucin 1 (*MUC1*) and N-cadherin (*NCAD*) by qRT-PCR and immunostaining, and of *miR-31, miR-135b, miR-132, miR-200c, miR-221* and *miR-222*. Unexpectedly, no correlation was found between the expression of these molecular markers and histopathological differentiation grade. Therefore, our data point toward necessary caution when predicting the evolution and prognosis of ICC on the basis of cell differentiation criteria.

## INTRODUCTION

Intrahepatic cholangiocarcinoma (ICC) is the second most common primary tumor of the liver. It represents less than 10% of cholangiocarcinoma cases, but in contrast to perihilar and distal cholangiocarcinoma, its incidence and mortality rates are rising (Khan et al., 2012; Razumilava and Gores, 2014; Wadsworth et al., 2013). When evaluating disease progression, several prognostic factors were proposed. These include tumor size, surgical strategy, serum markers, TNM staging, histological features, mutational profiles, gene expression signatures (mRNA, microRNA, lncRNA), or expression of individual genes at the mRNA, miRNA or protein level. Prognostic factors can also be evaluated combinatorially, for instance in the format of nomograms, to improve their prognostic value (Hyder et al., 2014).

Because of its ease of use in the clinic, differentiation of ICC is an often considered prognostic factor. Histopathologically, the proportion of gland formation serves as a differentiation criterium: well-differentiated tumors, which are associated with better survival, exhibit greater than 95% glandular tissue, moderately differentiated tumors show 50% to 95% gland formation, and poorly differentiated tumors have less than 50% glandular tissue (Fan et al., 2011; Mazur et al., 2012; Plieskatt et al., 2014; Uenishi et al., 2003). Interestingly, a number of markers that qualify as molecular differentiation markers because they were shown to promote differentiation of cholangiocytes or to be expressed specifically in the biliary lineage correspond to ICC prognostic factors. One would therefore expect that expression of molecular differentiation markers would overlap with the prognostic value of ICC. Consistently, Mazur and coworkers found that the transcription factor SRY-related HMG box transcription factor 9 (*SOX9*), which is required for bile duct morphogenesis and cholangiocyte polarity, is a prognostic factor for survival (Mazur et al., 2012). Moreover, Terashi *et al.* showed that lack of osteopontin (*OPN*), which is expressed in the cholangiocytes and not in hepatocytes (Antoniou et al., 2009a), is associated with poor patient outcome (Terashi et al., 2004). However, *SOX9* was not confirmed as a predictor of better survival in a different study (Matsushima et al., 2015), and not all molecular differentiation markers have a prognostic value: *HNF1β*,

which is cholangiocyte-specific in adult liver and which stimulates biliary development (Coffinier et al., 2002), is not associated with survival rate of ICC (Mazur et al., 2012; Yu et al., 2015). Again, Wang and coworkers showed that the transcription factor *SOX4*, which promotes cholangiocyte differentiation and bile duct formation (Poncy et al., 2015a), is unexpectedly a factor for poor prognosis of ICC (Wang et al., 2014).

These observations highlight a discrepancy between the prognostic value and the expression of molecular differentiation markers and prompted us to consider that the expression of molecular markers of cholangiocyte differentiation would have a stronger predicting value if supported by histopathological differentiation criteria. Here we analysed a cohort of surgically resected ICCs and verified if histopathological differentiation grade is correlated with expression of molecular differentiation markers. For the latter, our analysis included transcription factors that are well characterized as differentiation regulators. We also included a set of microRNAs (miRNAs) which have been shown to be differentially expressed between the different tumor grades (Plieskatt et al., 2014). Indeed, miRNAs are involved in cholangiocarcinoma where they modulate apoptosis, proliferation, migration and response to therapy (Munoz-Garrido et al., 2012; Papaconstantinou et al., 2012; Szabo and Bala, 2013; Wang et al., 2012) and several investigators characterized miRNA expression profiles in ICC to identify miRNA signatures for improved diagnosis and prognosis (Chen et al., 2009; Karakatsanis et al., 2013; Kawahigashi et al., 2009; Meng et al., 2006; Zhang et al., 2015).

Surprisingly, we found that molecular differentiation markers are expressed at similar levels regardless of the differentiation status of the tumor. Therefore, our data highlight a disparity between molecular- and histology-based classification and suggest caution when classifying ICC tumor samples.

**Table 1. Characteristics of tumors samples**

| ICC | |
|---|---|
| Size | 2-16 cm (mean= 5.9) |
| Macroscopic type | 17 mass forming<br>1 periductal infiltrative |
| Microscopic differentiation | 5 well-differentiated<br>6 moderately differentiated<br>6 poorly differentiated<br>1 with both well and poorly differentiated area |
| Mucin production | 5 present<br>13 absent |
| Background liver | 3 with cirrhosis<br>15 without cirrhosis |
| Pathological stage | 4 pT1N0; 2 pT1N1<br>6 pT2aN0; 1 pT2aN1<br>2 pT2bN0; 2 pT2bN1<br>1 pT4N1 |

## RESULTS

### Selection of tumor samples

We histologically classified 18 ICC samples from 16 patients (12 men and 4 women; age 39-75, mean: 60.2) as well (containing 95% glandular tissue), moderately (50% to 95% gland formation) or poorly differentiated (less than 50% glandular tissue) (Fig. 1A-C). None of the patients were receiving treatment, except for one of the two patients with a recurrence and who was treated with Gemcitabine. In one patient, the ICC contained both a well and a poorly differentiated area that were analysed separately. Two patients experienced a recurrence and each second tumor was also studied separately, leading to a total number of 19 samples of ICC characterized for their histological differentiation. We selected tumor areas in which *CK7*-positive cells represented more than 50% of the tumor surface (Fig. 1D-F), in order to reduce the contamination of epithelial cancer cells by non-epithelial cells during the RNA extraction procedure (see below). Tumor characteristics are described in Table 1.

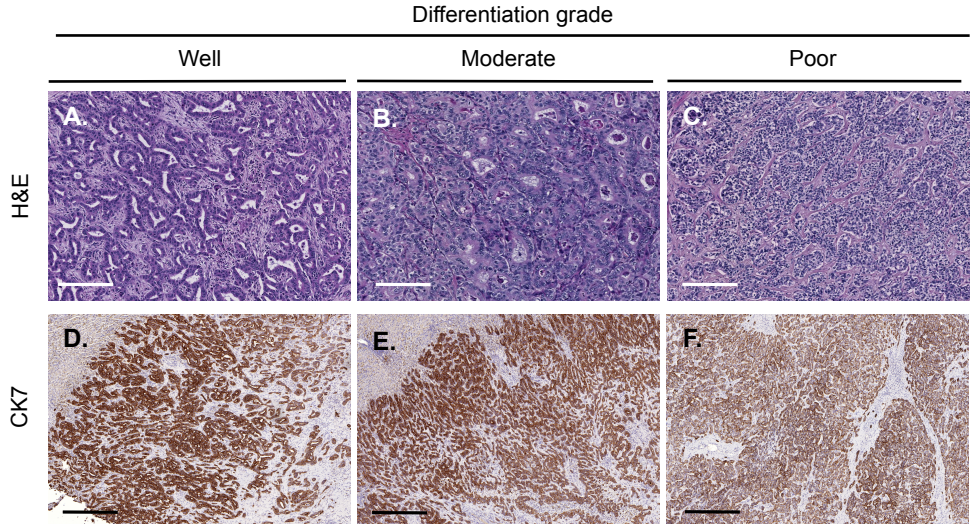



**Figure 1. Tumor classification and selection of tumor areas with high density of *CK7*+ cells. (A-C)** Tumors were classified as well-, moderately- and poorly-differentiated. **(D-F)** Immunohistochemical detection of *CK7* in representative histologically-graded ICCs. Areas with at least 50% of *CK7*

staining were selected for further RNA extraction and immunofluorescence stainings. White scale bars = 200 µm. Black scale bars = 500 µm

**Molecular differentiation markers in ICC: mRNA and microRNA expression**

To look for a potential correlation between histopathological differentiation grade and molecular differentiation markers in ICC, we measured the expression of the latter in the tumor samples. We focused on transcription factors that were shown to be stimulators of biliary differentiation. Total RNA was extracted from formalin-fixed paraffin-embedded tissue: ICC tissue was delineated using *CK7* and H&E staining in the adjacent sections, and non-tumor *CK7*-negative tissue from a distant sample of the same surgical specimen was used as control. We then measured by qRT-PCR the expression of biliary differentiation markers (*SOX4, SOX9, and HNF1*$\beta$) and of the hepatocyte marker *HNF4*$\alpha$. All biliary markers were expressed at lower levels in the tumor tissue than in the adjacent non-tumor tissue (Fig. 2A). *HNF4*$\alpha$ was low, confirming that the tumor samples were not contaminated with significant levels of hepatocytes.

Importantly, our analysis showed that none of the tested markers correlated with histological differentiation grade (Fig. 2B). In addition, when the ratio of expression in tumor *versus* non-tumor tissue was analysed, again no correlation was found between molecular marker expression and histological grade of the ICCs (Fig. 2C).

Since the transcription factors tested above did not correlate with ICC histological grade, we measured the expression of other markers (*OPN, MUC1, CK903, YAP, EPCAM, NCAD* and *CK19*) that are known to be biliary-specific and associated with ICC (Aishima et al., 2002; Braicu, 2009; Marti et al., 2015; Mosnier et al., 2009; Pei et al., 2015; Sirica et al., 2009; Sulpice et al., 2014). All those markers were expressed at lower levels in the tumor tissue than in the adjacent non-tumor tissue (Fig. 3A). Moreover, as observed previously, we did not found any correlation between the biliary markers and the histological grade of the tumors (Fig. 3B). Again, when considering the ratio of expression in tumor versus non-tumor tissue, no correlation was found (Fig. 3C).

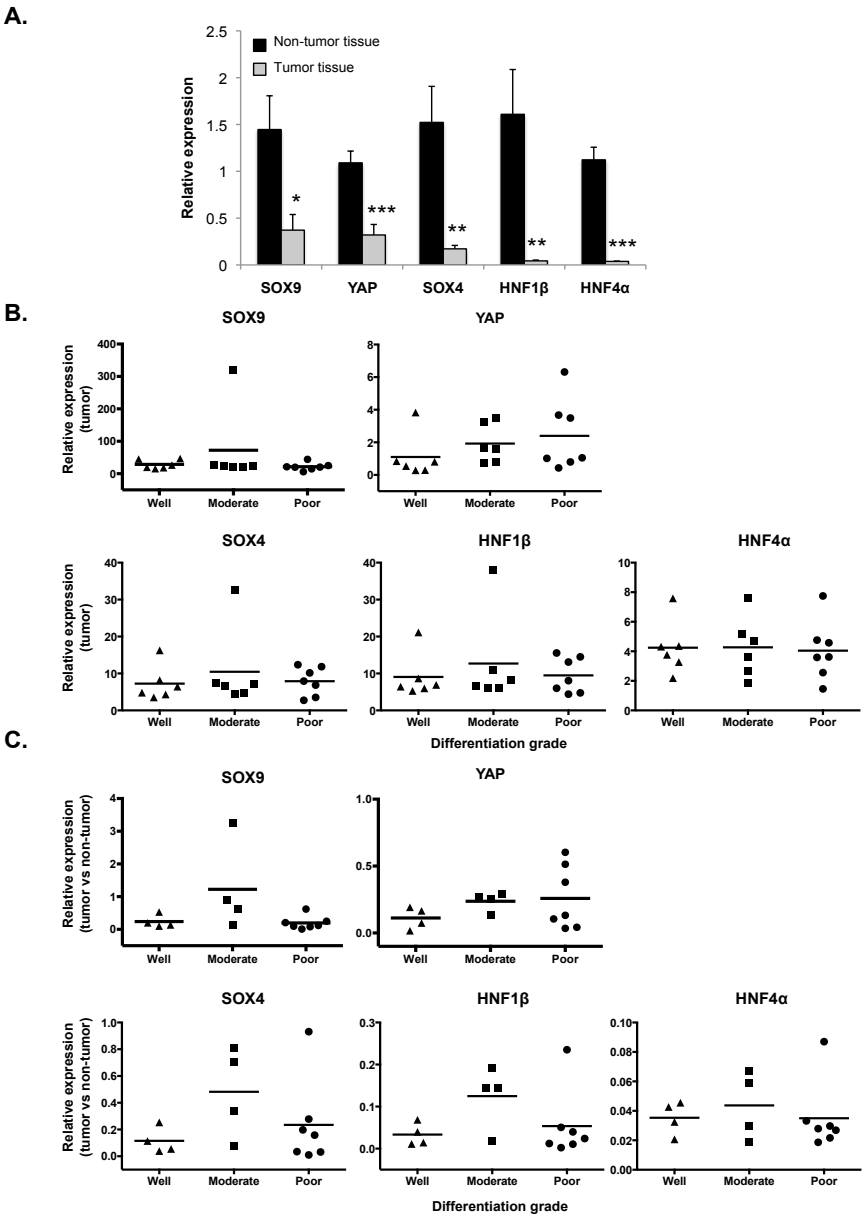



**Figure 2. Molecular biliary differentiation markers are not differentially expressed among histologically-graded iCC's. (A)** All biliary differentiation markers are expressed (qRT-PCR) at lower levels in ICC as compared to distant non-tumoral tissue. Low levels of *HNF4α* indicate lack of significant contamination with normal hepatocytes. (Mean ± SEM; *p<0.05, **p<0.01, ***p<0.001). **(B-C)** Lack of correlation between molecular differentiation marker expression and tumor grade when comparing **(B)** ICC samples or **(C)** the ratio of expression in tumor versus non-tumor tissue. Dots represent individual ICC samples and horizontal bars represent the mean of the samples.

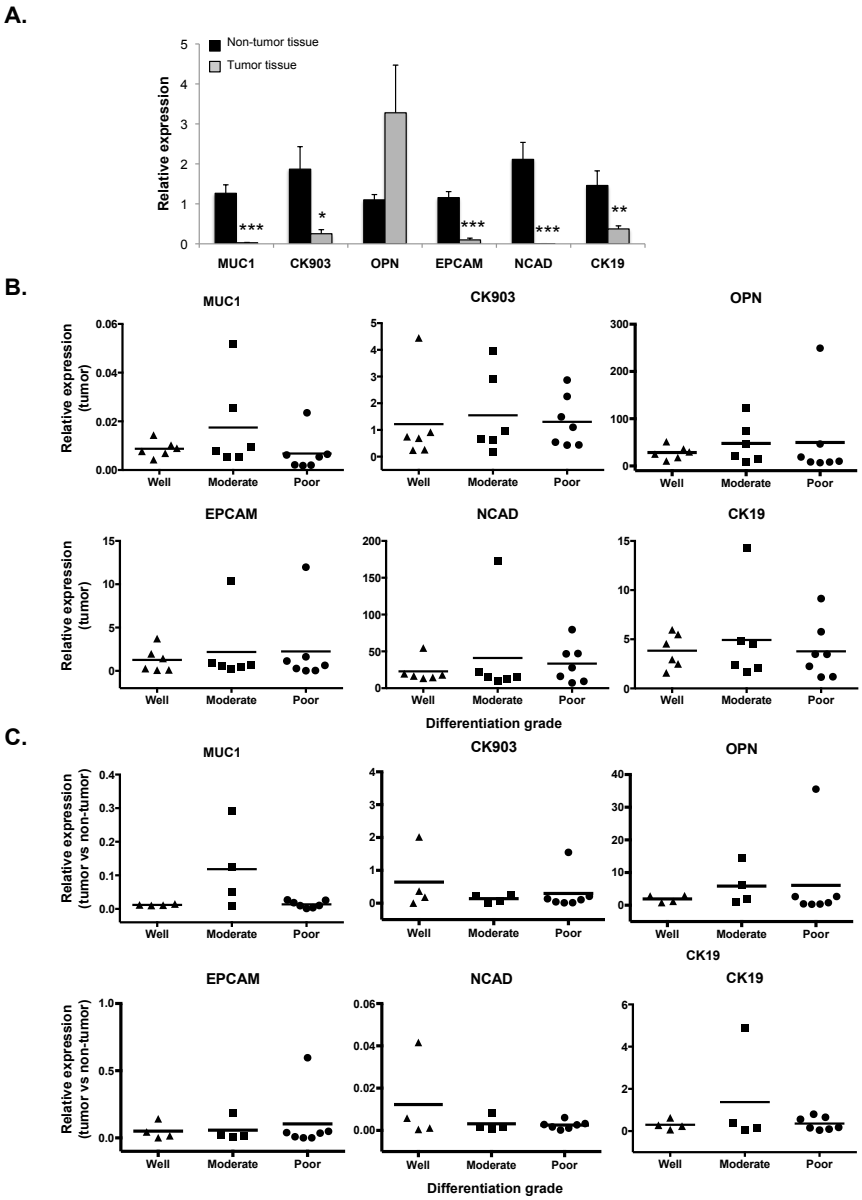



**Figure 3. Biliary-specific proteins are not differentially expressed among histologically-graded iCC's. (A)** All markers are expressed (qRT-PCR) at lower levels in ICC as compared to distant non-tumoral tissue. (Mean ± SEM; *p<0.05, **p<0.01, ***p<0.001). **(B-C)** Lack of correlation between molecular differentiation marker expression and tumor grade when comparing **(B)** ICC samples or **(C)** the ratio of expression in tumor versus non-tumor tissue. Dots represent individual ICC samples and horizontal bars represent mean of the samples.

We next investigated the expression of miRNAs in our ICC samples. Several studies have compared the expression of miRNAs in ICC and control tissue (Chen et al., 2009; Karakatsanis et al., 2013; Kawahigashi et al., 2009; Meng et al., 2006; Zhang et al., 2015). We here analysed miRNAs that were found to be dysregulated in earlier studies in which control tissue was compared with ICC, and whose dysregulation has been correlated with histological differentiation grade of ICCs (Table 2) (Plieskatt et al., 2014).

**Table 2.Selection of microRNAs associated with ICC differentiation grade.**

| microRNA | Dysregulation in ICC | Differential expression between ICC histological-grades[Plieskatt et al., 2014] |
|---|---|---|
| **miR-200c** | Up-[Plieskatt et al., 2015; Plieskatt et al., 2014] or Down-[Chen et al., 2009; Karakatsanis et al., 2013]regulated | Moderate > Well (FC=9,6) |
| **miR-221** | Up-[Plieskatt et al., 2015; Plieskatt et al., 2014] or Down-[Karakatsanis et al., 2013]regulated | Moderate > Well (FC=4,6) |
| **miR-31** | Up-[Plieskatt et al., 2015; Plieskatt et al., 2014] or Down-[Karakatsanis et al., 2013]regulated | Moderate > Well (FC=60,3) |
| **miR-222** | Down-regulated[Chen et al., 2009; Karakatsanis et al., 2013] | Moderate > Well (FC=4,8) |
| **miR-135b** | Up-regulated[Plieskatt et al., 2015; Plieskatt et al., 2014] | Moderate > Well (FC=22,7) |
| **miR-132** | No | Moderate > Well (FC=15,1) |

FC : Fold Change

Figure 4A shows that a subset of microRNAs (*miR-200c, miR-31 and miR-135b*) was expressed at higher levels in the tumor than in the non-tumor tissue. *miR-222* was not detectable in our ICC samples. When considering differentiation of the tumors, no correlation was found between histological grade and expression of the selected miRNAs, except for *miR-132*, which was low in the poorly differentiated tumors (Fig. 4B). However, when considering the ratio of expression in tumor *versus* non-tumor tissue, again no correlation was found with histological grade, even for *miR-132* (Fig. 4C). Finally, we analysed the expression of the six cholangiocyte-enriched microRNAs identified in the previous paper but found no correlation between their expression and the histological grade of the tumors (Supplementary Fig.1).

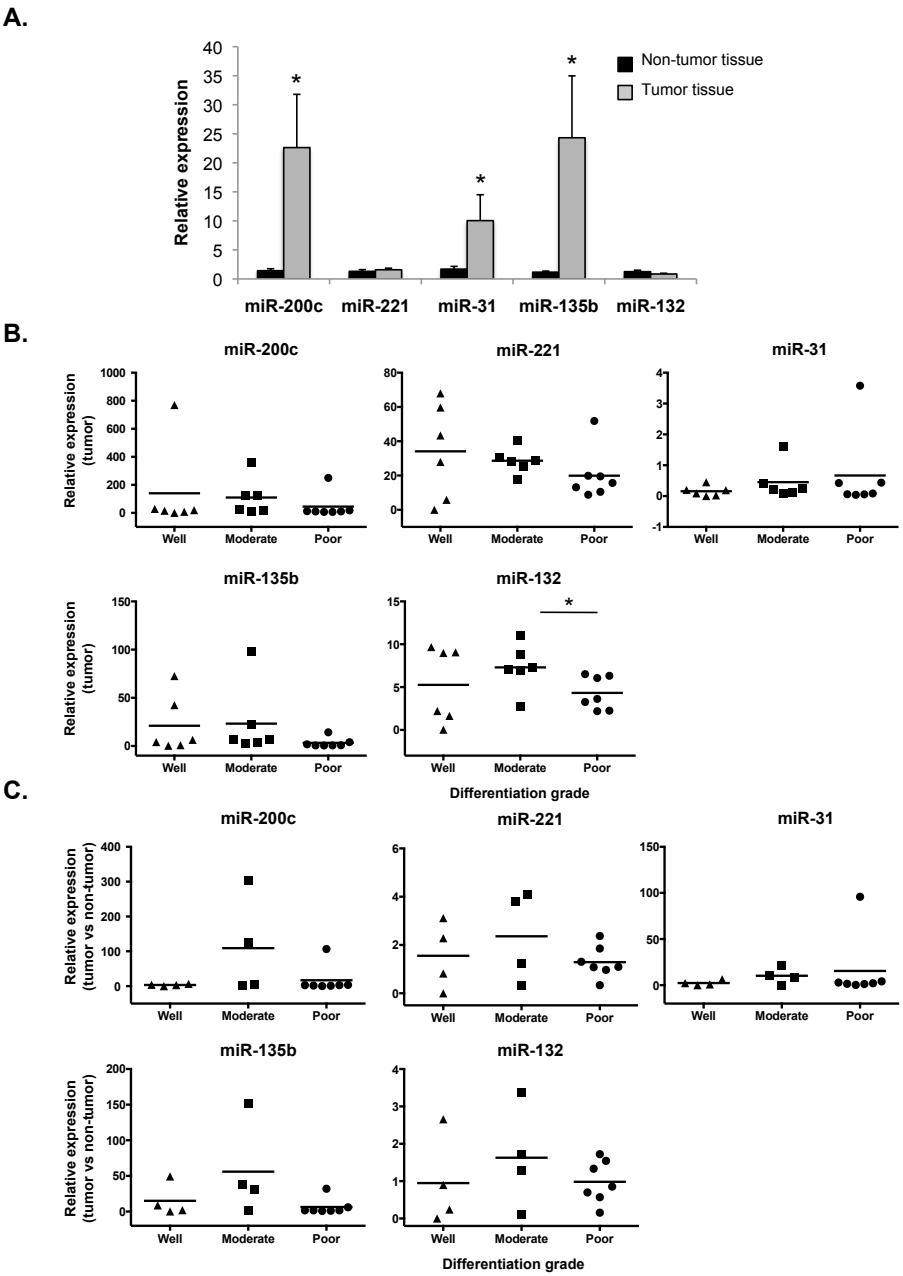



**Figure 4. ICC-associated microRNAs are not differentially expressed in histologically-graded iCC.** MicroRNAs known to be dysregulated in ICC and differentially expressed among tumor grades were selected for qRT-PCR analysis. **(A)** Three microRNAs are up-regulated in ICC when compared to distant non-tumoral tissues. (Mean ± SEM; *p<0.05). **(B-C)** Lack of correlation between microRNA expression and tumor differentiation grade when **(B)** comparing ICC samples, or**(C)** when analysing the ratio of expression in tumor *versus* non-tumor tissue. Dots represent individual ICC samples.

**Molecular differentiation markers in ICC - protein expression**

Since mRNA expression does not necessarily correlate with protein expression, we analysed the expression of SOX9, OPN, CK19 and HNF1β by immunostaining on two representative samples of each histologically-defined differentiation grade (Fig. 5). The results showed that the markers are expressed in the tumors regardless of their differentiation grade. SOX9, which is normally located in the nucleus, was restricted to the cytoplasm in well-differentiated ICC while it was expressed in both the cytoplasm and nucleus in moderately and poorly differentiated ICC (Fig. 5A-F). CK19 was expressed in all ICC samples (Fig. 5G-L). Similarly, OPN was expressed in all tumor types (Fig. 5M-R). However, in well-differentiated ICC, OPN was predominantly expressed at the apical pole of cells but a subset of cells also displayed cytoplasmic location (Fig. 5M-N, white and yellow arrowheads). In contrast, OPN was observed mainly in the cytoplasm of cells of moderately differentiated tumors, while only a subset of cells expressed OPN at the apical pole (Fig. 5O-P, white and yellow arrowheads). Poorly differentiated tumors have lost apico-basal polarity, preventing correct interpretation of polarity marker location. However, in those poorly differentiated tumors some cells expressed cytoplasmic OPN (Fig 5Q-R, yellow arrowheads). Therefore, overall expression of CK19, SOX9 and OPN protein does not correlate with histological differentiation grade, but subcellular location of SOX9 and OPN were related to ICC cell differentiation.

Surprisingly, in contrast to the qRT-PCR data, HNF1β protein expression was high in poorly differentiated ICC (Fig. 5 Q-R, Q'-R') and, low and mislocated, *i.e.* non-nuclear, in well differentiated tumors (Fig. 5M-N, M'-N'); moderately differentiated tumors showed intermediate expression levels (Fig. 5O-P, O'-P').

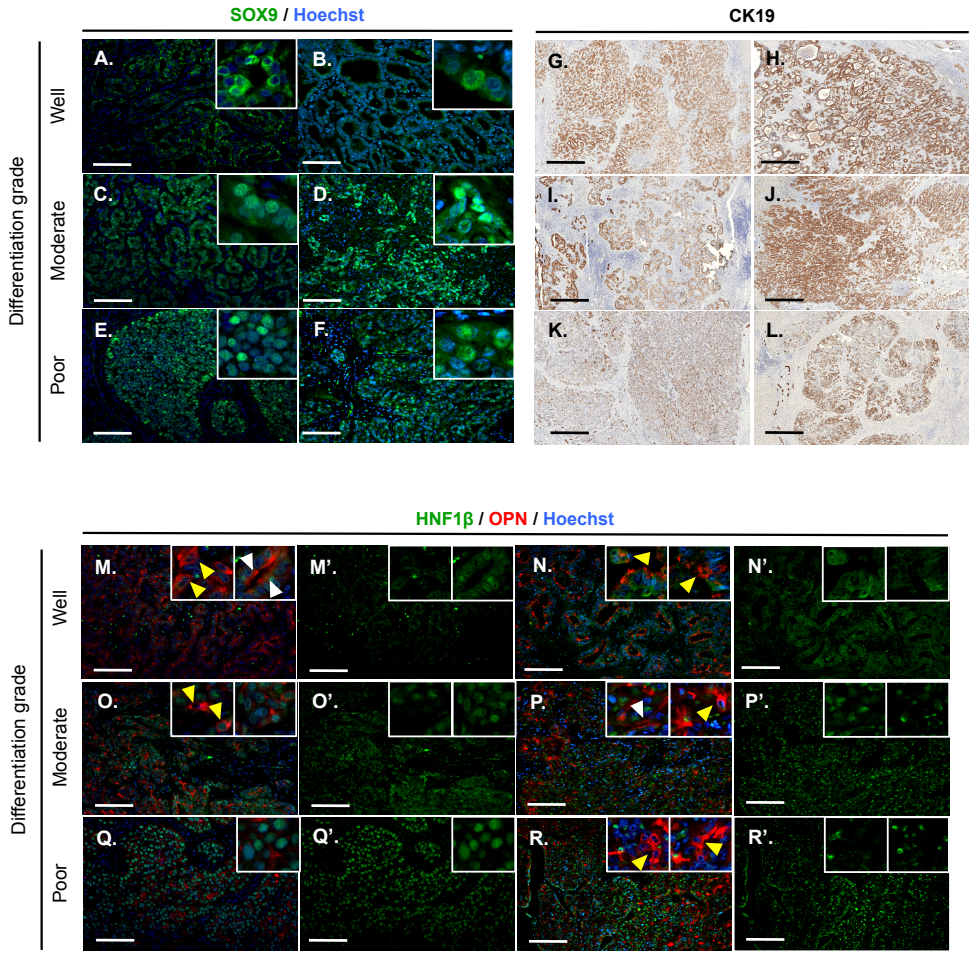



**Figure 5. Expression of molecular biliary markers in histologically-graded ICC's. (A-F)** SOX9 expression is detected in the cytoplasm of well-differentiated ICC cells (A-B) and both in the cytoplasm and nucleus of moderately and poorly differentiated tumor cells (C-F). **(G-L)** CK19 is expressed in all types of histologically-graded tumors. **(M-R)** OPN is detected in all types of histologically graded-ICC's. Its expression is mostly apical in well-differentiated tumor cells (M-N, white arrowheads), but cytoplasmic OPN is detected in moderately and poorly differentiated ICCs and in a subset of well-differentiated tumor cells (M-R, yellow arrowheads). **(M'-R')** HNF1β expression inversely correlates with ICC grade. White scale bar = 100 µm, black scale bar = 500 µm.

## DISCUSSION

In recent years, many efforts have been devoted to better classify ICCs and determine their prognosis. Since differentiation grade of the tumors, defined by histopathological criteria, is closely related to patient outcome (Mazur et al., 2012; Uenishi et al., 2003), in the present work we wished to strengthen histopathological differentiation criteria by correlating them with expression of molecular cholangiocyte differentiation markers. We assumed that well differentiated tumors would express high levels of cholangiocyte markers and that these levels would decrease in less differentiated tumors. However, our work unexpectedly revealed a lack of correlation between histopathological and molecular differentiation criteria in ICC.

Here, we analysed the expression of biliary markers in areas of ICCs where the tumoral cells (identified by the CK7 positive staining) represented more than 50% of the total area in order to limit contamination by non-tumor cells. All our carcinoma expressed lower levels of these markers compared to control tissues (Figs. 2-4), thereby suggesting that the epithelial cells are undergoing a dedifferentiation process, at least at the molecular level. In line with this observation, Mazur and coworkers previously proposed that *SOX9* expression decreases in the early step of ICC development (Mazur et al., 2012). These results raise the question of the real differentiation status of the tumors, and may explain why some differentiation markers are associated with good or poor prognosis in distinct studies (e.g. *SOX9*; (Matsushima et al., 2015; Mazur et al., 2012)), and why some other differentiation markers such as HNF1β are not associated with prognosis (Mazur et al., 2012; Yu et al., 2015).

We further showed by RT-qPCR and immunofluorescence that *SOX9* and *OPN* are expressed equally in all tumor types (Fig. 5). However, their subcellular location depended on the differentiation grade of the ICC. SOX9 is located in the cytoplasm of well-differentiated tumors investigated here, whereas it was nuclear or cytoplasmic in moderately and poorly differentiated tumors. Cytoplasmic expression of SOX9 has already been observed in pancreatic adenocarcinoma affected with p53 mutation (Huang et al.,

2015), in breast cancer cells (Chakravarty et al., 2011) and in biliary tract cancers (Mazur et al., 2012), suggesting that the location of SOX9 may depend on the mutational status of the cells. OPN is expressed in the cytoplasm of early biliary progenitors in the embryo, and becomes apical once the biliary cells become polarized (Antoniou et al., 2009a). The dual cytoplasmic and apical location of OPN found in well-differentiated tumors may reflect distinct levels of molecular differentiation of the cells within the same tumor. Regarding HNF1β, Mazur and coworkers, could not correlate HNF1β expression with survival rates of ICC (Mazur et al., 2012). This is at first sight at odds with our findings: since we found more HNF1β protein in poorly differentiated tumors, which are known to be associated with poor prognosis, our data suggest that HNF1β is a marker of poor prognosis. However, combining our data with those of Mazur and coworkers would be in agreement with the overall conclusion of the present work, namely that molecular differentiation markers do not correlate with histopathological differentiation criteria. Finally, HNF1β protein expression is higher in poorly differentiated tumors, while *HNF1$\beta$* mRNA does not correlate differentiation grade. This points toward potential post-transcriptional regulation and further underscores the care needed when interpreting expression of molecular differentiation markers in ICC.

When analysing our set of tumors, we were unable to corroborate the findings by Plieskatt and co-workers, who showed that *miR-200c, miR221, miR-31, miR-135b* and *miR-132* are differentially expressed between well differentiated, moderately differentiated and papillary carcinoma-type ICC (Plieskatt et al., 2015; Plieskatt et al., 2014). In line with this, several groups attempted to list dysregulated microRNAs in ICCs, but only little overlap can be found when comparing the proposed microRNA lists (Chen et al., 2009; Karakatsanis et al., 2013; Kawahigashi et al., 2009; Plieskatt et al., 2015; Plieskatt et al., 2014; Zhang et al., 2015). In addition, contradictory results were found.For instance, *miR-200c* was either down-regulated (Chen et al., 2009; Karakatsanis et al., 2013) or upregulated (Plieskatt et al., 2015; Plieskatt et al., 2014) (Fig. 3). This points towards necessary care when interpreting microRNA expression in ICC. The broad range of control tissue used to investigate microRNA expression could contribute to the observed

discrepancies. Indeed, control tissues selected by different authors were either normal hepatic bile duct tissue or total liver parenchyma, which are distinct tissues, and originated from liver associated with a variety of diseases such as cirrhosis, hepatitis, or infection with *Opisthorchis viverrini* (Plieskatt et al., 2015; Plieskatt et al., 2014; Razumilava and Gores, 2013). In that context, Plieskatt and coworkers showed that in *Opisthorchis viverrini*-induced ICC, miRNAs in distal non-tumor tissue clustered closer to the tumor than to non-tumor tissue from control individuals (Plieskatt et al., 2015). This is in line with our lack of correlation between miRNA or mRNA expression and ICC grade when considering the ratio of expression in tumor *versus* non-tumor tissue (Figs. 3C). Indeed, our controls were from non-tumor tissue taken from the patient affected with ICC.

## CONCLUSION

In this work we compared histologically-graded ICC rich in epithelial cells and found no correlation between expression of biliary molecular differentiation markers and the histological differentiation grade of the tumors. Therefore, our data point towards necessary caution when classifying ICC tumor samples and determining prognosis based on molecular differentiation criteria.

## ACKNOWLEDGMENTS

The authors thank the members of the Lemaigre lab for discussions, and the Department of Pathology of the Cliniques Universitaires Saint Luc for technical support.

## MATERIALS AND METHODS

### Ethics Statement

The work on human tissue samples was performed in compliance with the Belgian regulation, and with the 1975 Declaration of Helsinki. We studied 18 ICCs obtained from

16 patients (12 men; 4 women) surgically treated at the Cliniques Universitaires St Luc (Brussels, Belgium) by a surgeon who is not co-author of the present paper, prior to the start of the present analysis. An anonymous registration number was tagged on each sample and researchers who analysed the samples had no access to the name of the donor. The retrospective analysis of the surgical specimens was approved by the Commission on Biomedical Ethics of the Université Catholique de Louvain and Cliniques Universitaires Saint-Luc (Approval # 2013/08JUL/384). Informed consent is not required for retrospective analyses.

**Immunohistochemistry and Immunofluorescence.**

Immunohistochemistry for cytokeratin 7 (*CK7*) was performed on 4 µm sections of formalin-fixed paraffin-embedded tumors and carried out with a standardized protocol on a Ventana Benchmark system (Ventana Medical Systems, Tucson, AZ, USA). Immunofluorescence was performed on 5 µm sections of formalin-fixed paraffin-embedded tumors. Briefly, tissue sections were deparaffinized and micro-wave heated for 10 min in 10mM sodium citrate pH 6.0 for antigen unmasking. Sections were permeabilized for 5 min in phosphate-buffered saline (PBS)/0.3% Triton X-100 before blocking for 45 min in 0.3% milk/10% bovine serum albumin/0.3% Triton X-100 in PBS. Primary and secondary antibodies (listed in Supplementary Table 1) were diluted in blocking solution and incubated respectively at 4°C overnight and room temperature for 1 h. Pictures were taken with an Axiovert 200 fluorescent microscope using AxioVision system.

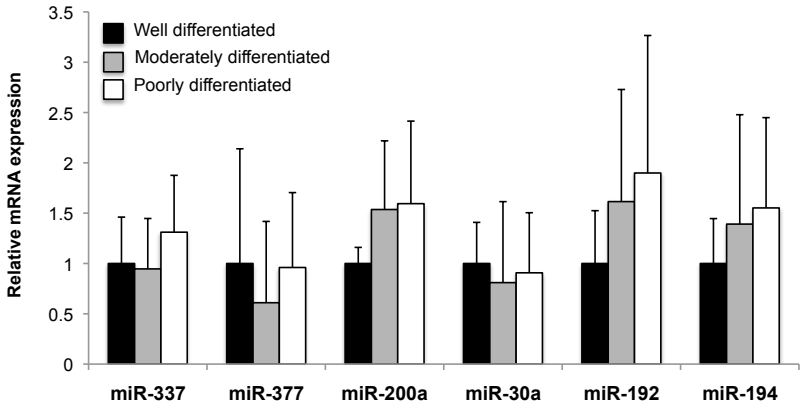
**RNA extraction and RT-qPCR**

Formalin-fixed paraffin-embedded tumors were sectioned at 10 µm and regions of interest were scraped from the glass slides with a surgical blade. Total RNA was isolated using the RecoverAll Total Nucleic Acid Isolation Kit for FFPE (#AM1975, Ambion). cDNA synthesis was performed with MMLV reverse transcriptase (#28025-13, Invitrogen) according to manufacturer's protocol. Gene expression was quantified by qPCR using Kapa SYBR Fast 2X Universal Master Mix (#KK4601, Sopachem). The primers are listed in

Supplementary Table 2. For measuring microRNA expression, specific stem-loop primers were used for reverse transcription and RT-qPCR was performed using a specific forward primer and a common universal reverse primer (Supplementary Table 3). mRNA and microRNA levels were normalized for β-*ACTIN* or *GAPDH* and *RNU6* or *RNU1a* respectively.

## SUPPORTING INFORMATION

**Supplementary Figure 1. Cholangiocyte-enriched microRNAs are not differentially expressed in histologically-graded iCCs.** Expression of the 6 cholangiocyte-enriched microRNAs identified in paper 1 was measured by qRT-PCR. Mean ± SEM.




**Supplementary Table 1: List of primary and secondary antibodies used for immunostaining experiments.**

| Primary antibody | Species | Dilution | Source | Reference number |
|---|---|---|---|---|
| CK7 | Mouse | 1/200 | Dako | M7018 |
| Sox9 | Rabbit | 1/250 | Chemicon | AB5535 |
| HNF1β | Rabbit | 1/100 | Santa Cruz | SC-22840 |
| OPN | Goat | 1/150 | R&D Systems | AF808 |

| Secondary antibody | Species | Dilution | Source | Reference number |
|---|---|---|---|---|
| Alexa Fluor 488 anti-rabbit | Donkey | 1/1000 | Invitrogen | A-21206 |
| Alexa Fluor 594 anti-goat | Donkey | 1/1000 | Invitrogen | A-11058 |
| Alexa Fluor 647 anti-mouse | Donkey | 1/1000 | Invitrogen | A-31571 |

**Supplementary Table 2: List of primer sequences used for RT-qPCR.**

| Gene | Primer sequence (5' → 3') |
|---|---|
| β-Actin | Fw - TCC TGA GCG CAA GTA CTC TGT<br>Rev - CTG ATC CAC ATC TGC TGG AAG |
| Gapdh | Fw - GGC CAA GGT CAT CCA TGA CA<br>Rev - TTC TAG ACG GCA GGT CAG GT |
| RNU6 | Fw – CTC GCT TCG GCA GCA CA<br>Rev – AAC GCT TCA CGA ATT TGC GT |
| RNU1a | Fw – CCA TGA TCA CGA AGG TGG TT<br>Rev – ATC CGG AGT GCA ATG GAT AA |
| Sox9 | Fw - CCT GGG ATT GCC CCG A<br>Rev - GAG CAG ACG CAC ATC TC |
| OPN | Fw – GCA ACC GAA GTT TTC ACT CC<br>Rev – ATT CAA CTC CTC GCT TTC CA |
| CK19 | Fw – CTG AAG GAA GAG CTG GCC TA<br>Rev – TCA TAT TGG CTT CGC ATG TC |
| Sox4 | Fw – GGT GCA AGA CCC CGA GTG<br>Rev – GCT GTC TTT GAG CAG CTT CC |
| HNF4α | Fw – CGT GCT GCT CCT AGG CAA<br>Rev – GTC AAG GAT GCG TAT GGA CAC |

| | |
|---|---|
| HNF1β | Fw – ACA CAC CTC CCA TCC TCA AG<br>Rev – CGC TTC TGG GTC TTC ATA GG |
| miR-200c | Fw – ACA CTC CAG CTG GGT AAT ACT GCC GGG TAA<br>Rev - CTC AAC TGG TGT CGT GGA GTC GGC AAT TCA GTT GAG TCC ATC ATT |
| miR-221 | Fw – ACA CTC CAG CTG GGA GCT ACA TTG TCT GC<br>Rev – CTC AAC TGG TGT CGT GGA GTC GGC AAT TCA GTT GAG GAA ACC CA |
| miR-31 | Fw – ACA CTC CAG CTG GGA GGC AAG ATG CTG GCA<br>Rev – CTC AAC TGG TGT CGT GGA GTC GGC AAT TCA GTT GAG CAG CTA TG |
| miR-135b | Fw – ACA CTC CAG CTG GGT ATG GCT TTT CAT TCC<br>Rev – CTC AAC TGG TGT CGT GGA GTC GGC AAT TCA GTT GAG TCA CAT AGG |
| miR-132 | Fw – ACA CTC CAG CTG GGT AAC AGT CTA CAG CCA<br>Rev – CTC AAC TGG TGT CGT GGA GTC GGC AAT TCA GTT GAG CGA CCA TG |

**Supplementary Table 3: List of stem-loop primers used for reverse transcription of miRNAs.**

| Gene | Primer sequence (5' ➔ 3') |
|---|---|
| miR-200c | Rev - CTC AAC TGG TGT CGT GGA GTC GGC AAT TCA GTT GAG TCC ATC ATT |
| miR-221 | Rev – CTC AAC TGG TGT CGT GGA GTC GGC AAT TCA GTT GAG GAA ACC CA |
| miR-31 | Rev – CTC AAC TGG TGT CGT GGA GTC GGC AAT TCA GTT GAG CAG CTA TG |
| miR-135b | Rev – CTC AAC TGG TGT CGT GGA GTC GGC AAT TCA GTT GAG TCA CAT AGG |
| miR-132 | Rev – CTC AAC TGG TGT CGT GGA GTC GGC AAT TCA GTT GAG CGA CCA TG |

# IV. GENERAL DISCUSSION AND PERSPECTIVES

In this thesis, we addressed the role of microRNAs in two aspects of hepatic cell differentiation. First, we looked into mechanisms regulating hepatic cell differentiation during embryogenesis and identified miR-337-3p as a novel regulator of liver development that sets the proper balance between hepatocyte and cholangiocyte gene expression during lineage segregation. Second, we investigated the expression of miRNAs in relation to the differentiation status of intrahepatic cholangiocarcinoma cells. Unexpectedly, we found no correlation between the expression of a specific set of microRNAs, cholangiocyte markers and the histological differentiation grade of the tumors.

## 1. INVESTIGATING MIR-337-3P FUNCTIONS DURING LIVER EMBRYOGENESIS

### 1.1. What are the miR-337-3p targets?

During hepatocyte development, LETFs form a dynamic network of autoregulatory and cross-regulatory loops whose numbers increase with time and which progressively stabilize the hepatocytic phenotype (Kyrmizi et al., 2006; Odom et al., 2006; Odom et al., 2004). Since LETFs are interconnected, downregulation of one LETF can perturb the expression of the others, making them good putative targets of miR-337-3p. Nevertheless, miR-337-3p most likely does not target HNF6 and HNF1β since their expression are maintained in forming bile ducts, a tissue in which miR-337-3p levels are elevated. The reduced expression of HNF6 and HNF1β observed in miR-337-3p hepatoblasts/hepatocytes is therefore probably a consequence of the downregulation of other LETFs. On the other hand, none of the core LETFs was predicted by bioinformatic tools as a direct miR-337-3p target, except for HNF4α for which we found no evidence for direct interaction with the microRNA (Dweep et al., 2011; Mestdagh et al., 2011; Reczko et al., 2012).

HNF4α would have been an ideal target since its inactivation in embryonic livers has been shown to result in a dramatic decrease of most the other LETFs (Kyrmizi et al., 2006). Interestingly, expression of three LETFs is unaffected by the embryonic deletion of HNF4α: C/EBPα, COUP-TFII and GATA6. Although COUP-TFII is predicted by bioinformatic tools to be a putative target of miR-337-3p, neither COUP-TFII nor GATA6 mRNA decrease when treating cultured hepatoblasts with miR-337-3p mimic (data not shown). Despite that we cannot rule out that miR-337-3p inhibits the translation of COUP-TFII, it is important to note that COUP-TFII and GATA6 play only limited role in the establishment of the LETFs network during embryogenesis and are not direct stimulators of HNF4α before birth (Figure1) (Kyrmizi et al., 2006). Therefore, the phenotype induced by miR-337-3p overexpression is unlikely to be a consequence of deregulation of COUP-TFII and GATA6. In contrast, C/EBPα is an excellent candidate. Indeed, C/EBPα is high in the LETFs cascade: it binds to HNF4α and FoxA2 (also known as HNF3β) regulatory regions starting at early stages of liver development (Figure 1) (Kyrmizi et al., 2006). Importantly, we demonstrated that C/EBPα expression is already low in E11.5 hepatoblasts of miR-337-3p Tg mice, and that C/EBPα levels decrease in a dose-dependent manner upon miR-337-3p transfection in cultured hepatoblasts. Therefore, C/EBPα could be a miR-337-3p target, and investigation of whether a direct interaction occurs between the two factors would be very informative.

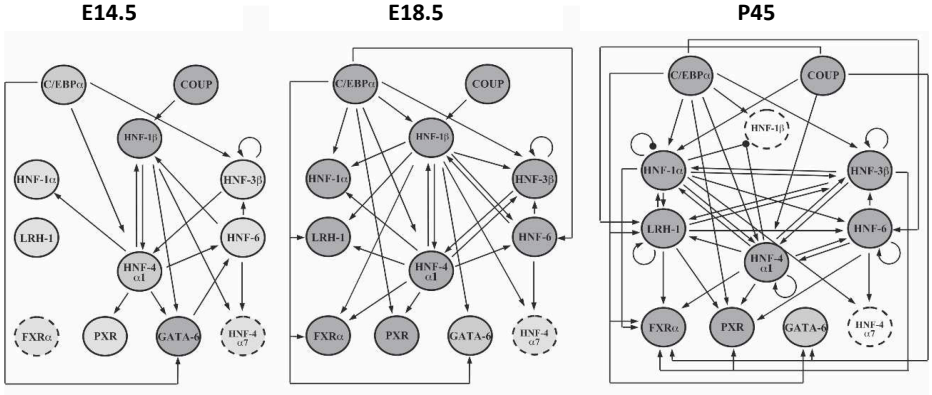



**Figure 1. Schematic representation of cross-regulatory interactions between LETFs** (from Kyrmizi et al., 2006). Interactions between factors are illustrated at E14.5, E18.5 and postnatal day 45 (P45). Arrows indicate an interaction with the regulatory elements of the transcription factor.

On the other hand, we demonstrated that miR-337-3p inhibits translation of STAT3, a known activator of HNF4α (Ito et al., 2000). Along the same lines, miR-337-3p could also repress other uninvestigated LETF stimulators. However, careful analysis of miR-337-3p mimic microarray did not reveal obvious candidates. MiR-337-3p could also target genes coding for DNA or histone modification enzymes as observed with miR-148a, which stimulates hepatocyte maturation by inhibiting DNMT1 expression (Gailhouste et al., 2013). Interestingly, cholangiocyte development is associated with increased methylation of CpG sequences in the promoter of both C/EBPα and HNF4α (Tanimizu et al., 2013) and DNMT1 expression shows a 2,2 fold increase after transfection of cultured hepatoblasts with miR-337-3p (data not shown). In consequence, miR-337-3p could repress hepatocyte markers expression by indirectly stimulating DNMT1 expression.

## 1.2. Mechanism of action of miR-337-3p

Our data demonstrate that miR-337-3p induces cholangiocyte differentiation *in vitro* and *in vivo*. *In vivo*, miR-337-3p Tg livers exhibit a reduced number of ductal plate cells. Since miR-337-3p Tg livers present with a lower number of hepatoblasts, we cannot rule out that this reduction in ductal plate cells is linked to that phenomenon. However, Tg livers show an increased SOX4 expression and cholangiocytes express more SOX9 per cell, thereby suggesting a role of miR-337-3p in cholangiocyte development. We demonstrated that miR-337-3p's effect on hepatoblasts differentiation is critically dependent on functional Notch and TGFβ signaling pathways. Notch signaling requires cell-to-cell contact and the portal vein surrounding mesenchyme is the major source of the Notch ligand Jagged 1 (Kodama et al., 2004; Tanimizu and Miyajima, 2004; Zong et al., 2009). Moreover, TGFβ signaling occurs as a gradient with maximum activity in the vicinity of the portal vein, while the TGFβ ligands TGFβ2 and TGFβ3 are abundantly expressed by the periportal mesenchyme (Antoniou et al., 2009; Clotman et al., 2005). Therefore, this suggests that in physiological conditions miR-337-3p predominantly acts on hepatoblasts surrounding the portal vein, namely the developing cholangiocytes, by repressing their acquisition of hepatocyte features and stimulating cholangiocyte-specific gene expression. However, it is important to note that the TGFβ ligand TGFβ1 is widely expressed in the

liver parenchyma, thereby allowing miR-337-3p to control gene expression in hepatoblasts and developing hepatocytes (Antoniou et al., 2009).

*In vitro* overexpression of miR-337-3p stimulates the biliary-promoting Notch and TGFβ signaling pathways. Since Yap is also a known stimulator of biliary development, we checked if *in vitro* overexpression of miR-337-3p was also stimulating the Hippo signaling pathway. Consistent with the stimulatory role of miR-337-3p on cholangiocyte gene expression, we found an upregulation of Hippo-related genes, notably TEAD2 and Ctgf which showed a 3- and 4- fold stimulation respectively (data not shown). On the other hand, since the effect of miR-337-3p is abrogated by γ-secretase and TGF-β receptor inhibitors (DAPT and SB431542), we expect that miR-337-3p directly targets these Notch and TGF-β mediators or upstream regulators thereof. It has been shown that Yap, the mediator of the Hippo pathway, participates in biliary commitment and is likely to be upstream of Notch (Yimlamai et al., 2014). Therefore, we verified if miR-337-3p function was also dependent on functional Hippo signaling pathway. On that purpose, we transfected cultured hepatoblasts with miR-337-3p in presence or absence of Verteporfin, a drug that inhibits TEAD-Yap association (Liu-Chittenden et al., 2012). As observed with Notch and TGFβ inhibitors, treatment with the TEAD-Yap inhibitor blocked the effects of miR-337-3p on hepatocyte and cholangiocyte gene expression (data not shown). However, we could not confirm that the effect was due to Yap inhibition. Indeed, when we analysed the expression of Hippo/Yap signaling markers Ctgf, Cyr61 and AmotL2 (Yimlamai et al., 2014), we found no repression of the Yap targets in presence of the inhibitor, suggesting either that Verteporfin was not functional as expected or did not specifically inhibit Yap. In addition, at all Verteporfin concentrations tested, cell death was unexpectedly high. Therefore, we were not able to safely conclude about the involvement of Hippo signaling in miR-337-3p function. As a note of caution, we also note that DAPT inhibits Notch signaling, but also E-Cadherin and EpCam signaling; the latter have not been investigated in the present work.

Together, these results point to the importance of miR-337-3p in the acquisition of cholangiocyte properties. *In vivo*, we overexpressed miR-337-3p in hepatoblasts using

AlfpCre-mediated recombination of the miR-337-3p-expressing transgene. In this model, recombination occurred in early hepatoblasts around E10.5 (Kellendonk et al., 2000), thereby allowing us to study the impact of miR-337-3p at the early stages of liver development. Nevertheless, in the microarray comparing miRNA expression between developing cholangiocytes and hepatocytes, we found that miR-337-3p was upregulated in E18.5 cholangiocytes, therefore suggesting a role of miR-337-3p during late stage of biliary development. We could not provide evidence supporting this hypothesis. First, during biliary tubulogenesis, hepatoblasts stimulated by TGFβ differentiate to the cholangiocyte lineage in which TβRII become repressed (Antoniou et al., 2009). Interestingly, TβRII is a validated target of miR-337-3p in chondrocytes (Zhong et al., 2012). Nevertheless, *in vitro* overexpression of miR-337-3p is not associated with TβRII repression (data not shown). Secondly, we managed to overexpressmiR-337-3p specifically in mid- to late stage cholangiocytes by using the tamoxifen-inducible SOX9CreER and OPNCreER. However, we failed to detect any phenotype. Taken together, these data suggest that miR-337-3p preferentially acts in early stages of liver development.

Interestingly, similarities are found concerning the role of miR-337-3p in developing liver and developing chondrocytes. Indeed, miR-337-3p stimulates cholangiocyte gene expression and controls hepatobiliary segregation notably by stimulating SOX4 and SOX9 expression. Similarly, miR-337-3p was found to regulate chondrogenesis, during which it induces cartilage-specific gene expression in chondrocytes (Zhong et al., 2012). Similarly to cholangiocyte development, SOX9 is essential for chondrocyte differentiation where it induces the expression of ECM-related genes (Leung et al., 2011). Moreover, *in vitro* experiments demonstrated that SOX4 is required to induce chondrocyte differentiation of human synovium-derived stem cells (Zhang et al., 2015). Therefore, miR-337-3p might be a regulator of cell differentiation in several organs.

## 2. MICRORNAS, FINE TUNERS OF DEVELOPMENTAL PROCESSES

During liver embryogenesis, small changes in gene expression can have a significant impact on cell differentiation. For instance, C/EBPα expression is progressively repressed during cholangiocyte development. However, cholangiocytes need to express small amounts of C/EBPα since complete loss of C/EBPα leads to development of tubular structures similar to extrahepatic bile ducts (Yamasaki et al., 2006). Similarly, a 1.7 fold induction in miR-122 expression is sufficient to accelerate hepatocyte differentiation and induce biliary hyperplasia. In agreement with these results, our mathematical model showed that optimal levels of miR-337-3p are required for normal hepatocyte development since either an increase or a decrease in its expression reduces HNF4α expression. Our proposal that miR-337-3p functions within a narrow range of concentration is further supported by our observation that a 2-fold overexpression of miR-337-3p destabilised the hepatocyte differentiation program *in vivo*. Taken together, these data highlight the importance of fine-tuned gene expression for time-specific and appropriate lineage segregation and cell differentiation during liver development.

Consistent with the role of miRNAs in fine-tuning of gene expression, we demonstrated that miR-337-3p is involved in an incoherent feed-forward loop that results in biphasic control on HNF4α, a master regulator of hepatocyte differentiation. Our loop model involves Stat3 and C/EBPα. We do not exclude that other components might participate to miR-337-3p-controlled expression of HNF4α. The regulation of C/EBPα by miR-337-3p can be indirect. Moreover the feed-forward loop might comprise an additional branch, and we have preliminary evidence that a miR-337-3p -I Snail -I HNF4α branch may contribute to the incoherent feed-forward motif. While feed-forward loop motifs are known to control metabolism in adult hepatocytes (Kyrmizi et al., 2006; Martinez-Jimenez et al., 2010; Odom et al., 2006) we provide, to our knowledge, the first demonstration of a incoherent feed-forward loop motif involved in embryonic liver.

## 3. *IN VITRO* GENERATION OF HEPATIC CELLS

In recent years, many efforts have been devoted to produce cholangiocytes *in vitro*. Indeed, cholangiocytes represent less than 5% of the total liver mass and proliferate slowly (Si-Tayeb et al., 2010). Moreover, cholangiocytes that are currently cultured *in vitro* cannot be considered as normal cells since they either correspond to large T antigen SV40 immortalized cholangiocytes or derive from cholangiocarcinomas. Therefore, availability of functional cholangiocytes is essential for understanding pathophysiology of biliary diseases and liver regeneration, and could be useful for therapeutic strategies and study of drug-induced liver toxicity.

The current strategy to generate cholangiocytes *in vitro* consists in reprogramming ESCs or induced pluripotent stem cells (iPSCs) toward the cholangiocyte lineage by mimicking developmental steps (Figure 2).

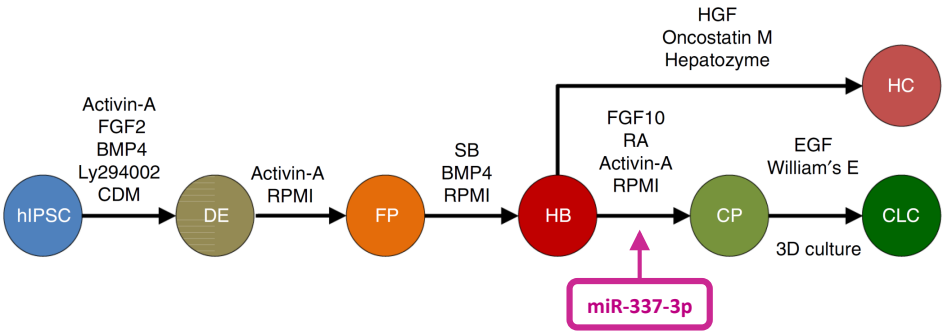



**Figure 2. Example of reprogramming protocol of iPSCs to hepatic cells** (adapted from Sampaziotis et al., 2015). Key stages of hepatic development stepwise differentiation of iPSCs. DE, definitive endoderm; FP, Foregut progenitor; HB, hepatoblast; CP, cholangiocyte precursor; CLC, cholangiocyte-like cell; HC, hepatocyte-like cell; BMP, bone morphogenetic protein; Ly294002 is a phosphatidylinositol-3-OH kinase inhibitor; CDM, chemically defined medium; RPMI, Roswell Park Memorial Institute medium; SB, SB-431542; HGF, hepatocyte growth factor; RA, retinoic acid; EGF, epidermal growth factor; FGF, fibroblast growth factor.

Using this approach, Dianat and coworkers successfully generated cholangiocyte-like cells from human ESCs (Dianat et al., 2014). These cells express biliary markers such as SOX9, CK7, OPN and HNF6 and repress HNF4α, while expressing genes important for cholangiocyte function such as the Cystic Fibrosis Transmembrane conductance Regulator

(CFTR) and the secretin receptor. In a 3D culture system, they acquire apico-basal polarity and form tubules and cysts. Moreover, using the same differentiation protocol, they also generated *in vitro* cholangiocytes from iPSCs or HepaRG cells, which is a human bipotent progenitor cell line (Marion et al., 2010). Using a similar approach, Sampaziotis and colleagues also reported generation of functional cholangiocyte-like cells from human iPSCs. Interestingly, they also generated cholangiocyte-like cells from healthy patients or from patients with polycystic liver diseases and successfully validated the use of two drugs for treating the disease (Sampaziotis et al., 2015). In the same lines, Ogawa and coworkers generated cholangiocyte-like cells from human iPSCs and demonstrated that functionally impaired iPSCs-derived cholangiocytes from cystic fibrosis patients were rescued by CFTR correctors (Ogawa et al., 2015). Finally, De Assuncao and colleagues also reported generation of iPSCs-derived cholangiocytes and demonstrated that the cells engrafted within mouse liver following retrograde intrabiliary infusion (De Assuncao et al., 2015).

A second strategy to generate *in vitro* cholangiocytes would be to directly reprogram fibroblasts into cholangiocytes by forcing the expression of cholangiocyte-specific transcription factors. Indeed, such approach has already been used to generate hepatocyte-like cells from human iPSCs (Takayama et al., 2012) or mouse fibroblasts (Huang et al., 2014; Sekiya and Suzuki, 2011). However, this method has not yet been achieved to produce *in vitro* cholangiocytes. Finally, Yu *et al*. reported successful generation of cholangiocyte-like and hepatocyte-like cells by combining the two approaches described above (Yu et al., 2013). Indeed, they first produced hepatoblast-like cells by forced expression of HNF1β and FoxA3 and further used specific growth factors and different culture conditions to induce differentiation toward hepatocyte or cholangiocyte lineages.

Our findings now demonstrate that monitoring miR-337-3p expression could enhance the cholangiocyte differentiation protocols, specifically in protocols that include a hepatoblastic step (Figure 3). In addition, since small variations of miR-337-3p expression levels decrease HNF4α expression, it would be interesting to monitor miR-337-3p expression in hepatocyte differentiation protocols too.

## 4. CHOLANGIOCYTE DIFFERENTIATION MARKERS, MICRORNAS AND ICCAS

In this part of the PhD thesis, as a first step to investigate the role of miRNAs in cholangiocarcinoma differentiation, we attempted to correlate the expression of cholangiocyte differentiation markers and miRNAs with the histopathological differentiation grade of iCCA. Surprisingly, we found no correlation. Interestingly, among the six investigated miRNAs, three were shown to be cholangiocyte-specific miRNAs, namely miR-200c, miR-222 and miR-221 (Chen et al., 2009).

In the first part of the thesis, we identified six cholangiocyte-enriched microRNAs (miR-200a-3p, miR-194-5p, miR-192-5p, miR-377-3p, miR-30a-5p and miR-337-3p) in developing livers at E18.5 and E14.5. Therefore, we measured their expression in histologically-graded iCCAs. Since the selected tumors are enriched in epithelial CK7-positive cells, we assumed that cholangiocyte-enriched miRNAs would be expressed at higher levels in well-differentiated tumors than in poorly-differentiated ones. However, we found similar expression of the cholangiocyte-enriched microRNAs in all iCCAs samples, regardless of their differentiation grade (data not shown). Taken together, these surprising results highlight discrepancies between molecular- and histology-based classifications and point toward a necessary caution when classifying iCCAs tumors. Classification of iCCAs according to molecular criteria instead of (or in addition to) histological criteria would be an option. However, combination of diagnostic tools for each patient is labor-intensive and not easily translated in routine clinical diagnosis.

In order to correlate hepatic differentiation markers with the histological grade of iCCAs, we selected tumor areas characterized by high epithelial cell density in order to avoid stromal contamination. We surprisingly found lower levels of differentiation markers, except for OPN, in the tumor tissue compared to the adjacent non-tumor tissue, suggesting that the epithelial part of the tumors was undergoing a dedifferentiation process. Intriguingly, when performing the same experiment in tumors areas with less than 30% of CK7-positive epithelial cells, we found that some of the differentiation markers, namely OPN, CK19 and SOX4 were upregulated in the tumor tissue compared to

adjacent non-tumor tissue, whereas SOX9 and Muc1 were not affected (data not shown). Importantly, when performing immunofluorescence staining in low- and high- CK7 positive areas, we found no difference in the differentiation marker expression. Along the same lines, Terashi and coworkers demonstrated that iCCA epithelial cells but not stromal cells were expressing OPN, and that lack of OPN expression was related with poor prognosis (Terashi et al., 2004). In contrast, Sulpice and coworkers detected high OPN expression in tumor stroma and demonstrated that stromal expression of OPN is an independent factor of poor prognosis (Sulpice et al., 2013). Taken together, these data suggest that stromal cells express molecular differentiation markers and may further contribute to the discrepancies observed between different studies. Consequently, it is important to distinguish epithelial and stromal cells when attempting to characterize iCCAs.

Finally, despite the lack of correlation between miR-337-3p expression and the differentiation grade of iCCAs, miR-337-3p is likely to have a function in this tumor type. Indeed, miR-337-3p expression was directly associated with patient survival in pancreatic ductal adenocarcinoma (Zhang et al., 2014). In parallel, miR-337-3p was shown to induce cellular senescence in colorectal cancers (Kim et al., 2012) and to reduce proliferation and progression of neuroblastomas and gastric cancers (Wang et al., 2013; Xiang et al., 2015). Moreover, miR-337-3p directly targets the proto-oncogene TWIST1, which correlates with acquired drug resistance and poor prognosis in human cancers.(Nairismagi et al., 2013). Together, these data indicate that miR-337-3p is a potential tumor-suppressor microRNA which displays anti-proliferative functions. Consistent with this hypothesis, cultured hepatoblasts transfected with miR-337-3p mimics or miR-337-3p hairpin inhibitors was associated with decreased or increased cell numbers, respectively. We conclude that miR-337-3p deserves investigation in cholangiocarcinoma.

# 5. GENERAL CONCLUSION AND PERSPECTIVES

In conclusion, our work improves our knowledge of hepatobiliary segregation and extends our knowledge about the role of miRNAs during liver embryogenesis. Indeed, we identified miR-337-3p as a new player in hepatic lineage segregation that sets the right balance between cholangiocyte and hepatocyte gene expression. Importantly, only small changes in miR-337-3p expression were sufficient to affect liver development, indicating that even minor quantitative changes in gene expression impact on hepatic cell differentiation. Therefore, it is worthwhile to monitor and modulate miR-337-3p expression during *in vitro* programming of mouse hepatic cells from stem cells. In addition, since miR-337-3p is well conserved in human, an interesting short-term perspective would be to confirm the role of miR-337-3p in human cells. Finally, our work prompted us to investigate the histological differentiation status of iCCAs and highlighted significant heterogeneity between tumors, thereby calling the histological classification value into question. Better understanding of molecular processes driving iCCA development could help in establishing a classification protocol that correlates with disease prognosis.

# V. ANNEXES

## 1. PROLIFERATION-INDEPENDENT INITIATION OF BILIARY CYSTS IN POLYCYSTIC LIVER DISEASES

I contributed to finalize the paper by performing experiments requested by the reviewers.

PLOS | ONE

RESEARCH ARTICLE

# Proliferation-Independent Initiation of Biliary Cysts in Polycystic Liver Diseases

**Jean-Bernard Beaudry[1], Sabine Cordi[1], Céline Demarez[1], Sébastien Lepreux[2], Christophe E. Pierreux[1], Frédéric P. Lemaigre[1]***

**1** Université catholique de Louvain, de Duve Institute, Brussels, Belgium, **2** INSERM U889, Université Bordeaux 2, Bordeaux, France

* frederic.lemaigre@uclouvain.be

CrossMark
click for updates

OPEN ACCESS

**Citation:** Beaudry J-B, Cordi S, Demarez C, Lepreux S, Pierreux CE, Lemaigre FP (2015) Proliferation-Independent Initiation of Biliary Cysts in Polycystic Liver Diseases. PLoS ONE 10(6): e0132295. doi:10.1371/journal.pone.0132295

**Editor:** Wan-Xi Yang, Zhejiang University, CHINA

**Received:** January 16, 2015

**Accepted:** June 11, 2015

**Published:** June 30, 2015

**Copyright:** © 2015 Beaudry et al. This is an open access article distributed under the terms of the Creative Commons Attribution License, which permits unrestricted use, distribution, and reproduction in any medium, provided the original author and source are credited.

**Data Availability Statement:** All relevant data are within the paper and its Supporting Information files.

**Funding:** This work was supported by the Interuniversity Attraction Pole Programme (Belgian Science Policy (BELSPO, grant PVII-47; http://www.belspo.be/), the D.G. Higher Education and Scientific Research of the French Community of Belgium (grant 10/15-029), the Alphonse and Jean Forton Fund (grant 2011-R10150-004; http://www.kbs-frb.be/fund.aspx?id=293586&langtype=2060), and the Fonds de la Recherche Scientifique Médicale (grant 3.4536.10F; http://www.fnrs.be/). CEP is research associate of the F.R.S.-FNRS (Belgium). The funders had no role in study design, data collection and

## Abstract

Biliary cysts in adult patients affected by polycystic liver disease are lined by cholangiocytes that proliferate, suggesting that initiation of cyst formation depends on proliferation. Here, we challenge this view by analyzing cyst-lining cell proliferation and differentiation in *Cpk* mouse embryos and in livers from human fetuses affected by Autosomal Recessive Polycystic Kidney Disease (ARPKD), at early stages of cyst formation. Proliferation of fetal cholangiocyte precursors, measured by immunostaining in human and mouse livers, was low and did not differ between normal and ARPKD or *Cpk* livers, excluding excessive proliferation as an initiating cause of liver cysts. Instead, our analyses provide evidence that the polycystic livers exhibit increased and accelerated differentiation of hepatoblasts into cholangiocyte precursors, eventually coalescing into large biliary cysts. Lineage tracing experiments, performed in mouse embryos, indicated that the cholangiocyte precursors in *Cpk* mice generate cholangiocytes and periportal hepatocytes, like in wild-type animals. Therefore, contrary to current belief, cyst formation in polycystic liver disease does not necessarily depend on overproliferation. Combining our prenatal data with available data from adult livers, we propose that polycystic liver can be initiated by proliferation-independent mechanisms at a fetal stage, followed by postnatal proliferation-dependent cyst expansion.

## Introduction

Polycystic disease of the liver is characterized by the presence of biliary cysts leading to hepatomegaly. It is found in patients with polycystic kidney disease—both the autosomal dominant and recessive forms—but when associated with mutations in the Protein kinase C substrate 80K-H, *SEC63* or Low density lipoprotein receptor-related protein 5 genes, it presents as an isolated liver disease. Liver cysts are also found in syndromes that are collectively characterized by dysfunction of primary cilia [1, 2].

The large size of hepatic cysts and their connection to the biliary tree led to the hypothesis that hepatic cysts start to develop in fetuses through excessive proliferation of biliary precursors, although this was not experimentally demonstrated [3–6]. Indeed, Autosomal Recessive Polycystic Kidney Disease (ARPKD) is caused by mutations in *PKHD1*, which codes for

analysis, decision to publish, or preparation of the manuscript.

**Competing Interests:** No competing interest.

fibrocystin/polyductin, a protein associated with the apical membrane and the primary cilium [7–9]. The association of fibrocystin/polyductin with primary cilia led to the speculation that cyst formation and expansion result from ciliary dysfunction. Since primary cilia regulate multiple functions including proliferation, it was suggested that hyperproliferation initiates liver cyst formation in ARPKD [3, 5, 6, 10–12]. This suggestion was supported by reports indicating that cyst-lining cells in PCK rat livers overproliferate [13–15]. However, all data where proliferation was measured, *i.e.* not simply deduced from histological phenotypes, were collected in adult livers, and fetal studies were not statistically validated [15]. Therefore, careful analysis of proliferation in mouse models and in human ARPKD at fetal stages is lacking.

During normal liver development, cholangiocytes differentiate from hepatoblasts and from ductal plate cells located around the portal vein [16]. Primitive ductal structures (PDS) then develop within the ductal plate. Their lumina are lined on the portal side by cholangiocytes and on the parenchymal side by hepatoblasts [17]. By the end of gestation PDS differentiate to bile ducts entirely lined by cholangiocytes and surrounded by mesenchyme, while the ductal plate cells not involved in bile duct formation differentiate into periportal hepatocytes, canals of Hering and adult progenitors [18]. Duct development progresses from the hilum to the periphery of the lobes, explaining why distinct stages of duct development can be identified within the same lobe in fetal liver. Importantly, cholangiocyte proliferation in fetal liver is low, indicating that bile ducts grow by recruiting hepatoblasts that differentiate into cholangiocytes [18]. This raises the possibility that cyst development in polycystic diseases is initiated in a proliferation-independent manner. Here, we address this hypothesis by analysing liver samples from human fetuses affected by ARPKD. We also investigate cyst formation in *Cpk* mice, which develop cysts as a result from mutations in *Cystin1*, a gene coding for a cilium-associated protein [19, 20].

## Materials and Methods

### Animals

*Cpk* [21] and *Sox9-CreER;Rosa*$^{YFP}$ mice [18] were backcrossed for at least 6 generations in a Balb/C background. Bromodeoxyuridine (BrdU) labeling was performed by injecting pregnant females at the indicated time with a single intraperitoneal dose of BrdU (20 mg/kg). Embryos were collected 1 h after injection. Tamoxifen (Sigma (T5648), Bornem, Belgium) was dissolved in corn oil (Sigma (C8267), Bornem, Belgium) at a concentration of 30 mg/ml and intraperitoneally injected into embryonic day (E)14.5 pregnant mothers at 100 mg/kg body weight. Tamoxifen had no adverse effects on embryos but induced late delivery and caused the mothers to devour the pups at birth. Thus, following cesarean birth at E19.0, newborn pups were transferred to foster mothers and collected 24 h later.

### Human fetal liver

ARPKD fetuses had mutations in the *PKHD1* gene [22] and showed kidneys with radially oriented dilation of the medullary collecting ducts [23]. The human samples have been studied in previous studies and were collected prior to the start of the present work [23, 24]. We analyzed 1 normal liver at 13 weeks of gestation (W), 1 normal liver at 22W, 1 ARPKD liver at 13W and 2 ARPKD livers at 22W. The normal livers were from a fetus suffering from trisomia 18 (13W) and from a foetus suffering from infection (22W).

## Ethics statement

The work on human tissue samples was performed in compliance with the French regulation (section L. 1241–5 Code of Public Health), and with the 1975 Declaration of Helsinki. The samples were collected in France by a pathologist who is not co-author of the present paper, prior to the start of the present analysis. An anonymous registration number was tagged on each sample at the time of collection, and researchers who analyzed the samples had no access to the name of the donor. The French regulation does not require referral to a research ethic committee for tissue samples used for scientific purposes aimed to investigate the causes of the spontaneous or therapeutic abortions. The women who underwent an abortion gave their written consent after receiving adequate information about the purposes of such samples.

All experimental procedures involving the use of animals were approved by the Animal Ethics Committee of the Université catholique de Louvain (permit number 2012/UCL/MD/021) and were conducted in compliance with the animal welfare regulations of Belgium. Animals received humane care according to the criteria outlined in the "Guide for the Care and Use of Laboratory Animals" prepared by the National Academy of Sciences (NIH publication 86–23 revised 1985).

## Immunofluorescence

Liver tissues were formalin-fixed and paraffin-embedded. Five μm-thick slides were stained as described [18] using antibodies and conditions listed in S1 Table. Pictures were taken with an Axiovert 200 fluorescent microscope using AxioVision system or a Cell Observer Spinning Disk confocal microscope (both from Carl Zeiss, Zaventem, Belgium). The number of proliferating cholangiocytes was established by determining the proportion of $Ki67^+$;$Sox9^+$ cells compared to the total number of $Sox9^+$ cells ($(n^{Ki67+;Sox9+}/n^{Sox9+}) \times 100$).

In human embryos, numbers of $Sox9^+$ cells counted were 726 (control 13W), 498 (control 22W), 830 (ARPKD 13W), 906 and 1086 (ARPKD 22W samples). The percentage of $Ki67^+$;$Sox9^+$/$Sox9^+$ cells was measured per image field for each sample. A total of 9 (control 13W), 11 (control 22W), 6 (ARPKD 13W), 8 and 5 image fields (ARPKD 22W samples) were analyzed.

In mouse embryos, we counted 275 and 600 $Sox9^+$ cells in WT and *Cpk* embryos, respectively (n = 3), and calculated the percentage of $Ki67^+$;$Sox9^+$/$Sox9^+$ cells per animal. We applied Student's t test to the mouse samples to determine statistically significant differences.

## Microarray

Total RNA was extracted from WT and *Cpk* embryos at E18.5 (n = 3) using TriPure reagent (Roche). Quality and integrity of RNA samples were assessed using a Bioanalyzer RNA 6000 Nano kit (Agilent Technologies). Genome-wide expression was assessed using GeneChip Mouse Genome 2.0 ST arrays (Affymetrix). Results are provided in S2 Table. Gene set enrichment analysis was performed as described [25].

## Microdissection of embryonic portal spaces

WT and *Cpk* livers at E17.5 were formalin-fixed and paraffin-embedded. Series of adjacent 10 μm-thick sections were cut, the first of which was subjected to H&E staining to locate portal spaces, which were manually dissected out of the adjacent slides. Approximately 45 portal spaces from as many tissue slides were pooled from each liver and subjected to RNA extraction using RecoverAll Total Nucleic Acid Isolation Kit (Ambion). The experiment was performed separately on 2 WT and 2 *Cpk* embryos. A total of 500 ng RNA was reverse-transcribed using MMLV (Invitrogen). qPCR was performed on 5 ng RNA on a C1000 Themocycler coupled to

a CFX96 Real-Time system (BioRad) using Kapa SYBR FAST qPCR Master Mix (Sopachem). Two-tailed Student's t-test was applied to determine statistically significant differences ($p<0.05$). qPCR primer sequences are available upon request.

## Results

### Developing biliary cells do not proliferate in two models of polycystic liver

Human fetuses affected by ARPKD develop cysts around the portal vein, which is consistent with a ductal plate origin [23]. No subcapsular cysts are detected. In many instances the ductal plate was almost entirely cystic from 13 weeks of gestation (13W) onwards, suggesting that most cholangiocytes in the ductal plate are involved in cyst formation (Fig 1A). We assessed proliferation of differentiating cholangiocytes in normal fetuses and ARPKD individuals at 13W and 22W of gestation. We measured proliferation of biliary cells by coimmunofluorescent staining against Sex-determining region Y–related HMG box transcription factor 9 (Sox9) and Ki67, which mark biliary cells and cycling cells from G1- to M-phase, respectively. Biliary cells from wild-type (WT) fetuses exhibited low proliferation, extending earlier data on mouse fetal liver [18] (Fig 1A). Importantly, Sox9/Ki67 co-stainings revealed no difference in proliferation of biliary cells between WT and ARPKD fetuses (Fig 1A), irrespective of gestational stage. This was confirmed by quantification (Fig 1B). We reached similar conclusions by analyzing proliferation using staining against the phosphorylated form of histone H3 (P.H3), which specifically marks cells in M-phase (data not shown). The percentage of proliferating biliary cells in human fetuses was similar to that measured in the mouse model (see below). Thus, biliary cysts in ARPKD fetuses, despite their significant size, do not result from excessive proliferation of biliary precursors.

To extend these observations in a second model of polycystic liver, we measured the proliferation of cholangiocytes in embryonic livers from WT and *Cpk* mice [19]. *Cpk* mice develop periportal liver cysts when bred in the appropriate genetic background [19, 21, 26–28]. In these mice, large cysts are readily detected around portal veins by E17.5 [24]. We measured proliferation of $Sox9^+$ biliary cells by staining for Ki67, P.H3, and BrdU. The latter, which marks nuclei of cells during S-phase, had been injected one hour prior to collection of the fetuses. Embryonic biliary cells exhibited very limited proliferation in WT embryos (Fig 2). Moreover, staining for BrdU, Ki67 and P.H3 in *Cpk* livers at E17.5 did not reveal any increase in proliferation within cysts (Fig 2A and 2B).

### Accelerated differentiation of biliary cells in *Cpk* liver

Analysis of embryos at several stages of liver development revealed that cyst formation in homozygous *Cpk* livers occurred very abruptly. Indeed, while no cyst was detected at E15.5 (Fig 3A), at E16.5 the ductal plate became locally irregular and showed some dilated PDS, full-blown cysts were detected at E17.5 with a near 100% penetrance. Importantly, at E15.5 and E16.5, prior to cyst formation, there was no increase in biliary cell proliferation in *Cpk* livers (Fig 3A). At birth, the number of proliferating biliary cells increased slightly in WT pups, as expected [18], but did not differ between WT and *Cpk* pups (Fig 3A). These data indicate that prenatal initiation of cyst formation in *Cpk* livers does not result from increased proliferation of biliary precursors.

Development of cysts cannot result from reduced apoptosis, since the ductal plate and developing bile ducts do not undergo apoptosis [18]. Therefore we envisaged that abnormal cell fate determination might lead to accumulation of biliary cells in *Cpk* livers. Indeed, by the end of gestation the ductal plate normally generates bile ducts but also periportal hepatocytes that progressively lose expression of Sox9 and acquire hepatocytic markers. In polycystic liver,

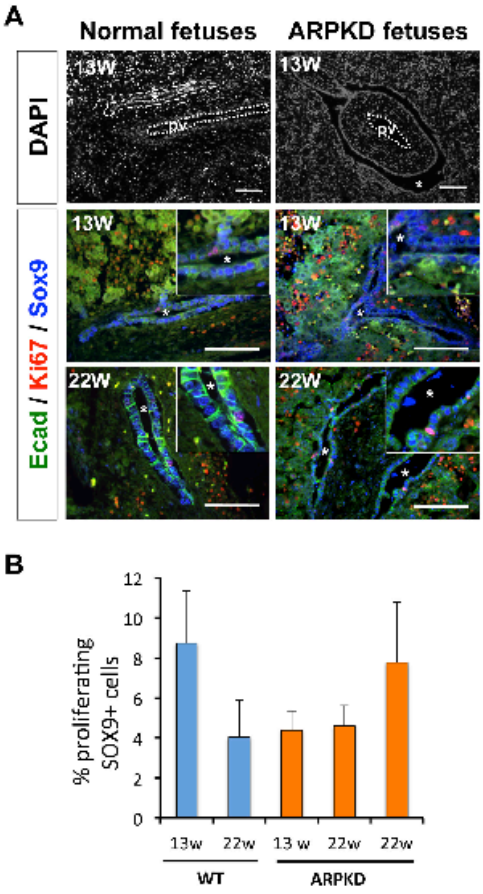



**Fig 1. Liver cysts in human ARPKD fetuses do not exhibit increased proliferation. (A)** *(Upper panels)* Comparison of WT and ARPKD fetal livers. Tissue sections were stained with DAPI. Cysts in ARPKD fetuses almost entirely surround the portal vein. Asterisks indicate cysts and ducts. *(Middle and lower panels)* Immunofluorescent stainings showing the occasional presence of $Sox9^+/Ki67^+$ cells in WT and ARPKD livers. Bars: 100 μm. **(B)** Percentage of proliferating $Sox9^+$ cholangiocyte precursors, using the following formula: $(n^{Ki67+;Sox9+}/n^{Sox9+}) \times 100$. Over 500 (WT) and 800 (ARPKD) $Sox9^+$ cells per liver were counted. The

two ARPKD livers at 22W of gestation were analysed separately. Data are shown as mean +/- SEM (see methods).

doi:10.1371/journal.pone.0132295.g001

ductal plate cells may fail to differentiate to periportal hepatocytes, leading to an accumulation of differentiating biliary cells and expansion of cysts. To test this hypothesis, we traced the fate of Sox9$^+$ ductal plate cells from the fetal period until birth in *Sox9-CreER;Rosa*$^{YFP}$ mice [18] backcrossed in the *Cpk* background. To label Sox9$^+$ cells, we induced CreER-mediated YFP expression at E14.5 by a single injection of Tamoxifen in pregnant mothers (Fig 3B), and analyzed the livers at postnatal day P1. YFP$^+$ hepatocytes were still detected in the periportal areas *of Cpk* pups with near maximal YFP-labeling of biliary cells (Fig 3C). Thus, lack of differentiation of ductal plate cells to hepatocytes in *Cpk* mice is unlikely to be a major cause of biliary cyst formation. Low and variable efficiency of ductal plate cell labeling by Sox9-CreER in a *Cpk* background prevented us to perform accurate quantifications of the lineage tracings. Therefore, our lineage tracings do not exclude that a small proportion of ductal plate cells maintains its biliary fate and fails to convert to hepatocytes, thereby contributing to some extent to perinatal cyst expansion.

Since defective differentiation of ductal plate cells to periportal hepatocytes is unlikely to explain the formation of biliary cysts, we reasoned that excessive and accelerated differentiation of hepatoblasts into biliary cells might cause cyst formation. Our earlier work has shown that biliary cells lining cysts in *Cpk* mice and human ARPKD were well differentiated [24]. Further analysis now revealed that biliary differentiation was accelerated in *Cpk* livers. Indeed, at E17.5 the biliary cysts were invariably symmetrical throughout the lobes (Fig 4): all cells lining the cysts were Sox9$^+$ and the cysts were nearly completely surrounded by mesenchyme. In contrast, the WT littermates showed the expected hilar-to-peripheral gradient of differentiation: PDS adjacent to the hilum were entirely lined by Sox9$^+$ cells, but did not yet show alpha-Smooth Muscle Actin ($\alpha$SMA)$^+$ mesenchyme on their parenchymal side; at a distance of the hilum, most PDS in WT livers were still asymmetrical since they were lined by Sox9$^-$ cells on their parenchymal side; a limited number of symmetrical PDS could be observed but lacked $\alpha$SMA$^+$ mesenchyme. We concluded that excessive and accelerated biliary differentiation contributed to cystogenesis in *Cpk* mice.

To identify potential genes and pathways involved in this phenomenon we performed genome-wide microarray expression assays on WT and *Cpk* embryonic whole livers at E18.5. Mutants could be identified at dissection by the cystic extrahepatic biliary tissue and the pancreatic duct, while PCR confirmed the *Cpk* genotype. Nonetheless, WT and *Cpk* livers exhibited similar expression profiles, indicating that global levels of gene expression remain unaltered in *Cpk* livers. Known regulators of biliary differentiation were not significantly up- or downregulated (S2 Table), and gene set enrichment analysis did not uncover significant anomalies of signaling pathways known to promote biliary differentiation. However, the latter analysis uncovered that a gene set comprising apical junction genes is enriched in the *cpk* livers (Fig 5A; S3 Table). This gene set comprises several claudin genes, including Claudin 7 which in liver is biliary-specific [29]; claudins are associated with tight junctions and were shown to be required for normal bile duct formation [30].

Since gene expression is minimally affected in whole *Cpk* embryonic livers, we focused on the portal tracts. The latter were microdissected from WT and *Cpk* livers at E18.5 (Fig 5B) and qRT-PCR analyses were performed to analyze the expression of transcriptional regulators and signaling effectors known to control biliary differentiation (Fig 5C–5H). Since biliary cells are more numerous in *Cpk* liver portal tracts than in controls, we normalized the expression of the tested genes to the expression of the biliary marker Sox9. While the mean values for hepatocyte

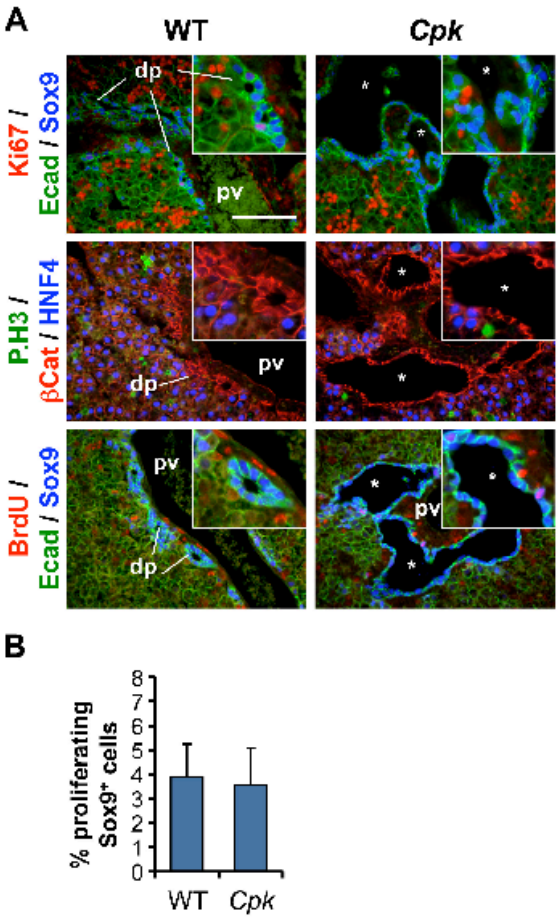



**Fig 2. No excessive proliferation during biliary cyst formation in mouse *Cpk* embryonic livers. (A)** Immunofluorescent staining against the indicated markers was performed on tissue slides from WT and *Cpk* mouse livers at E17.5. Proliferation rates, revealed by Ki67, P.H3 and BrdU stainings, are low in WT and *Cpk* cholangiocytes, while the rest of the liver exhibits higher levels of proliferation. *, cysts; pv, portal vein; dp, ductal plate. Bars: 100 μm. Insets: 2-fold higher magnifications. **(B)** Percentage of proliferating Sox9$^+$ cholangiocyte precursors, calculated using the formula ($n^{Ki67+/Sox9+}/n^{Sox9+}$) x 100, like in Fig 1B (n = 3 for each genotype). Data are mean +/- SD. Two-tailed t-test was performed, and a p-value <0.05 was considered significant.

doi:10.1371/journal.pone.0132295.g002

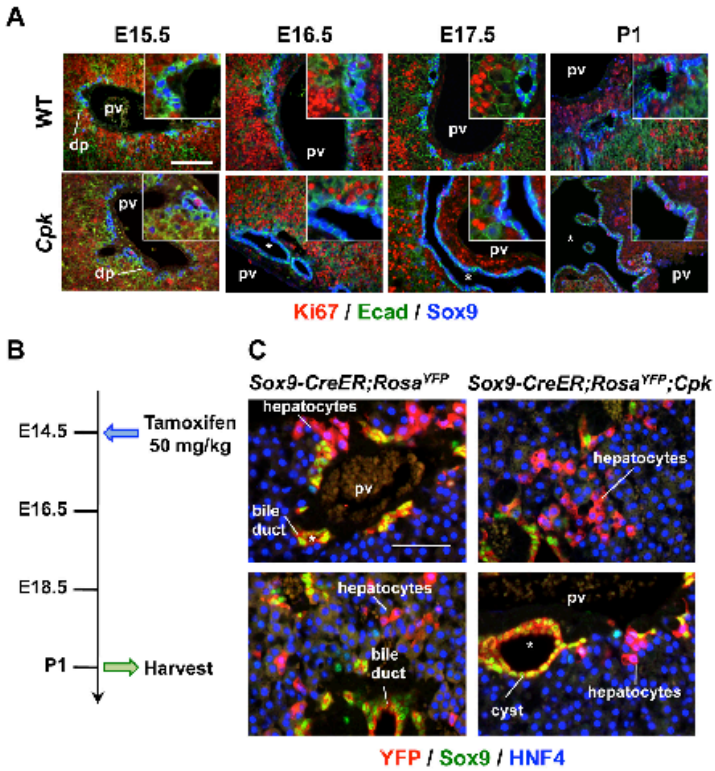



**Fig 3. Cysts form in *Cpk* embryos, without excessive proliferation and with normal differentiation of ductal plate cells into periportal hepatocytes.** **(A)** Time-course analysis of biliary cyst formation in *Cpk* mouse embryos. First signs of biliary cysts can be observed at E16.5; full-blown cysts are observed with 100% penetrance from E17.5. *, cysts, pv, portal vein; dp, ductal plate. Bars: 100 μm. **(B)** Scheme of the Sox9 lineage tracing experiment experiment. Pregnant mothers bearing *Sox9-CreER;Rosa*$^{YFP}$*;Cpk*$^{mut}$ embryos were injected at E14.5 with a single dose of tamoxifen, and newborn pups were collected at P1. **(C)** Sox9$^{+}$ ductal plate cells can give rise to periportal hepatocytes in *Cpk* livers. Lineage tracing of *Sox9-CreER;Rosa*$^{YFP}$*;Cpk*$^{mut}$ ductal plate cells detected differentiation of periportal HNF4$^{+}$/Sox9$^{-}$/YFP$^{+}$ hepatocytes in *Cpk* mouse livers at P1. Bars: 100 μm.

doi:10.1371/journal.pone.0132295.g003

and mesenchymal gene expression were slightly reduced, consistent with a lower number of hepatocytes and mesenchymal cells in the *Cpk* portal tracts, this reduction did not reach statistical significance (Fig 5D). Similarly, mean values of biliary markers (Fig 5C) and of Wnt signaling effectors (Fig 5E) were upregulated in *Cpk* portal tracts, but the data were not

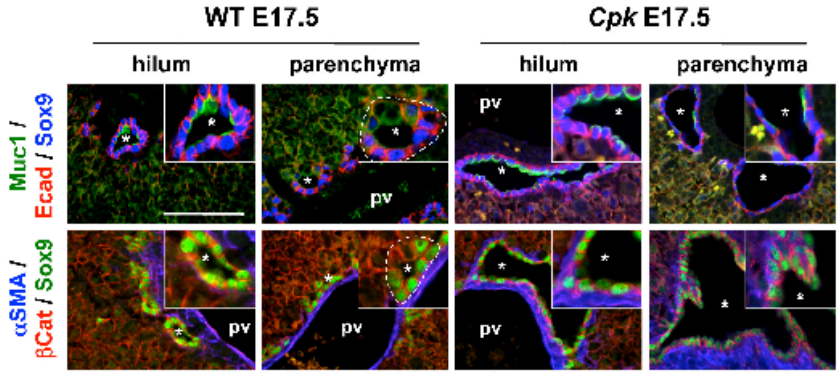



**Fig 4. *Cpk* embryonic livers show excessive and accelerated biliary differentiation.** Biliary differentiation was assessed by immunofluorescent staining against the indicated markers in E17.5 WT and *Cpk* livers. In WT livers, most PDS were asymmetrical, lacked expression of the maturation marker Muc1 and were not surrounded by mesenchyme, except for some PDS adjacent to the hilum. In contrast, all cystic structures in *Cpk* livers were symmetrical both at the hilum and in the parenchyma, expressed biliary maturation markers, and were surrounded by mesenchyme. Bars: 100 μm. Insets: 2-fold higher magnifications.

doi:10.1371/journal.pone.0132295.g004

statistically significant. Analysis of Notch (Fig 5F), FGF and VEGF (Fig 5G), and of Hippo signaling (Fig 5H) did not support an involvement of these pathways. When the measured values were not normalized for Sox9 expression, only *Osteopontin*, *Axin2*, *Hes1*, *Fgfr2 and Ctgf* showed slight but statistically significant upregulation (not shown). Together, these observations do not identify a specific mechanism promoting biliary differentiation in *Cpk* livers but leave open the possibility that combined alterations of several mechanisms contribute to the formation of cysts in ARPKD embryos. These alterations should preferentially occur in periportal cells, explaining why cysts are systematically located near periportal areas.

## Discussion

Initiation of biliary cyst formation in polycystic liver disease is usually considered to result from overproliferation of cyst-lining cells. This commonly held view is based on histological stainings of fetal liver without *bona fide* measurements of proliferation or without statistical validation of proliferation data [15, 31]; it also relies on analyses of postnatal liver cells, and on the observation that cysts in adult liver contain growth factors and cytokines known to promote proliferation [13–15, 32, 33]. Therefore, analysis of proliferation in polycystic livers at fetal stages was lacking. We decided to address this question in human ARPKD and in a mouse model with polycystic liver. ARPKD is caused by mutation in *PKHD1*. To broaden the scope of our analysis, we selected a mouse model that has a mutation in a distinct gene, namely the *Cpk* mouse which has a mutated *Cystin1* gene. Here we show that there is no increase in proliferation rate in ductal plates before and during cyst initiation in two models of polycystic livers, in human and mouse. We propose that cyst formation is proliferation-independent, and provide

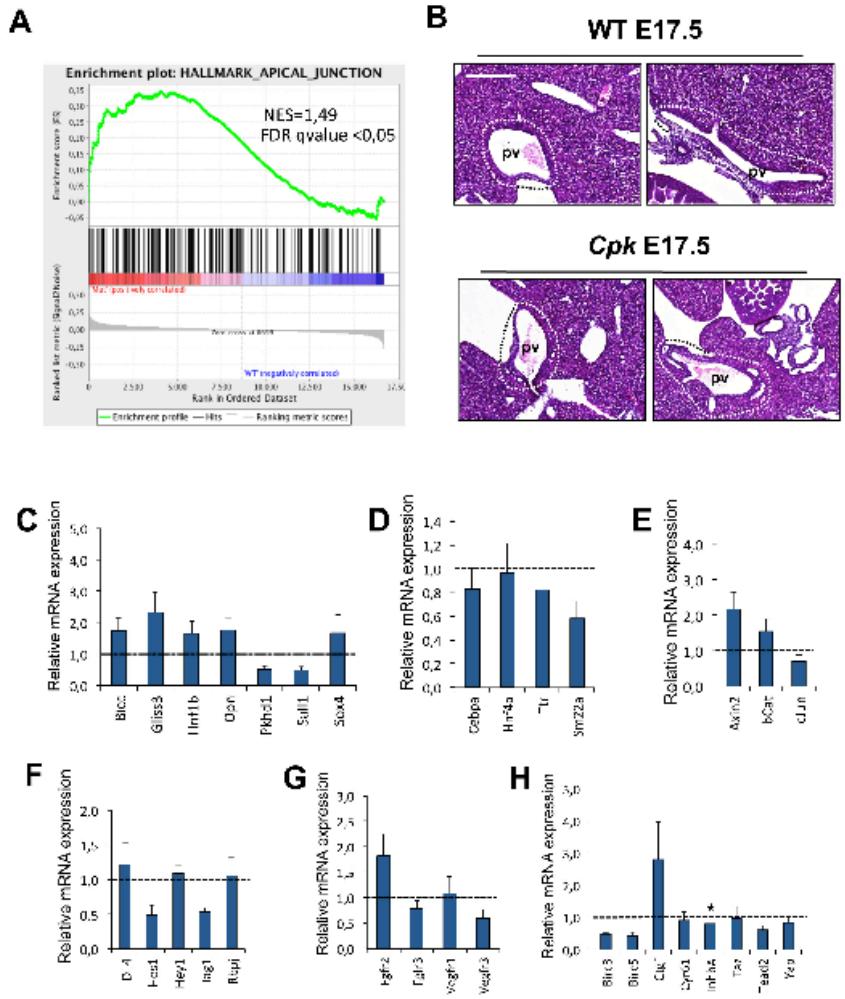

A
Enrichment plot: HALLMARK_APICAL_JUNCTION
NES=1,49
FDR qvalue <0,05
Rank in Ordered Dataset
Enrichment profile
Hits
Ranking metric scores
B
WT E17.5
pv
pv
Cpk E17.5
pv
pv
C
Relative mRNA expression
Bicc1
Gli3s3
Inf1b
Osn
Pkhd1
Sall1
Sox4
D
Relative mRNA expression
Cebpa
Hnf4a
Tr
Smr22a
E
Relative mRNA expression
Axin2
bCat
cJun
F
Relative mRNA expression
D-1
Hes1
Hey1
Ng1
Rbpj
G
Relative mRNA expression
Fgfr2
Fgfr3
Vegfr1
Vegfr3
H
Relative mRNA expression
Birc3
Birc5
Ctgf
Cyr61
Inhba
Tac
Tead2
Yap

**Fig 5. Expression of genes in *Cpk* livers. (A)** Gene set enrichment analysis revealed enrichment of apical junction proteins. The gene set is shown in S3 Table. **(B)** Manual microdissection of WT and *Cpk* portal tracts at E17.5 on formalin-fixed, paraffin-embedded livers. Representative H&E staining of 2 individuals of each genotype are shown. The area of microdissected tissue is delineated by a dotted line. Bar, 400 μm. **(C-J)** qRT-PCR analysis in WT and *Cpk* portal tracts. Shown here are differentiation markers of **C:** cholangiocytes, **D:** hepatocytes and mesenchyme (*Sm22a*); markers of signaling activity of the **E:** Wnt/βCatenin, **F:** Notch, **G:** FGF and VEGF, **H:** YAP/Hippo pathways (n = 3 for WT, n = 5 for cpk). All gene expression data were normalized for the expression for the biliary marker Sox9. Student's t-test was applied to determine significant difference (*, $p<0.05$).

doi:10.1371/journal.pone.0132295.g005

evidence that excessive differentiation contributes to cystogenesis at least in a subset of polycystic liver diseases.

Cysts develop around branches of the portal veins, suggesting that in human ARPKD and *Cpk* embryos hepatoblasts display an excessive response to a biliary differentiation-inducing signal emitted by the portal endothelium or surrounding mesenchyme. Cystin1 is associated with the cilium [19, 20] and the latter organelle regulates the activity of several signaling pathways involved in cellular differentiation, including pathways known to stimulate biliary differentiation such as the Notch and Wnt pathways [34–37]. However, overexpression of Notch or Wnt effectors does not induce polycystic livers [35, 38]. Thus, it is likely that none of the known pathways involved in biliary differentiation can, upon perturbation, lead to liver cyst formation single-handedly. However, we cannot rule out that slight perturbations of mutiple pathways combinatorially induce polycystic liver. In this context, our gene set enrichment analysis revealed that apical junction proteins are enriched in *Cpk* livers. Defective cilia function is associated with perturbed expression of the tight junction-associated proteins claudins, including upregulation of a subset of claudins [39]. Claudins are required for normal bile duct development [30]. Taken together, data in human ARPKD and in *Cpk* mice open the possibility that tight junction regulation and biliary differentiation are intimately connected.

Enrichment of cystin and/or fibrocystin in cells located close to the periportal area may explain why cysts develop only around portal veins. In line with this, purified embryonic cholangiocytes show a dramatic enrichment of cystin and fibrocystin mRNA expression as compared to hepatoblasts (data not shown). Dynamic three-dimensional analysis of bile duct development revealed that it normally starts in close vicinity of the portal vein with formation of small cysts, defined by a size that is smaller than 40 μm and with a luminal diameter larger than 5 μm; subsequently, segments of larger size form, most likely by connection and elongation of small cysts [40]. In the present work, we noticed that polycystosis in *Cpk* livers starts at E16.5, a developmental stage at which cyst and segment formation increases in normal embryos. Therefore, acceleration of this early stage of biliary construction is a hallmark of the polycystic liver models studied here. The dynamic model of biliary development revealed that after birth, biliary network density decreases while bile ducts enlarge, elongate and move at some distance away from the portal vein [40]. Takashima and coworkers suggested that postnatal reduction of the biliary network may result from conversion of a subset of biliary cells to hepatocytes [18, 40]. We therefore hypothesized that cyst formation or expansion may result from failure to reduce the network by lack of conversion of a subset of biliary cells to hepatocytes. However, our lineage tracings do not support this hypothesis.

In the present work we provide evidence that cyst initiation results from increased differentiation of biliary cells.

Several mechanisms are proposed to contribute to cyst development. These are increased cell proliferation, enhanced fluid secretion, abnormal cell–matrix interactions, alterations in cell polarity, abnormal ciliary structure or function, and autocrine and paracrine angiogenic signaling [4, 6]. In the models studied here, ciliary dysfunction is likely a key driver of cyst initiation, as mentioned above. However, most studies link ciliary dysfunction with hyperproliferation and altered fluid secretion, for instance via perturbed $Ca^{2+}$ and cAMP levels. Our data do

not show biliary cell hyperproliferation and the histology of the cysts do not show evidence for fluid-induced tension. Still, further work is required to determine whether $Ca^{2+}$ and cAMP levels, and fluid secretion might regulate cholangiocyte differentiation.

## Conclusions

Our data indicate that initiation of liver cyst formation does not necessarily depend on overproliferation of cyst-lining cells at fetal stages. Since overproliferation occurs postnatally, cyst formation thus appears to be a two-step mechanism, most likely initiated by excessive differentiation of biliary precursors *in utero* followed by proliferative growth after birth. Therefore, in addition to controlling the proliferative growth of pre-established cysts, efforts aiming at preventing the excessive differentiation that causes biliary cyst formation may provide therapeutic benefits.

## Supporting Information

**S1 Table. List of antibodies used in this study.**
(PDF)

**S2 Table. Microarray data comparing liver RNA from E18.5 wild-type and *Cpk* embryos.**
(PDF)

**S3 Table. Apical junction gene set enriched in E18.5 *Cpk* embryos as compared to wild-type embryos.**
(PDF)

## Acknowledgments

The authors thank Ahmed Essaghir for help with microarray data, Bianca Pastorelli for assistance, and the members of the Lemaigre lab for discussions. We also thank Mrs S. Desjardins from the direction of clinical research of the Bordeaux hospital (CHU Bordeaux) for her research ethics expertise.

## Author Contributions

Conceived and designed the experiments: JBB CEP FPL. Performed the experiments: JBB SC. Analyzed the data: JBB SC CD CEP FPL. Contributed reagents/materials/analysis tools: SL. Wrote the paper: JBB SC CD SL CEP FPL.

## References

1. Cnossen WR, te Morsche RH, Hoischen A, Gilissen C, Chrispijn M, Venselaar H, et al. Whole-exome sequencing reveals LRP5 mutations and canonical Wnt signaling associated with hepatic cystogenesis. Proc Natl Acad Sci U S A. 2014; 111: 5343–5348. doi: 10.1073/pnas.1309438111 PMID: 24706814
2. Wills ES, Roepman R, Drenth JP. Polycystic liver disease: ductal plate malformation and the primary cilium. Trends Mol Med. 2014; 20: 261–270. doi: 10.1016/j.molmed.2014.01.003 PMID: 24506938
3. Masyuk T, LaRusso N. Polycystic liver disease: new insights into disease pathogenesis. Hepatology. 2006; 43: 906–908. PMID: 16628666
4. Onori P, Franchitto A, Mancinelli R, Carpino G, Alvaro D, Francis H, et al. Polycystic liver diseases. Dig Liver Dis. 2010; 42: 261–271. doi: 10.1016/j.dld.2010.01.006 PMID: 20138815
5. Strazzabosco M, Fabris L. Development of the bile ducts: essentials for the clinical hepatologist. J Hepatol. 2012; 56: 1159–1170. doi: 10.1016/j.jhep.2011.09.022 PMID: 22245898
6. Strazzabosco M, Somlo S. Polycystic liver diseases: congenital disorders of cholangiocyte signaling. Gastroenterology. 2011; 140: 1855–1859. doi: 10.1053/j.gastro.2011.04.030 PMID: 21515270

7. Tao B, Bu S, Yang Z, Siroky B, Kappes JC, Kispert A, et al. Cystin localizes to primary cilia via membrane microdomains and a targeting motif. J Am Soc Nephrol. 2009; 20: 2570–2580. doi: 10.1681/ASN.2009020188 PMID: 19850956

8. Gallagher AR, Esquivel EL, Briere TS, Tian X, Mitobe M, Menezes LF, et al. Biliary and pancreatic dysgenesis in mice harboring a mutation in Pkhd1. Am J Pathol. 2008; 172: 417–429. doi: 10.2353/ajpath.2008.070381 PMID: 18202188

9. Woollard JR, Punyashtiti R, Richardson S, Masyuk TV, Whelan S, Huang BQ, et al. A mouse model of autosomal recessive polycystic kidney disease with biliary duct and proximal tubule dilatation. Kidney Int. 2007; 72: 328–336. PMID: 17519956

10. Johnson CA, Gissen P, Sergi C. Molecular pathology and genetics of congenital hepatorenal fibrocystic syndromes. J Med Genet. 2003; 40: 311–319. PMID: 12746391

11. Masyuk AI, Masyuk TV, LaRusso NF. Cholangiocyte primary cilia in liver health and disease. Dev Dyn. 2008; 237: 2007–2012. doi: 10.1002/dvdy.21530 PMID: 18407555

12. Muchatuta MN, Gattone VH 2nd, Witzmann FA, Blazer-Yost BL. Structural and functional analyses of liver cysts from the BALB/c-cpk mouse model of polycystic kidney disease. Exp Biol Med. 2009; 234: 17–27.

13. Gradilone SA, Masyuk TV, Huang BQ, Banales JM, Lehmann GL, Radtke BN, et al. Activation of Trpv4 reduces the hyperproliferative phenotype of cystic cholangiocytes from an animal model of ARPKD. Gastroenterology. 2010; 139: 304–314. doi: 10.1053/j.gastro.2010.04.010 PMID: 20399209

14. Muff MA, Masyuk TV, Stroope AJ, Huang BQ, Splinter PL, Lee SO, et al. Development and characterization of a cholangiocyte cell line from the PCK rat, an animal model of Autosomal Recessive Polycystic Kidney Disease. Lab Invest. 2006; 86: 940–950. PMID: 16783394

15. Sanzen T, Harada K, Yasoshima M, Kawamura Y, Ishibashi M, Nakanuma Y. Polycystic kidney rat is a novel animal model of Caroli's disease associated with congenital hepatic fibrosis. Am J Pathol. 2001; 158: 1605–1612. PMID: 11337358

16. Raynaud P, Carpentier R, Antoniou A, Lemaigre FP. Biliary differentiation and bile duct morphogenesis in development and disease. Int J Biochem Cell Biol. 2011; 43: 245–256. doi: 10.1016/j.biocel.2009.07.020 PMID: 19735739

17. Antoniou A, Raynaud P, Cordi S, Zong Y, Tronche F, Stanger B, et al. Intrahepatic bile ducts develop according to a new mode of tubulogenesis regulated by the transcription factor SOX9. Gastroenterology. 2009; 136: 2325–2333. doi: 10.1053/j.gastro.2009.02.051 PMID: 19403103

18. Carpentier R, Suner RE, Van Hul N, Kopp JL, Beaudry JB, Cordi S, et al. Embryonic ductal plate cells give rise to cholangiocytes, periportal hepatocytes, and adult liver progenitor cells. Gastroenterology. 2011; 141: 1432–1438. doi: 10.1053/j.gastro.2011.06.049 PMID: 21708104

19. Hou X, Mrug M, Yoder BK, Lefkowitz EJ, Kremmidiotis G, D'Eustachio P, et al. Cystin, a novel cilia-associated protein, is disrupted in the cpk mouse model of polycystic kidney disease. J Clin Invest. 2002; 109: 533–540. PMID: 11854326

20. Yoder BK, Hou X, Guay-Woodford LM. The polycystic kidney disease proteins, polycystin-1, polycystin-2, polaris, and cystin, are co-localized in renal cilia. J Am Soc Nephrol. 2002; 13: 2508–2516. PMID: 12239239

21. Preminger GM, Koch WE, Fried FA, McFarland E, Murphy ED, Mandell J. Murine congenital polycystic kidney disease: a model for studying development of cystic disease. J Urol. 1982; 127: 556–560. PMID: 7062441

22. Denamur E, Delezoide AL, Alberti C, Bourillon A, Gubler MC, Bouvier R, et al. Genotype-phenotype correlations in fetuses and neonates with autosomal recessive polycystic kidney disease. Kidney Int. 2010; 77: 350–358. doi: 10.1038/ki.2009.440 PMID: 19940839

23. Villeneuve J, Pelluard-Nehme F, Combe C, Carles D, Chaponnier C, Ripoche J, et al. Immunohistochemical study of the phenotypic change of the mesenchymal cells during portal tract maturation in normal and fibrous (ductal plate malformation) fetal liver. Comp Hepatol. 2009; 8:5. doi: 10.1186/1476-5926-8-5 PMID: 19602240

24. Raynaud P, Tate J, Callens C, Cordi S, Vandersmissen P, Carpentier R, et al. A classification of ductal plate malformations based on distinct pathogenic mechanisms of biliary dysmorphogenesis. Hepatology. 2011; 53: 1959–1966. doi: 10.1002/hep.24292 PMID: 21391226

25. Subramanian A, Tamayo P, Mootha VK, Mukherjee S, Ebert BL, Gillette MA, et al. Gene set enrichment analysis: a knowledge-based approach for interpreting genome-wide expression profiles. Proc Natl Acad Sci U S A. 2005; 102: 15545–15550. PMID: 16199517

26. Guay-Woodford LM, Green WJ, Lindsey JR, Beier DR. Germline and somatic loss of function of the mouse cpk gene causes biliary ductal pathology that is genetically modulated. Hum Mol Genet. 2000; 9: 769–778. PMID: 10749984

27. Harris PC, Rossetti S. Molecular genetics of autosomal recessive polycystic kidney disease. Mol Genet Metab. 2004; 8: 75–85.

28. Nagao S, Kugita M, Yoshihara D, Yamaguchi T. Animal models for human polycystic kidney disease. Exp Anim. 2012; 61: 477–488. PMID: 23095811

29. Seth A, Ye J, Yu N, Guez F, Bedford DC, Neale GA, et al. Prox1 ablation in hepatic progenitors causes defective hepatocyte specification and increases biliary cell commitment. Development. 2014; 141: 538–547. doi: 10.1242/dev.099481 PMID: 24449835

30. Cheung ID, Bagnat M, Ma TP, Datta A, Evason K, Moore JC, et al. Regulation of intrahepatic biliary duct morphogenesis by Claudin 15-like b. Dev Biol. 2012; 361: 68–78. doi: 10.1016/j.ydbio.2011.10.004 PMID: 22020048

31. Moser M, Matthiesen S, Kirfel J, Schorle H, Bergmann C, Senderek J, et al. A mouse model for cystic biliary dysgenesis in autosomal recessive polycystic kidney disease (ARPKD). Hepatology. 2005; 41: 1113–1121. PMID: 15830394

32. Masyuk TV, Masyuk AI, Torres VE, Harris PC, Larusso NF. Octreotide inhibits hepatic cystogenesis in a rodent model of polycystic liver disease by reducing cholangiocyte adenosine 3',5'-cyclic monophosphate. Gastroenterology. 2007; 132: 1104–1116. PMID: 17383431

33. Lai X, Blazer-Yost BL, Gattone VH 2nd, Muchatuta MN, Witzmann FA. Protein composition of liver cyst fluid from the BALB/c-cpk/+ mouse model of autosomal recessive polycystic kidney disease. Proteomics. 2009; 9: 3775–3782. doi: 10.1002/pmic.200800379 PMID: 19639592

34. Gerdes JM, Davis EE, Katsanis N. The vertebrate primary cilium in development, homeostasis, and disease. Cell. 2009; 137: 32–45. doi: 10.1016/j.cell.2009.03.023 PMID: 19345185

35. Decaens T, Godard C, de Reynies A, Rickman DS, Tronche F, Couty JP, et al. Stabilization of beta-catenin affects mouse embryonic liver growth and hepatoblast fate. Hepatology. 2008; 47: 247–258. PMID: 18038450

36. Tan X, Yuan Y, Zeng G, Apte U, Thompson MD, Cieply B, et al. Beta-catenin deletion in hepatoblasts disrupts hepatic morphogenesis and survival during mouse development. Hepatology. 2008; 47: 1667–1679. doi: 10.1002/hep.22225 PMID: 18393386

37. Zong Y, Panikkar A, Xu J, Antoniou A, Raynaud P, Lemaigre F, et al. Notch signaling controls liver development by regulating biliary differentiation. Development. 2009; 136: 1727–1739. doi: 10.1242/dev.029140 PMID: 19369401

38. Yanger K, Zong Y, Maggs LR, Shapira SN, Maddipati R, Aiello NM, et al. Robust cellular reprogramming occurs spontaneously during liver regeneration. Genes Dev. 2013; 27: 719–724. doi: 10.1101/gad.207803.112 PMID: 23520387

39. Overgaard CE, Sanzone KM, Spiczka KS, Sheff DR, Sandra A, Yeaman C. Deciliation is associated with dramatic remodeling of epithelial cell junctions and surface domains. Mol Biol Cell. 2009; 20: 102–113. doi: 10.1091/mbc.E08-07-0741 PMID: 19005211

40. Takashima Y, Terada M, Kawabata M, Suzuki A. Dynamic three-dimensional morphogenesis of intrahepatic bile ducts in mouse liver development. Hepatology. 2015; 61: 1003–1011. doi: 10.1002/hep.27436 PMID: 25212491

## Supplemental Table 1: List of antibodies used in this study

| Primary antibody | Species/Isotype | Dilution | Manufacturer | Catalog number |
|---|---|---|---|---|
| HNF4 | mouse IgG2a | 1/300 | R&D Systems | PP-H1415-OO |
| Ecad | mouse | 1/250 | BD Biosciences | 610182 |
| Sox9 | rabbit | 1/500 | Chemicon | AB5535 |
| Muc1 | hamster | 1/500 | Neomarkers | HM-1630-P |
| Ki67 | mouse IgG1 | 1/250 | BD Biosciences | 556003 |
| Brdu | mouse IgG1 | 1/20 | DSHB | G3G4 |
| P.H3 | rabbit | 1/100 | Cell Signaling | 9701 |
| aSMA | mouse IgG2a | 1/50 | Dako | M0851 |
| bCat | mouse IgG1 | 1/1000 | BD Biosciences | 610154 |
| YFP | goat | 1/250 | Abcam | ab6673 |

| Secondary antibody | Dilution | Manufacturer | Catalog number |
|---|---|---|---|
| donkey anti-mouse Alexa Fluor 647 | 1/1000 | Invitrogen | A31571 |
| goat anti-mouse IgG2a Alexa Fluor 488 | 1/1000 | Invitrogen | A21131 |
| goat anti-mouse IgG2a Alexa Fluor 594 | 1/1000 | Invitrogen | A21135 |
| goat anti-mouse IgG2a Alexa Fluor 647 | 1/1000 | Invitrogen | A21241 |
| goat anti-mouse IgG1 Alexa Fluor 594 | 1/1000 | Invitrogen | A21125 |
| donkey anti-rabbit Alexa Fluor 488 | 1/1000 | Invitrogen | A21206 |
| donkey anti-rabbit Alexa Fluor 647 | 1/1000 | Invitrogen | A31573 |
| donkey anti-goat Alexa Fluor 594 | 1/1000 | Invitrogen | A11058 |
| biotinylated anti-hamster | 1/500 | Jackson ImmunoResearch | 127-065-160 |
| streptavidin Alexa Fluor 488 | 1/1000 | Invitrogen | S11223 |

# VI. REFERENCES


Aishima, S., Asayama, Y., Taguchi, K., Sugimachi, K., Shirabe, K., Shimada, M., Sugimachi, K., Tsuneyoshi, M., 2002. The utility of keratin 903 as a new prognostic marker in mass-forming-type intrahepatic cholangiocarcinoma. Mod Pathol 15, 1181-1190.

Alder, O., Cullum, R., Lee, S., Kan, A.C., Wei, W., Yi, Y., Garside, V.C., Bilenky, M., Griffith, M., Morrissy, A.S., Robertson, G.A., Thiessen, N., Zhao, Y., Chen, Q., Pan, D., Jones, S.J., Marra, M.A., Hoodless, P.A., 2014. Hippo signaling influences HNF4A and FOXA2 enhancer switching during hepatocyte differentiation. Cell Rep 9, 261-271.

Alon, U., 2007. Network motifs: theory and experimental approaches. Nat Rev Genet 8, 450-461.

Antoniou, A., Raynaud, P., Cordi, S., Zong, Y., Tronche, F., Stanger, B., Jacquemin, P., Pierreux, C.E., Clotman, F., Lemaigre, F.P., 2009a. Intrahepatic bile ducts develop according to a new mode of tubulogenesis regulated by the transcription factor SOX9. Gastroenterology 136, 2325-2333.

Antoniou, A., Raynaud, P., Cordi, S., Zong, Y., Tronche, F., Stanger, B.Z., Jacquemin, P., Pierreux, C.E., Clotman, F., Lemaigre, F.P., 2009b. Intrahepatic bile ducts develop according to a new mode of tubulogenesis regulated by the transcription factor SOX9. Gastroenterology 136, 2325-2333.

Arts, F.A., Velghe, A.I., Stevens, M., Renauld, J.C., Essaghir, A., Demoulin, J.B., 2015. Idiopathic basal ganglia calcification-associated PDGFRB mutations impair the receptor signalling. Journal of cellular and molecular medicine 19, 239-248.

Bartel, D.P., 2009. MicroRNAs: target recognition and regulatory functions. Cell 136, 215-233.

Battle, M.A., Konopka, G., Parviz, F., Gaggl, A.L., Yang, C., Sladek, F.M., Duncan, S.A., 2006. Hepatocyte nuclear factor 4alpha orchestrates expression of cell adhesion proteins during the epithelial transformation of the developing liver. Proc Natl Acad Sci U S A 103, 8419-8424.

Beaudry, J.B., Pierreux, C.E., Hayhurst, G.P., Plumb-Rudewiez, N., Weiss, M.C., Rousseau, G.G., Lemaigre, F.P., 2006. Threshold levels of hepatocyte nuclear factor 6 (HNF-6) acting in synergy with HNF-4 and PGC-1alpha are required for time-specific gene expression during liver development. Mol Cell Biol 26, 6037-6046.

Berg, T., Rountree, C.B., Lee, L., Estrada, J., Sala, F.G., Choe, A., Veltmaat, J.M., De Langhe, S., Lee, R., Tsukamoto, H., Crooks, G.M., Bellusci, S., Wang, K.S., 2007. Fibroblast growth factor 10 is critical for liver growth during embryogenesis and controls hepatoblast survival via beta-catenin activation. Hepatology 46, 1187-1197.

Bernstein, E., Kim, S.Y., Carmell, M.A., Murchison, E.P., Alcorn, H., Li, M.Z., Mills, A.A., Elledge, S.J., Anderson, K.V., Hannon, G.J., 2003. Dicer is essential for mouse development. Nature genetics 35, 215-217.

Bernuzzi, F., Marabita, F., Lleo, A., Carbone, M., Mirolo, M., Marzioni, M., Alpini, G., Alvaro, D., Muri Boberg, K., Locati, M., Torzilli, G., Rimassa, L., Piscaglia, F., He, X.S., Bowlus, C.L., Yang, G.X., Eric Gershwin, M., Invernizzi, P., 2016. Serum microrna as novel biomarkers for primary sclerosing cholangitis and cholangiocarcinoma. Clinical and experimental immunology.

Blechacz, B., Gores, G.J., 2008. Cholangiocarcinoma: advances in pathogenesis, diagnosis, and treatment. Hepatology 48, 308-321.

Blouin, A., Bolender, R.P., Weibel, E.R., 1977. Distribution of organelles and membranes between hepatocytes and nonhepatocytes in the rat liver parenchyma. A stereological study. The Journal of cell biology 72, 441-455.

Bochkis, I.M., Rubins, N.E., White, P., Furth, E.E., Friedman, J.R., Kaestner, K.H., 2008. Hepatocyte-specific ablation of Foxa2 alters bile acid homeostasis and results in endoplasmic reticulum stress. Nature medicine 14, 828-836.

Bort, R., Signore, M., Tremblay, K., Martinez Barbera, J.P., Zaret, K.S., 2006. Hex homeobox gene controls the transition of the endoderm to a pseudostratified, cell emergent epithelium for liver bud development. Dev Biol 290, 44-56.

Bossard, P., Zaret, K.S., 1998. GATA transcription factors as potentiators of gut endoderm differentiation. Development 125, 4909-4917.

Braicu, C., 2009. Molecular Markers in the Pathogenesis of Cholangiocarcinoma: Potential for Early Detection and Selection of Appropriate Treatment. Gastroenterology Research 2, 132-140.

Calmont, A., Wandzioch, E., Tremblay, K.D., Minowada, G., Kaestner, K.H., Martin, G.R., Zaret, K.S., 2006. An FGF response pathway that mediates hepatic gene induction in embryonic endoderm cells. Dev Cell 11, 339-348.

Carpentier, R., Suner, R.E., van Hul, N., Kopp, J.L., Beaudry, J.B., Cordi, S., Antoniou, A., Raynaud, P., Lepreux, S., Jacquemin, P., Leclercq, I.A., Sander, M., Lemaigre, F.P., 2011. Embryonic ductal plate cells give rise to cholangiocytes, periportal

hepatocytes, and adult liver progenitor cells. Gastroenterology 141, 1432-1438, 1438 e1431-1434.

Chakravarty, G., Rider, B., Mondal, D., 2011. Cytoplasmic compartmentalization of SOX9 abrogates the growth arrest response of breast cancer cells that can be rescued by trichostatin A treatment. Cancer Biol Ther 11, 71-83.

Cheloufi, S., Dos Santos, C.O., Chong, M.M., Hannon, G.J., 2010. A dicer-independent miRNA biogenesis pathway that requires Ago catalysis. Nature 465, 584-589.

Chen, L., Yan, H.X., Yang, W., Hu, L., Yu, L.X., Liu, Q., Li, L., Huang, D.D., Ding, J., Shen, F., Zhou, W.P., Wu, M.C., Wang, H.Y., 2009. The role of microRNA expression pattern in human intrahepatic cholangiocarcinoma. J Hepatol 50, 358-369.

Chiang, H.R., Schoenfeld, L.W., Ruby, J.G., Auyeung, V.C., Spies, N., Baek, D., Johnston, W.K., Russ, C., Luo, S., Babiarz, J.E., Blelloch, R., Schroth, G.P., Nusbaum, C., Bartel, D.P., 2010. Mammalian microRNAs: experimental evaluation of novel and previously annotated genes. Genes Dev 24, 992-1009.

Chong, M.M., Zhang, G., Cheloufi, S., Neubert, T.A., Hannon, G.J., Littman, D.R., 2010. Canonical and alternate functions of the microRNA biogenesis machinery. Genes Dev 24, 1951-1960.

Cifuentes, D., Xue, H., Taylor, D.W., Patnode, H., Mishima, Y., Cheloufi, S., Ma, E., Mane, S., Hannon, G.J., Lawson, N.D., Wolfe, S.A., Giraldez, A.J., 2010. A novel miRNA processing pathway independent of Dicer requires Argonaute2 catalytic activity. Science 328, 1694-1698.

Cirillo, L.A., Lin, F.R., Cuesta, I., Friedman, D., Jarnik, M., Zaret, K.S., 2002. Opening of compacted chromatin by early developmental transcription factors HNF3 (FoxA) and GATA-4. Mol Cell 9, 279-289.

Clotman, F., Jacquemin, P., Plumb-Rudewiez, N., Pierreux, C.E., Van der Smissen, P., Dietz, H.C., Courtoy, P.J., Rousseau, G.G., Lemaigre, F.P., 2005. Control of liver cell fate decision by a gradient of TGF beta signaling modulated by Onecut transcription factors. Genes Dev 19, 1849-1854.

Clotman, F., Lannoy, V.J., Reber, M., Cereghini, S., Cassiman, D., Jacquemin, P., Roskams, T., Rousseau, G.G., Lemaigre, F.P., 2002. The onecut transcription factor HNF6 is required for normal development of the biliary tract. Development 129, 1819-1828.

Coffinier, C., Gresh, L., Fiette, L., Tronche, F., Schutz, G., Babinet, C., Pontoglio, M., Yaniv, M., Barra, J., 2002. Bile system morphogenesis defects and liver dysfunction upon targeted deletion of HNF1beta. Development 129, 1829-1838.

Coffinier, C., Thepot, D., Babinet, C., Yaniv, M., Barra, J., 1999. Essential role for the homeoprotein vHNF1/HNF1beta in visceral endoderm differentiation. Development 126, 4785-4794.

Collins, A.L., Wojcik, S., Liu, J., Frankel, W.L., Alder, H., Yu, L., Schmittgen, T.D., Croce, C.M., Bloomston, M., 2014. A differential microRNA profile distinguishes cholangiocarcinoma from pancreatic adenocarcinoma. Annals of surgical oncology 21, 133-138.

Cordi, S., Godard, C., Saandi, T., Jacquemin, P., Monga, S.P., Colnot, S., Lemaigre, F.P., 2016. Role of beta-catenin in development of bile ducts. Differentiation, 42-49.

Croniger, C., Trus, M., Lysek-Stupp, K., Cohen, H., Liu, Y., Darlington, G.J., Poli, V., Hanson, R.W., Reshef, L., 1997. Role of the isoforms of CCAAT/enhancer-binding protein in the initiation of phosphoenolpyruvate carboxykinase (GTP) gene transcription at birth. J Biol Chem 272, 26306-26312.

Decaens, T., Godard, C., de Reynies, A., Rickman, D.S., Tronche, F., Couty, J.P., Perret, C., Colnot, S., 2008. Stabilization of beta-catenin affects mouse embryonic liver growth and hepatoblast fate. Hepatology 47, 247-258.

DeLaForest, A., Nagaoka, M., Si-Tayeb, K., Noto, F.K., Konopka, G., Battle, M.A., Duncan, S.A., 2011. HNF4A is essential for specification of hepatic progenitors from human pluripotent stem cells. Development 138, 4143-4153.

Deng, X.G., Qiu, R.L., Wu, Y.H., Li, Z.X., Xie, P., Zhang, J., Zhou, J.J., Zeng, L.X., Tang, J., Maharjan, A., Deng, J.M., 2014. Overexpression of miR-122 promotes the hepatic differentiation and maturation of mouse ESCs through a miR-122/FoxA1/HNF4a-positive feedback loop. Liver Int 34, 281-295.

Denson, L.A., McClure, M.H., Bogue, C.W., Karpen, S.J., Jacobs, H.C., 2000. HNF3beta and GATA-4 transactivate the liver-enriched homeobox gene, Hex. Gene 246, 311-320.

Du, L., Subauste, M.C., DeSevo, C., Zhao, Z., Baker, M., Borkowski, R., Schageman, J.J., Greer, R., Yang, C.R., Suraokar, M., Wistuba, II, Gazdar, A.F., Minna, J.D., Pertsemlidis, A., 2012. miR-337-3p and its targets STAT3 and RAP1A modulate taxane sensitivity in non-small cell lung cancers. PLoS One 7, e39167.

Dweep, H., Gretz, N., 2015. miRWalk2.0: a comprehensive atlas of microRNA-target interactions. Nature methods 12, 697.

Ebert, M.S., Sharp, P.A., 2012. Roles for microRNAs in conferring robustness to biological processes. Cell 149, 515-524.

Enomoto, H., Yoshida, K., Kishima, Y., Kinoshita, T., Yamamoto, M., Everett, A.D., Miyajima, A., Nakamura, H., 2002. Hepatoma-derived growth factor is highly expressed in developing liver and promotes fetal hepatocyte proliferation. Hepatology 36, 1519-1527.

Fan, B., Malato, Y., Calvisi, D.F., Naqvi, S., Razumilava, N., Ribback, S., Gores, G.J., Dombrowski, F., Evert, M., Chen, X., Willenbring, H., 2012. Cholangiocarcinomas can originate from hepatocytes in mice. J Clin Invest 122, 2911-2915.

Fan, L., He, F., Liu, H., Zhu, J., Liu, Y., Yin, Z., Wang, L., Guo, Y., Wang, Z., Yan, Q., Huang, G., 2011. CD133: a potential indicator for differentiation and prognosis of human cholangiocarcinoma. BMC Cancer 11, 320.

Fava, G., Lorenzini, I., 2012. Molecular pathogenesis of cholangiocarcinoma. International journal of hepatology 2012, 630543.

Friedman, R.C., Farh, K.K., Burge, C.B., Bartel, D.P., 2009. Most mammalian mRNAs are conserved targets of microRNAs. Genome Res 19, 92-105.

Gailhouste, L., Gomez-Santos, L., Hagiwara, K., Hatada, I., Kitagawa, N., Kawaharada, K., Thirion, M., Kosaka, N., Takahashi, R.-u., Shibata, T., Miyajima, A., Ochiya, T., 2013. miR-148a plays a pivotal role in the liver by promoting the hepatospecific phenotype and suppressing the invasiveness of transformed cells. Hepatology 58, 1153-1165.

Gebhardt, R., Baldysiak-Figiel, A., Krugel, V., Ueberham, E., Gaunitz, F., 2007. Hepatocellular expression of glutamine synthetase: an indicator of morphogen actions as master regulators of zonation in adult liver. Progress in histochemistry and cytochemistry 41, 201-266.

Geisler, F., Nagl, F., Mazur, P.K., Lee, M., Zimber-Strobl, U., Strobl, L.J., Radtke, F., Schmid, R.M., Siveke, J.T., 2008. Liver-specific inactivation of Notch2, but not Notch1, compromises intrahepatic bile duct development in mice. Hepatology 48, 607-616.

Gong, S., Zheng, C., Doughty, M.L., Losos, K., Didkovsky, N., Schambra, U.B., Nowak, N.J., Joyner, A., Leblanc, G., Hatten, M.E., Heintz, N., 2003. A gene expression atlas of the central nervous system based on bacterial artificial chromosomes. Nature 425, 917-925.

Griffiths-Jones, S., Grocock, R.J., van Dongen, S., Bateman, A., Enright, A.J., 2006. miRBase: microRNA sequences, targets and gene nomenclature. Nucleic Acids Res 34, D140-144.

Gualdi, R., Bossard, P., Zheng, M., Hamada, Y., Coleman, J.R., Zaret, K.S., 1996. Hepatic specification of the gut endoderm in vitro: cell signaling and transcriptional control. Genes Dev 10, 1670-1682.

Guglielmi, A., Ruzzenente, A., Campagnaro, T., Pachera, S., Valdegamberi, A., Nicoli, P., Cappellani, A., Malfermoni, G., Iacono, C., 2009. Intrahepatic cholangiocarcinoma: prognostic factors after surgical resection. World journal of surgery 33, 1247-1254.

Haga, H., Patel, T., 2015. Molecular diagnosis of intrahepatic cholangiocarcinoma. Journal of Hepato-Biliary-Pancreatic Sciences 22, 114-123.

Hand, N.J., Master, Z.R., Eauclaire, S.F., Weinblatt, D.E., Matthews, R.P., Friedman, J.R., 2009a. The microRNA-30 family is required for vertebrate hepatobiliary development. Gastroenterology 136, 1081-1090.

Hand, N.J., Master, Z.R., Le Lay, J., Friedman, J.R., 2009b. Hepatic function is preserved in the absence of mature microRNAs. Hepatology 49, 618-626.

Hatziapostolou, M., Polytarchou, C., Aggelidou, E., Drakaki, A., Poultsides, G.A., Jaeger, S.A., Ogata, H., Karin, M., Struhl, K., Hadzopoulou-Cladaras, M., Iliopoulos, D., 2011. An HNF4alpha-miRNA inflammatory feedback circuit regulates hepatocellular oncogenesis. Cell 147, 1233-1247.

Hayhurst, G.P., Lee, Y.H., Lambert, G., Ward, J.M., Gonzalez, F.J., 2001. Hepatocyte nuclear factor 4alpha (nuclear receptor 2A1) is essential for maintenance of hepatic gene expression and lipid homeostasis. Mol Cell Biol 21, 1393-1403.

Hofmann, J.J., Zovein, A.C., Koh, H., Radtke, F., Weinmaster, G., Iruela-Arispe, M.L., 2010. Jagged1 in the portal vein mesenchyme regulates intrahepatic bile duct development: insights into Alagille syndrome. Development 137, 4061-4072.

Huang, L., Holtzinger, A., Jagan, I., BeGora, M., Lohse, I., Ngai, N., Nostro, C., Wang, R., Muthuswamy, L.B., Crawford, H.C., Arrowsmith, C., Kalloger, S.E., Renouf, D.J., Connor, A.A., Cleary, S., Schaeffer, D.F., Roehrl, M., Tsao, M.S., Gallinger, S., Keller, G., Muthuswamy, S.K., 2015. Ductal pancreatic cancer modeling and drug screening using human pluripotent stem cell- and patient-derived tumor organoids. Nat Med 21, 1364-1371.

Hunter, M.P., Wilson, C.M., Jiang, X., Cong, R., Vasavada, H., Kaestner, K.H., Bogue, C.W., 2007. The homeobox gene Hhex is essential for proper hepatoblast differentiation and bile duct morphogenesis. Dev Biol 308, 355-367.

Hyder, O., Marques, H., Pulitano, C., Marsh, J.W., Alexandrescu, S., Bauer, T.W., Gamblin, T.C., Sotiropoulos, G.C., Paul, A., Barroso, E., Clary, B.M., Aldrighetti, L., Ferrone,

C.R., Zhu, A.X., Popescu, I., Gigot, J.F., Mentha, G., Feng, S., Pawlik, T.M., 2014. A nomogram to predict long-term survival after resection for intrahepatic cholangiocarcinoma: an Eastern and Western experience. JAMA Surg 149, 432-438.

Ito, Y., Matsui, T., Kamiya, A., Kinoshita, T., Miyajima, A., 2000. Retroviral gene transfer of signaling molecules into murine fetal hepatocytes defines distinct roles for the STAT3 and ras pathways during hepatic development. Hepatology 32, 1370-1376.

Jeliazkova, P., Jors, S., Lee, M., Zimber-Strobl, U., Ferrer, J., Schmid, R.M., Siveke, J.T., Geisler, F., 2013. Canonical Notch2 signaling determines biliary cell fates of embryonic hepatoblasts and adult hepatocytes independent of Hes1. Hepatology 57, 2469-2479.

Jochheim, A., Cieslak, A., Hillemann, T., Cantz, T., Scharf, J., Manns, M.P., Ott, M., 2003. Multi-stage analysis of differential gene expression in BALB/C mouse liver development by high-density microarrays. Differentiation 71, 62-72.

Jung, J., Zheng, M., Goldfarb, M., Zaret, K.S., 1999. Initiation of mammalian liver development from endoderm by fibroblast growth factors. Science 284, 1998-2003.

Kamiya, A., Kinoshita, T., Ito, Y., Matsui, T., Morikawa, Y., Senba, E., Nakashima, K., Taga, T., Yoshida, K., Kishimoto, T., Miyajima, A., 1999. Fetal liver development requires a paracrine action of oncostatin M through the gp130 signal transducer. The EMBO journal 18, 2127-2136.

Karakatsanis, A., Papaconstantinou, I., Gazouli, M., Lyberopoulou, A., Polymeneas, G., Voros, D., 2013. Expression of microRNAs, miR-21, miR-31, miR-122, miR-145, miR-146a, miR-200c, miR-221, miR-222, and miR-223 in patients with hepatocellular carcinoma or intrahepatic cholangiocarcinoma and its prognostic significance. Mol Carcinog 52, 297-303.

Kawahigashi, Y., Mishima, T., Mizuguchi, Y., Arima, Y., Yokomuro, S., Kanda, T., Ishibashi, O., Yoshida, H., Tajiri, T., Takizawa, T., 2009. MicroRNA profiling of human intrahepatic cholangiocarcinoma cell lines reveals biliary epithelial cell-specific microRNAs. J Nippon Med Sch 76, 188-197.

Kellendonk, C., Opherk, C., Anlag, K., Schutz, G., Tronche, F., 2000. Hepatocyte-specific expression of Cre recombinase. Genesis 26, 151-153.

Keng, V.W., Yagi, H., Ikawa, M., Nagano, T., Myint, Z., Yamada, K., Tanaka, T., Sato, A., Muramatsu, I., Okabe, M., Sato, M., Noguchi, T., 2000. Homeobox gene Hex is essential for onset of mouse embryonic liver development and differentiation of the monocyte lineage. Biochem Biophys Res Commun 276, 1155-1161.

Khan, S.A., Emadossadaty, S., Ladep, N.G., Thomas, H.C., Elliott, P., Taylor-Robinson, S.D., Toledano, M.B., 2012. Rising trends in cholangiocarcinoma: is the ICD classification system misleading us? J Hepatol 56, 848-854.

Kim, D., Kwon, Y.K., Cho, K.H., 2008. The biphasic behavior of incoherent feed-forward loops in biomolecular regulatory networks. Bioessays 30, 1204-1211.

Kinoshita, T., Sekiguchi, T., Xu, M.J., Ito, Y., Kamiya, A., Tsuji, K., Nakahata, T., Miyajima, A., 1999. Hepatic differentiation induced by oncostatin M attenuates fetal liver hematopoiesis. Proc Natl Acad Sci U S A 96, 7265-7270.

Kiyohashi, K., Kakinuma, S., Kamiya, A., Sakamoto, N., Nitta, S., Yamanaka, H., Yoshino, K., Fujiki, J., Murakawa, M., Kusano-Kitazume, A., Shimizu, H., Okamoto, R., Azuma, S., Nakagawa, M., Asahina, Y., Tanimizu, N., Kikuchi, A., Nakauchi, H., Watanabe, M., 2013. Wnt5a signaling mediates biliary differentiation of fetal hepatic stem/progenitor cells in mice. Hepatology 57, 2502-2513.

Kodama, Y., Hijikata, M., Kageyama, R., Shimotohno, K., Chiba, T., 2004. The role of notch signaling in the development of intrahepatic bile ducts. Gastroenterology 127, 1775-1786.

Komuta, M., Govaere, O., Vandecaveye, V., Akiba, J., Van Steenbergen, W., Verslype, C., Laleman, W., Pirenne, J., Aerts, R., Yano, H., Nevens, F., Topal, B., Roskams, T., 2012. Histological diversity in cholangiocellular carcinoma reflects the different cholangiocyte phenotypes. Hepatology 55, 1876-1888.

Komuta, M., Spee, B., Borght, S.V., De Vos, R., Verslype, C., Aerts, R., Yano, H., Suzuki, T., Matsuda, M., Fujii, H., Desmet, V.J., Kojiro, M., Roskams, T., 2008. Clinicopathological study on cholangiolocellular carcinoma suggesting hepatic progenitor cell origin. Hepatology 47, 1544-1556.

Krupczak-Hollis, K., Wang, X., Kalinichenko, V.V., Gusarova, G.A., Wang, I.C., Dennewitz, M.B., Yoder, H.M., Kiyokawa, H., Kaestner, K.H., Costa, R.H., 2004. The mouse Forkhead Box m1 transcription factor is essential for hepatoblast mitosis and development of intrahepatic bile ducts and vessels during liver morphogenesis. Dev Biol 276, 74-88.

Kyrmizi, I., Hatzis, P., Katrakili, N., Tronche, F., Gonzalez, F.J., Talianidis, I., 2006. Plasticity and expanding complexity of the hepatic transcription factor network during liver development. Genes Dev 20, 2293-2305.

Lagos-Quintana, M., Rauhut, R., Yalcin, A., Meyer, J., Lendeckel, W., Tuschl, T., 2002. Identification of tissue-specific microRNAs from mouse. Current biology : CB 12, 735-739.

Lahuna, O., Rastegar, M., Maiter, D., Thissen, J.P., Lemaigre, F.P., Rousseau, G.G., 2000. Involvement of STAT5 (signal transducer and activator of transcription 5) and HNF-4 (hepatocyte nuclear factor 4) in the transcriptional control of the hnf6 gene by growth hormone. Molecular endocrinology (Baltimore, Md.) 14, 285-294.

Laudadio, I., Manfroid, I., Achouri, Y., Schmidt, D., Wilson, M.D., Cordi, S., Thorrez, L., Knoops, L., Jacquemin, P., Schuit, F., Pierreux, C.E., Odom, D.T., Peers, B., Lemaigre, F.P., 2012. A feedback loop between the liver-enriched transcription factor network and miR-122 controls hepatocyte differentiation. Gastroenterology 142, 119-129.

Lazaridis, K.N., Gores, G.J., 2005. Cholangiocarcinoma. Gastroenterology 128, 1655-1667.

Lee, C.S., Friedman, J.R., Fulmer, J.T., Kaestner, K.H., 2005. The initiation of liver development is dependent on Foxa transcription factors. Nature 435, 944-947.

Lekstrom-Himes, J., Xanthopoulos, K.G., 1998. Biological role of the CCAAT/enhancer-binding protein family of transcription factors. J Biol Chem 273, 28545-28548.

Lemaigre, F.P., 2009. Mechanisms of liver development: concepts for understanding liver disorders and design of novel therapies. Gastroenterology 137, 62-79.

Li, J., Ning, G., Duncan, S.A., 2000. Mammalian hepatocyte differentiation requires the transcription factor HNF-4alpha. Genes Dev 14, 464-474.

Li, L., Krantz, I.D., Deng, Y., Genin, A., Banta, A.B., Collins, C.C., Qi, M., Trask, B.J., Kuo, W.L., Cochran, J., Costa, T., Pierpont, M.E., Rand, E.B., Piccoli, D.A., Hood, L., Spinner, N.B., 1997. Alagille syndrome is caused by mutations in human Jagged1, which encodes a ligand for Notch1. Nature genetics 16, 243-251.

Li, Z., White, P., Tuteja, G., Rubins, N., Sackett, S., Kaestner, K.H., 2009. Foxa1 and Foxa2 regulate bile duct development in mice. J Clin Invest 119, 1537-1545.

Li, Z.Y., Xi, Y., Zhu, W.N., Zeng, C., Zhang, Z.Q., Guo, Z.C., Hao, D.L., Liu, G., Feng, L., Chen, H.Z., Chen, F., Lv, X., Liu, D.P., Liang, C.C., 2011. Positive regulation of hepatic miR-122 expression by HNF4alpha. J Hepatol 55, 602-611.

Liberzon, A., Birger, C., Thorvaldsdottir, H., Ghandi, M., Mesirov, J.P., Tamayo, P., 2015. The Molecular Signatures Database (MSigDB) hallmark gene set collection. Cell Syst 1, 417-425.

Liu-Chittenden, Y., Huang, B., Shim, J.S., Chen, Q., Lee, S.J., Anders, R.A., Liu, J.O., Pan, D., 2012. Genetic and pharmacological disruption of the TEAD-YAP complex suppresses the oncogenic activity of YAP. Genes Dev 26, 1300-1305.

Locker, J., 2011. Transcriptional Control of Hepatocyte Differentiation, in: Monga, S.S.P. (Ed.), Molecular Pathology of Liver Diseases. Springer US, Boston, MA, pp. 193-211.

Loh, K.M., Ang, L.T., Zhang, J., Kumar, V., Ang, J., Auyeong, J.Q., Lee, K.L., Choo, S.H., Lim, C.Y., Nichane, M., Tan, J., Noghabi, M.S., Azzola, L., Ng, E.S., Durruthy-Durruthy, J., Sebastiano, V., Poellinger, L., Elefanty, A.G., Stanley, E.G., Chen, Q., Prabhakar, S., Weissman, I.L., Lim, B., 2014. Efficient endoderm induction from human pluripotent stem cells by logically directing signals controlling lineage bifurcations. Cell Stem Cell 14, 237-252.

Lokmane, L., Haumaitre, C., Garcia-Villalba, P., Anselme, I., Schneider-Maunoury, S., Cereghini, S., 2008. Crucial role of vHNF1 in vertebrate hepatic specification. Development 135, 2777-2786.

Lorent, K., Moore, J.C., Siekmann, A.F., Lawson, N., Pack, M., 2010. Reiterative use of the notch signal during zebrafish intrahepatic biliary development. Dev Dyn 239, 855-864.

Lorent, K., Yeo, S.Y., Oda, T., Chandrasekharappa, S., Chitnis, A., Matthews, R.P., Pack, M., 2004. Inhibition of Jagged-mediated Notch signaling disrupts zebrafish biliary development and generates multi-organ defects compatible with an Alagille syndrome phenocopy. Development 131, 5753-5766.

Lozier, J., McCright, B., Gridley, T., 2008. Notch signaling regulates bile duct morphogenesis in mice. PLoS One 3, e1851.

Ludtke, T.H., Christoffels, V.M., Petry, M., Kispert, A., 2009. Tbx3 promotes liver bud expansion during mouse development by suppression of cholangiocyte differentiation. Hepatology 49, 969-978.

Maeda, T., Adachi, E., Kajiyama, K., Sugimachi, K., Tsuneyoshi, M., 1995. Combined hepatocellular and cholangiocarcinoma: proposed criteria according to cytokeratin expression and analysis of clinicopathologic features. Human pathology 26, 956-964.

Mangan, S., Alon, U., 2003. Structure and function of the feed-forward loop network motif. Proc Natl Acad Sci U S A 100, 11980-11985.

Margagliotti, S., Clotman, F., Pierreux, C.E., Beaudry, J.B., Jacquemin, P., Rousseau, G.G., Lemaigre, F.P., 2007. The Onecut transcription factors HNF-6/OC-1 and OC-2 regulate early liver expansion by controlling hepatoblast migration. Dev Biol 311, 579-589.

Marti, P., Stein, C., Blumer, T., Abraham, Y., Dill, M.T., Pikiolek, M., Orsini, V., Jurisic, G., Megel, P., Makowska, Z., Agarinis, C., Tornillo, L., Bouwmeester, T., Ruffner, H., Bauer, A., Parker, C.N., Schmelzle, T., Terracciano, L.M., Heim, M.H., Tchorz, J.S., 2015. YAP promotes proliferation, chemoresistance, and angiogenesis in human cholangiocarcinoma through TEAD transcription factors. Hepatology 62, 1497-1510.

Martinez Barbera, J.P., Clements, M., Thomas, P., Rodriguez, T., Meloy, D., Kioussis, D., Beddington, R.S., 2000. The homeobox gene Hex is required in definitive endodermal tissues for normal forebrain, liver and thyroid formation. Development 127, 2433-2445.

Martinez-Jimenez, C.P., Kyrmizi, I., Cardot, P., Gonzalez, F.J., Talianidis, I., 2010. Hepatocyte nuclear factor 4alpha coordinates a transcription factor network regulating hepatic fatty acid metabolism. Mol Cell Biol 30, 565-577.

Matsumoto, K., Miki, R., Nakayama, M., Tatsumi, N., Yokouchi, Y., 2008. Wnt9a secreted from the walls of hepatic sinusoids is essential for morphogenesis, proliferation, and glycogen accumulation of chick hepatic epithelium. Dev Biol 319, 234-247.

Matsumoto, K., Yoshitomi, H., Rossant, J., Zaret, K.S., 2001. Liver organogenesis promoted by endothelial cells prior to vascular function. Science 294, 559-563.

Matsushima, H., Kuroki, T., Kitasato, A., Adachi, T., Tanaka, T., Hirabaru, M., Hirayama, T., Kuroshima, N., Hidaka, M., Soyama, A., Takatsuki, M., Kinoshita, N., Sano, K., Nishida, N., Eguchi, S., 2015a. Sox9 expression in carcinogenesis and its clinical significance in intrahepatic cholangiocarcinoma. Dig Liver Dis 47, 1067-1075.

Matsushima, H., Kuroki, T., Kitasato, A., Adachi, T., Tanaka, T., Hirabaru, M., Hirayama, T., Kuroshima, N., Hidaka, M., Soyama, A., Takatsuki, M., Kinoshita, N., Sano, K., Nishida, N., Eguchi, S., 2015b. Sox9 expression in carcinogenesis and its clinical significance in intrahepatic cholangiocarcinoma. Dig Liver Dis.

Mazur, P.K., Riener, M.O., Jochum, W., Kristiansen, G., Weber, A., Schmid, R.M., Siveke, J.T., 2012. Expression and clinicopathological significance of notch signaling and cell-fate genes in biliary tract cancer. The American journal of gastroenterology 107, 126-135.

McDaniell, R., Warthen, D.M., Sanchez-Lara, P.A., Pai, A., Krantz, I.D., Piccoli, D.A., Spinner, N.B., 2006. NOTCH2 mutations cause Alagille syndrome, a heterogeneous disorder of the notch signaling pathway. Am J Hum Genet 79, 169-173.

McGuire, S., 2016. World Cancer Report 2014. Geneva, Switzerland: World Health Organization, International Agency for Research on Cancer, WHO Press, 2015. Advances in nutrition (Bethesda, Md.) 7, 418-419.

McLin, V.A., Rankin, S.A., Zorn, A.M., 2007. Repression of Wnt/beta-catenin signaling in the anterior endoderm is essential for liver and pancreas development. Development 134, 2207-2217.

Meng, F., Henson, R., Lang, M., Wehbe, H., Maheshwari, S., Mendell, J.T., Jiang, J., Schmittgen, T.D., Patel, T., 2006. Involvement of human micro-RNA in growth and response to chemotherapy in human cholangiocarcinoma cell lines. Gastroenterology 130, 2113-2129.

Miller, D.L., Ortega, S., Bashayan, O., Basch, R., Basilico, C., 2000. Compensation by fibroblast growth factor 1 (FGF1) does not account for the mild phenotypic defects observed in FGF2 null mice. Mol Cell Biol 20, 2260-2268.

Moll, R., Franke, W.W., Schiller, D.L., Geiger, B., Krepler, R., 1982. The catalog of human cytokeratins: patterns of expression in normal epithelia, tumors and cultured cells. Cell 31, 11-24.

Monga, S.P., Mars, W.M., Pediaditakis, P., Bell, A., Mule, K., Bowen, W.C., Wang, X., Zarnegar, R., Michalopoulos, G.K., 2002. Hepatocyte growth factor induces Wnt-independent nuclear translocation of beta-catenin after Met-beta-catenin dissociation in hepatocytes. Cancer research 62, 2064-2071.

Mosnier, J.F., Kandel, C., Cazals-Hatem, D., Bou-Hanna, C., Gournay, J., Jarry, A., Laboisse, C.L., 2009. N-cadherin serves as diagnostic biomarker in intrahepatic and perihilar cholangiocarcinomas. Mod Pathol 22, 182-190.

Munoz-Garrido, P., Garcia-Fernandez de Barrena, M., Hijona, E., Carracedo, M., Marin, J.J., Bujanda, L., Banales, J.M., 2012. MicroRNAs in biliary diseases. World J Gastroenterol 18, 6189-6196.

Nakanuma, Y., Kakuda, Y., 2015. Pathologic classification of cholangiocarcinoma: New concepts. Best practice & research. Clinical gastroenterology 29, 277-293.

Oda, T., Elkahloun, A.G., Pike, B.L., Okajima, K., Krantz, I.D., Genin, A., Piccoli, D.A., Meltzer, P.S., Spinner, N.B., Collins, F.S., Chandrasekharappa, S.C., 1997. Mutations in the human Jagged1 gene are responsible for Alagille syndrome. Nature genetics 16, 235-242.

Odom, D.T., Dowell, R.D., Jacobsen, E.S., Nekludova, L., Rolfe, P.A., Danford, T.W., Gifford, D.K., Fraenkel, E., Bell, G.I., Young, R.A., 2006. Core transcriptional regulatory circuitry in human hepatocytes. Mol Syst Biol 2, 2006 0017.

Odom, D.T., Zizlsperger, N., Gordon, D.B., Bell, G.W., Rinaldi, N.J., Murray, H.L., Volkert, T.L., Schreiber, J., Rolfe, P.A., Gifford, D.K., Fraenkel, E., Bell, G.I., Young, R.A.,

2004. Control of pancreas and liver gene expression by HNF transcription factors. Science 303, 1378-1381.

Oikawa, T., Kamiya, A., Kakinuma, S., Zeniya, M., Nishinakamura, R., Tajiri, H., Nakauchi, H., 2009. Sall4 regulates cell fate decision in fetal hepatic stem/progenitor cells. Gastroenterology 136, 1000-1011.

Papaconstantinou, I., Karakatsanis, A., Gazouli, M., Polymeneas, G., Voros, D., 2012. The role of microRNAs in liver cancer. Eur J Gastroenterol Hepatol 24, 223-228.

Pare, J.F., Malenfant, D., Courtemanche, C., Jacob-Wagner, M., Roy, S., Allard, D., Belanger, L., 2004. The fetoprotein transcription factor (FTF) gene is essential to embryogenesis and cholesterol homeostasis and is regulated by a DR4 element. J Biol Chem 279, 21206-21216.

Parviz, F., Matullo, C., Garrison, W.D., Savatski, L., Adamson, J.W., Ning, G., Kaestner, K.H., Rossi, J.M., Zaret, K.S., Duncan, S.A., 2003. Hepatocyte nuclear factor 4alpha controls the development of a hepatic epithelium and liver morphogenesis. Nature genetics 34, 292-296.

Pei, T., Li, Y., Wang, J., Wang, H., Liang, Y., Shi, H., Sun, B., Yin, D., Sun, J., Song, R., Pan, S., Sun, Y., Jiang, H., Zheng, T., Liu, L., 2015. YAP is a critical oncogene in human cholangiocarcinoma. Oncotarget 6, 17206-17220.

Petkov, P.M., Zavadil, J., Goetz, D., Chu, T., Carver, R., Rogler, C.E., Bottinger, E.P., Shafritz, D.A., Dabeva, M.D., 2004. Gene expression pattern in hepatic stem/progenitor cells during rat fetal development using complementary DNA microarrays. Hepatology 39, 617-627.

Pierreux, C.E., Stafford, J., Demonte, D., Scott, D.K., Vandenhaute, J., O'Brien, R.M., Granner, D.K., Rousseau, G.G., Lemaigre, F.P., 1999. Antiglucocorticoid activity of hepatocyte nuclear factor-6. Proc Natl Acad Sci U S A 96, 8961-8966.

Plieskatt, J., Rinaldi, G., Feng, Y., Peng, J., Easley, S., Jia, X., Potriquet, J., Pairojkul, C., Bhudhisawasdi, V., Sripa, B., Brindley, P.J., Bethony, J., Mulvenna, J., 2015. A microRNA profile associated with Opisthorchis viverrini-induced cholangiocarcinoma in tissue and plasma. BMC Cancer 15, 309.

Plieskatt, J.L., Rinaldi, G., Feng, Y., Peng, J., Yonglitthipagon, P., Easley, S., Laha, T., Pairojkul, C., Bhudhisawasdi, V., Sripa, B., Brindley, P.J., Mulvenna, J.P., Bethony, J.M., 2014. Distinct miRNA signatures associate with subtypes of cholangiocarcinoma from infection with the tumourigenic liver fluke Opisthorchis viverrini. J Hepatol 61, 850-858.

Plumb-Rudewiez, N., Clotman, F., Strick-Marchand, H., Pierreux, C.E., Weiss, M.C., Rousseau, G.G., Lemaigre, F.P., 2004. Transcription factor HNF-6/OC-1 inhibits the stimulation of the HNF-3alpha/Foxa1 gene by TGF-beta in mouse liver. Hepatology 40, 1266-1274.

Poncy, A., Antoniou, A., Cordi, S., Pierreux, C.E., Jacquemin, P., Lemaigre, F.P., 2015a. Transcription factors SOX4 and SOX9 cooperatively control development of bile ducts. Dev Biol 404, 136-148.

Poncy, A., Antoniou, A., Cordi, S., Pierreux, C.E., Jacquemin, P., Lemaigre, F.P., 2015b. Transcription factors SOX4 and SOX9 cooperatively control development of bile ducts. Dev Biol 402, 136-148.

Pontoglio, M., Barra, J., Hadchouel, M., Doyen, A., Kress, C., Bach, J.P., Babinet, C., Yaniv, M., 1996. Hepatocyte nuclear factor 1 inactivation results in hepatic dysfunction, phenylketonuria, and renal Fanconi syndrome. Cell 84, 575-585.

Rastegar, M., Rousseau, G.G., Lemaigre, F.P., 2000. CCAAT/enhancer-binding protein-alpha is a component of the growth hormone-regulated network of liver transcription factors. Endocrinology 141, 1686-1692.

Raynaud, P., Carpentier, R., Antoniou, A., Lemaigre, F.P., 2011. Biliary differentiation and bile duct morphogenesis in development and disease. Int J Biochem Cell Biol 43, 245-256.

Razumilava, N., Gores, G.J., 2013. Classification, diagnosis, and management of cholangiocarcinoma. Clin Gastroenterol Hepatol 11, 13-21 e11; quiz e13-14.

Razumilava, N., Gores, G.J., 2014. Cholangiocarcinoma. Lancet (London, England) 383, 2168-2179.

Rizvi, S., Gores, G.J., 2013. Pathogenesis, diagnosis, and management of cholangiocarcinoma. Gastroenterology 145, 1215-1229.

Roelandt, P., Antoniou, A., Libbrecht, L., Van Steenbergen, W., Laleman, W., Verslype, C., Van der Merwe, S., Nevens, F., De Vos, R., Fischer, E., Pontoglio, M., Lemaigre, F., Cassiman, D., 2012. HNF1B deficiency causes ciliary defects in human cholangiocytes. Hepatology 56, 1178-1181.

Rogler, C.E., Levoci, L., Ader, T., Massimi, A., Tchaikovskaya, T., Norel, R., Rogler, L.E., 2009. MicroRNA-23b cluster microRNAs regulate transforming growth factor-beta/bone morphogenetic protein signaling and liver stem cell differentiation by targeting Smads. Hepatology 50, 575-584.

Rossi, J.M., Dunn, N.R., Hogan, B.L., Zaret, K.S., 2001. Distinct mesodermal signals, including BMPs from the septum transversum mesenchyme, are required in combination for hepatogenesis from the endoderm. Genes Dev 15, 1998-2009.

Sablin, E.P., Blind, R.D., Uthayaruban, R., Chiu, H.J., Deacon, A.M., Das, D., Ingraham, H.A., Fletterick, R.J., 2015. Structure of Liver Receptor Homolog-1 (NR5A2) with PIP3 hormone bound in the ligand binding pocket. Journal of structural biology 192, 342-348.

Schmidt, C., Bladt, F., Goedecke, S., Brinkmann, V., Zschiesche, W., Sharpe, M., Gherardi, E., Birchmeier, C., 1995. Scatter factor/hepatocyte growth factor is essential for liver development. Nature 373, 699-702.

Schrem, H., Klempnauer, J., Borlak, J., 2002. Liver-enriched transcription factors in liver function and development. Part I: the hepatocyte nuclear factor network and liver-specific gene expression. Pharmacol Rev 54, 129-158.

Sekine, S., Ogawa, R., Ito, R., Hiraoka, N., McManus, M.T., Kanai, Y., Hebrok, M., 2009a. Disruption of Dicer1 induces dysregulated fetal gene expression and promotes hepatocarcinogenesis. Gastroenterology 136, 2304-2315 e2301-2304.

Sekine, S., Ogawa, R., McManus, M.T., Kanai, Y., Hebrok, M., 2009b. Dicer is required for proper liver zonation. J Pathol 219, 365-372.

Sekiya, S., Suzuki, A., 2012. Intrahepatic cholangiocarcinoma can arise from Notch-mediated conversion of hepatocytes. J Clin Invest 122, 3914-3918.

Sempoux, C., Jibara, G., Ward, S.C., Fan, C., Qin, L., Roayaie, S., Fiel, M.I., Schwartz, M., Thung, S.N., 2011. Intrahepatic cholangiocarcinoma: new insights in pathology. Seminars in liver disease 31, 49-60.

Serls, A.E., Doherty, S., Parvatiyar, P., Wells, J.M., Deutsch, G.H., 2005. Different thresholds of fibroblast growth factors pattern the ventral foregut into liver and lung. Development 132, 35-47.

Seth, A., Ye, J., Yu, N., Guez, F., Bedford, D.C., Neale, G.A., Cordi, S., Brindle, P.K., Lemaigre, F.P., Kaestner, K.H., Sosa-Pineda, B., 2014. Prox1 ablation in hepatic progenitors causes defective hepatocyte specification and increases biliary cell commitment. Development 141, 538-547.

Shiojiri, N., Takeshita, K., Yamasaki, H., Iwata, T., 2004. Suppression of C/EBP alpha expression in biliary cell differentiation from hepatoblasts during mouse liver development. J Hepatol 41, 790-798.

Si-Tayeb, K., Lemaigre, F.P., Duncan, S.A., 2010. Organogenesis and development of the liver. Dev Cell 18, 175-189.

Sirica, A.E., Dumur, C.I., Campbell, D.J., Almenara, J.A., Ogunwobi, O.O., Dewitt, J.L., 2009. Intrahepatic cholangiocarcinoma progression: prognostic factors and basic mechanisms. Clin Gastroenterol Hepatol 7, S68-78.

Slim, C.L., Lazaro-Dieguez, F., Bijlard, M., Toussaint, M.J., de Bruin, A., Du, Q., Musch, A., van Ijzendoorn, S.C., 2013. Par1b induces asymmetric inheritance of plasma membrane domains via LGN-dependent mitotic spindle orientation in proliferating hepatocytes. PLoS Biol 11, e1001739.

Sosa-Pineda, B., Wigle, J.T., Oliver, G., 2000. Hepatocyte migration during liver development requires Prox1. Nature genetics 25, 254-255.

Stanulovic, V.S., Kyrmizi, I., Kruithof-de Julio, M., Hoogenkamp, M., Vermeulen, J.L., Ruijter, J.M., Talianidis, I., Hakvoort, T.B., Lamers, W.H., 2007. Hepatic HNF4alpha deficiency induces periportal expression of glutamine synthetase and other pericentral enzymes. Hepatology 45, 433-444.

Stern, P., Astrof, S., Erkeland, S.J., Schustak, J., Sharp, P.A., Hynes, R.O., 2008. A system for Cre-regulated RNA interference in vivo. Proc Natl Acad Sci U S A 105, 13895-13900.

Strick-Marchand, H., Weiss, M.C., 2002. Inducible differentiation and morphogenesis of bipotential liver cell lines from wild-type mouse embryos. Hepatology (Baltimore, Md.) 36, 794-804.

Subramanian, A., Tamayo, P., Mootha, V.K., Mukherjee, S., Ebert, B.L., Gillette, M.A., Paulovich, A., Pomeroy, S.L., Golub, T.R., Lander, E.S., Mesirov, J.P., 2005. Gene set enrichment analysis: a knowledge-based approach for interpreting genome-wide expression profiles. Proc Natl Acad Sci U S A 102, 15545-15550.

Sulpice, L., Rayar, M., Turlin, B., Boucher, E., Bellaud, P., Desille, M., Meunier, B., Clement, B., Boudjema, K., Coulouarn, C., 2014. Epithelial cell adhesion molecule is a prognosis marker for intrahepatic cholangiocarcinoma. J Surg Res 192, 117-123.

Suzuki, A., 2003. Role for growth factors and extracellular matrix in controlling differentiation of prospectively isolated hepatic stem cells. Development 130, 2513-2524.

Suzuki, T., Kanai, Y., Hara, T., Sasaki, J., Sasaki, T., Kohara, M., Maehama, T., Taya, C., Shitara, H., Yonekawa, H., Frohman, M.A., Yokozeki, T., Kanaho, Y., 2006. Crucial Role of the Small GTPase ARF6 in Hepatic Cord Formation during Liver Development. Molecular and Cellular Biology 26, 6149-6156.

Szabo, G., Bala, S., 2013. MicroRNAs in liver disease. Nat Rev Gastroenterol Hepatol 10, 542-552.

Takashima, Y., Terada, M., Kawabata, M., Suzuki, A., 2015. Dynamic three-dimensional morphogenesis of intrahepatic bile ducts in mouse liver development. Hepatology 61, 1003-1011.

Takayama, K., Kawabata, K., Nagamoto, Y., Inamura, M., Ohashi, K., Okuno, H., Yamaguchi, T., Tashiro, K., Sakurai, F., Hayakawa, T., Okano, T., Furue, M.K., Mizuguchi, H., 2014. CCAAT/enhancer binding protein-mediated regulation of TGFbeta receptor 2 expression determines the hepatoblast fate decision. Development 141, 91-100.

Tan, X., Yuan, Y., Zeng, G., Apte, U., Thompson, M.D., Cieply, B., Stolz, D.B., Michalopoulos, G.K., Kaestner, K.H., Monga, S.P., 2008. Beta-catenin deletion in hepatoblasts disrupts hepatic morphogenesis and survival during mouse development. Hepatology 47, 1667-1679.

Tanaka, M., Hirabayashi, Y., Sekiguchi, T., Inoue, T., Katsuki, M., Miyajima, A., 2003. Targeted disruption of oncostatin M receptor results in altered hematopoiesis. Blood 102, 3154-3162.

Tanaka, S., Hirohashi, K., Uenishi, T., Yamamoto, T., Hamba, H., Kubo, S., Tanaka, H., Shuto, T., Ogawa, M., Kinoshita, H., 2004. A mixed hepatocellular carcinoma and cholangiocarcinoma: dual expression of biliary-type cytokeratin and hepatocyte specific marker. Hepato-gastroenterology 51, 839-841.

Tanimizu, N., 2003. Isolation of hepatoblasts based on the expression of Dlk/Pref-1. Journal of Cell Science 116, 1775-1786.

Tanimizu, N., Kikkawa, Y., Mitaka, T., Miyajima, A., 2012. alpha1- and alpha5-containing laminins regulate the development of bile ducts via beta1 integrin signals. J Biol Chem 287, 28586-28597.

Tanimizu, N., Kobayashi, S., Ichinohe, N., Mitaka, T., 2014. Downregulation of miR122 by grainyhead-like 2 restricts the hepatocytic differentiation potential of adult liver progenitor cells. Development 141, 4448-4456.

Tanimizu, N., Miyajima, A., 2004. Notch signaling controls hepatoblast differentiation by altering the expression of liver-enriched transcription factors. J Cell Sci 117, 3165-3174.

Tanimizu, N., Miyajima, A., Mostov, K.E., 2007. Liver progenitor cells develop cholangiocyte-type epithelial polarity in three-dimensional culture. Mol Biol Cell 18, 1472-1479.

Tanimizu, N., Nakamura, Y., Ichinohe, N., Mizuguchi, T., Hirata, K., Mitaka, T., 2013. Hepatic biliary epithelial cells acquire epithelial integrity but lose plasticity to differentiate into hepatocytes in vitro during development. J Cell Sci 126, 5239-5246.

Tanimizu, N., Saito, H., Mostov, K., Miyajima, A., 2004. Long-term culture of hepatic progenitors derived from mouse Dlk+ hepatoblasts. J Cell Sci 117, 6425-6434.

Tchorz, J.S., Kinter, J., Muller, M., Tornillo, L., Heim, M.H., Bettler, B., 2009. Notch2 signaling promotes biliary epithelial cell fate specification and tubulogenesis during bile duct development in mice. Hepatology 50, 871-879.

Terashi, T., Aishima, S., Taguchi, K., Asayama, Y., Sugimachi, K., Matsuura, S., Shimada, M., Maehara, S., Maehara, Y., Tsuneyoshi, M., 2004. Decreased expression of osteopontin is related to tumor aggressiveness and clinical outcome of intrahepatic cholangiocarcinoma. Liver Int 24, 38-45.

Torre, C., Perret, C., Colnot, S., 2011. Transcription dynamics in a physiological process: beta-catenin signaling directs liver metabolic zonation. Int J Biochem Cell Biol 43, 271-278.

Tremblay, K.D., Zaret, K.S., 2005. Distinct populations of endoderm cells converge to generate the embryonic liver bud and ventral foregut tissues. Dev Biol 280, 87-99.

Treyer, A., Musch, A., 2013. Hepatocyte polarity. Compr Physiol 3, 243-287.

Tsang, J., Zhu, J., van Oudenaarden, A., 2007. MicroRNA-mediated feedback and feedforward loops are recurrent network motifs in mammals. Mol Cell 26, 753-767.

Tsukita, S., Furuse, M., Itoh, M., 2001. Multifunctional strands in tight junctions. Nat Rev Mol Cell Biol 2, 285-293.

Uenishi, T., Kubo, S., Yamamoto, T., Shuto, T., Ogawa, M., Tanaka, H., Tanaka, S., Kaneda, K., Hirohashi, K., 2003. Cytokeratin 19 expression in hepatocellular carcinoma predicts early postoperative recurrence. Cancer science 94, 851-857.

Van Eyken, P., Sciot, R., Desmet, V., 1988. Intrahepatic bile duct development in the rat: a cytokeratin-immunohistochemical study. Laboratory investigation; a journal of technical methods and pathology 59, 52-59.

Vanderpool, C., Sparks, E.E., Huppert, K.A., Gannon, M., Means, A.L., Huppert, S.S., 2012. Genetic interactions between hepatocyte nuclear factor-6 and Notch signaling regulate mouse intrahepatic bile duct development in vivo. Hepatology 55, 233-243.

von Ahlfen, S., Missel, A., Bendrat, K., Schlumpberger, M., 2007. Determinants of RNA quality from FFPE samples. PLoS One 2, e1261.

Wadsworth, C.A., Lim, A., Taylor-Robinson, S.D., Khan, S.A., 2013. The risk factors and diagnosis of cholangiocarcinoma. Hepatology international 7, 377-393.

Wandzioch, E., Zaret, K.S., 2009. Dynamic signaling network for the specification of embryonic pancreas and liver progenitors. Science 324, 1707-1710.

Wang, M., Tan, Y., Costa, R.H., Holterman, A.X., 2004. In vivo regulation of murine CYP7A1 by HNF-6: a novel mechanism for diminished CYP7A1 expression in biliary obstruction. Hepatology 40, 600-608.

Wang, N.D., Finegold, M.J., Bradley, A., Ou, C.N., Abdelsayed, S.V., Wilde, M.D., Taylor, L.R., Wilson, D.R., Darlington, G.J., 1995. Impaired energy homeostasis in C/EBP alpha knockout mice. Science 269, 1108-1112.

Wang, W., Zhang, J., Zhan, X., Lin, T., Yang, M., Hu, J., Han, B., Hu, S., 2014. SOX4 is associated with poor prognosis in cholangiocarcinoma. Biochem Biophys Res Commun 452, 614-621.

Wang, X.W., Heegaard, N.H., Orum, H., 2012. MicroRNAs in liver disease. Gastroenterology 142, 1431-1443.

Wang, Z., Dolle, P., Cardoso, W.V., Niederreither, K., 2006. Retinoic acid regulates morphogenesis and patterning of posterior foregut derivatives. Dev Biol 297, 433-445.

Watt, A.J., Zhao, R., Li, J., Duncan, S.A., 2007. Development of the mammalian liver and ventral pancreas is dependent on GATA4. BMC Dev Biol 7, 37.

Weinstein, M., Monga, S.P., Liu, Y., Brodie, S.G., Tang, Y., Li, C., Mishra, L., Deng, C.X., 2001. Smad proteins and hepatocyte growth factor control parallel regulatory pathways that converge on beta1-integrin to promote normal liver development. Mol Cell Biol 21, 5122-5131.

Westmacott, A., Burke, Z.D., Oliver, G., Slack, J.M., Tosh, D., 2006. C/EBPalpha and C/EBPbeta are markers of early liver development. Int J Dev Biol 50, 653-657.

Xu, H., He, J.H., Xiao, Z.D., Zhang, Q.Q., Chen, Y.Q., Zhou, H., Qu, L.H., 2010. Liver-enriched transcription factors regulate microRNA-122 that targets CUTL1 during liver development. Hepatology 52, 1431-1442.

Yamasaki, H., Sada, A., Iwata, T., Niwa, T., Tomizawa, M., Xanthopoulos, K.G., Koike, T., Shiojiri, N., 2006. Suppression of C/EBPalpha expression in periportal

hepatoblasts may stimulate biliary cell differentiation through increased Hnf6 and Hnf1b expression. Development 133, 4233-4243.

Yanai, M., Tatsumi, N., Hasunuma, N., Katsu, K., Endo, F., Yokouchi, Y., 2008. FGF signaling segregates biliary cell-lineage from chick hepatoblasts cooperatively with BMP4 and ECM components in vitro. Dev Dyn 237, 1268-1283.

Yang, J.S., Lai, E.C., 2011. Alternative miRNA biogenesis pathways and the interpretation of core miRNA pathway mutants. Mol Cell 43, 892-903.

Yimlamai, D., Christodoulou, C., Galli, G.G., Yanger, K., Pepe-Mooney, B., Gurung, B., Shrestha, K., Cahan, P., Stanger, B.Z., Camargo, F.D., 2014. Hippo pathway activity influences liver cell fate. Cell 157, 1324-1338.

Yoshida, Y., Hughes, D.E., Rausa, F.M., 3rd, Kim, I.M., Tan, Y., Darlington, G.J., Costa, R.H., 2006. C/EBPalpha and HNF6 protein complex formation stimulates HNF6-dependent transcription by CBP coactivator recruitment in HepG2 cells. Hepatology 43, 276-286.

Yu, D.D., Jing, Y.Y., Guo, S.W., Ye, F., Lu, W., Li, Q., Dong, Y.L., Gao, L., Yang, Y.T., Yang, Y., Wu, M.C., Wei, L.X., 2015. Overexpression Of Hepatocyte Nuclear Factor-1beta Predicting Poor Prognosis Is Associated With Biliary Phenotype In Patients With Hepatocellular Carcinoma. Sci Rep 5, 13319.

Yuan, H., Wen, B., Liu, X., Gao, C., Yang, R., Wang, L., Chen, S., Chen, Z., de The, H., Zhou, J., Zhu, J., 2015. CCAAT/enhancer-binding protein alpha is required for hepatic outgrowth via the p53 pathway in zebrafish. Sci Rep 5, 15838.

Zaret, K.S., Grompe, M., 2008. Generation and regeneration of cells of the liver and pancreas. Science 322, 1490-1494.

Zhang, L., Rubins, N.E., Ahima, R.S., Greenbaum, L.E., Kaestner, K.H., 2005. Foxa2 integrates the transcriptional response of the hepatocyte to fasting. Cell Metab 2, 141-148.

Zhang, M.Y., Li, S.H., Huang, G.L., Lin, G.H., Shuang, Z.Y., Lao, X.M., Xu, L., Lin, X.J., Wang, H.Y., Li, S.P., 2015. Identification of a novel microRNA signature associated with intrahepatic cholangiocarcinoma (ICC) patient prognosis. BMC Cancer 15, 64.

Zhang, N., Bai, H., David, K.K., Dong, J., Zheng, Y., Cai, J., Giovannini, M., Liu, P., Anders, R.A., Pan, D., 2010. The Merlin/NF2 tumor suppressor functions through the YAP oncoprotein to regulate tissue homeostasis in mammals. Dev Cell 19, 27-38.

Zhao, R., Duncan, S.A., 2005. Embryonic development of the liver. Hepatology 41, 956-967.

Zhao, R., Watt, A.J., Li, J., Luebke-Wheeler, J., Morrisey, E.E., Duncan, S.A., 2005. GATA6 is essential for embryonic development of the liver but dispensable for early heart formation. Mol Cell Biol 25, 2622-2631.

Zong, Y., Panikkar, A., Xu, J., Antoniou, A., Raynaud, P., Lemaigre, F., Stanger, B.Z., 2009. Notch signaling controls liver development by regulating biliary differentiation. Development 136, 1727-1739.